

Gravitational Lensing

Yannick Mellier

IAP and Obs. de Paris / LERMA

1. short history
2. Theory, useful concept and definitions
3. Clusters of galaxies
4. Halos of galaxies
5. Cosmic shear

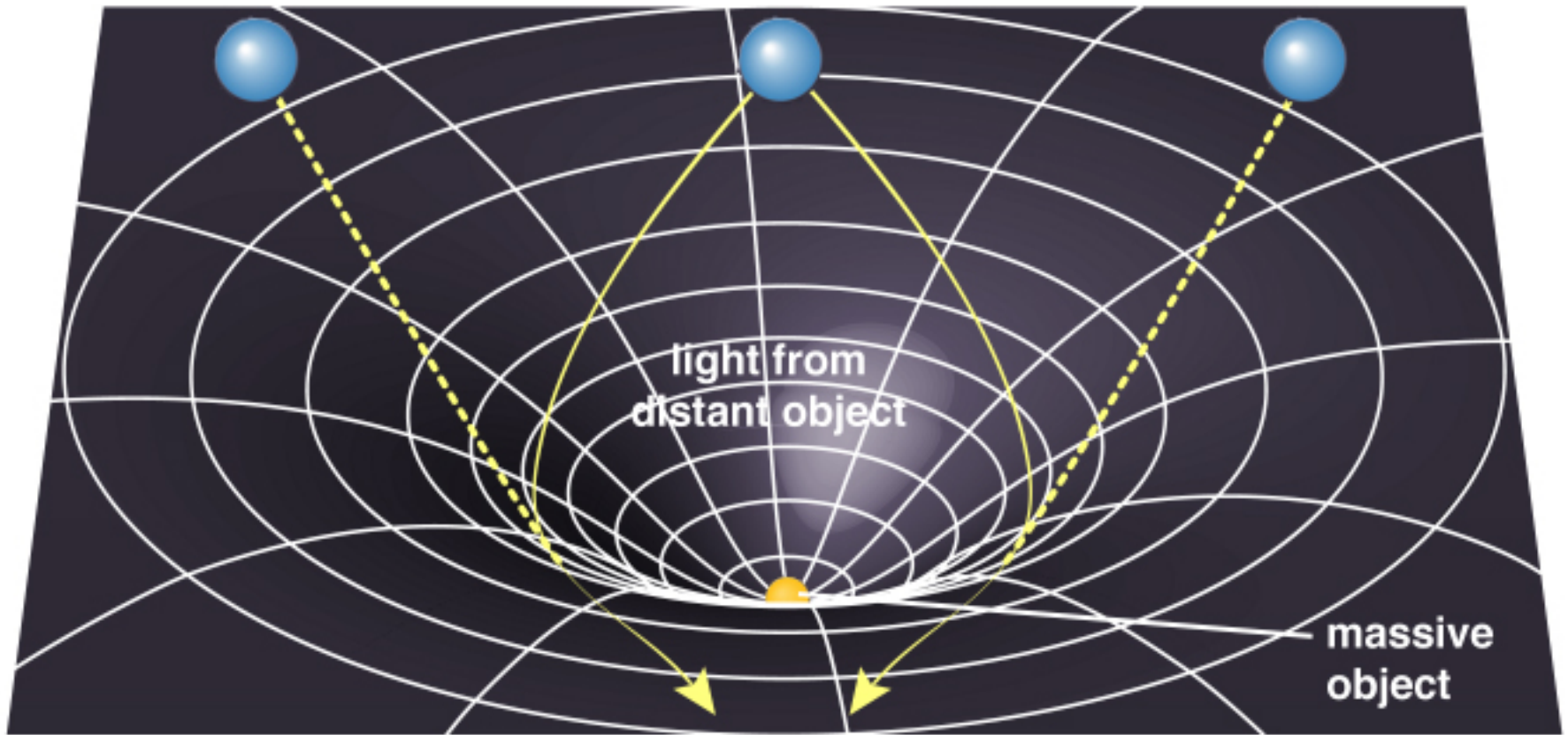
I. **Gravitational Lensing:**

theory, concepts and
definitions

General relativity:

curvature of space time locally modified by mass condensation

Apparent position of a first image Real image Apparent position of a second image



to Earth

Deflection of light, magnification, image multiplication distortion of objects : directly **depend on the amount of matter**

Gravitational lensing effect is **achromatic** (photons follow geodesics regardless their energy)

Lensing : a short history

- 1804:** Soldner works on the deflection of light by gravity
- 1915:** General Relativity
- 1919:** Deflection angle of stars behind the Sun
- 1936:** Einstein's work on lensing by stellar objects
- 1937:** F. Zwicky visions on « extragalactic nebulae » as lenses
- 1964:** Refsdal: time delay and H_0
- 1979:** Multiple image of quasars (0957+561)
- 1987:** Giant arcs in clusters of galaxies (A370, A2218, CL244)
- 1987:** First Einstein ring
- 1993:** EROS and MACHO microlensing experiments
- 2000:** Detection of cosmic shear signal
- 2006:** The « Bullet » cluster and existence of dark matter
- 2007:** First detection of lensing on CMB anisotropies

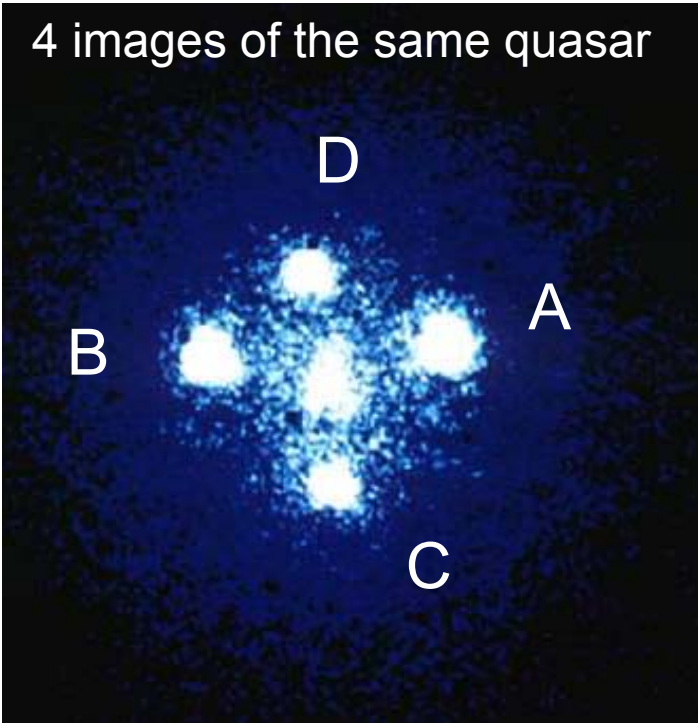
Multiple images: The « Einstein Cross »

Galaxy 2227+030

Redshift $z=0.0394$

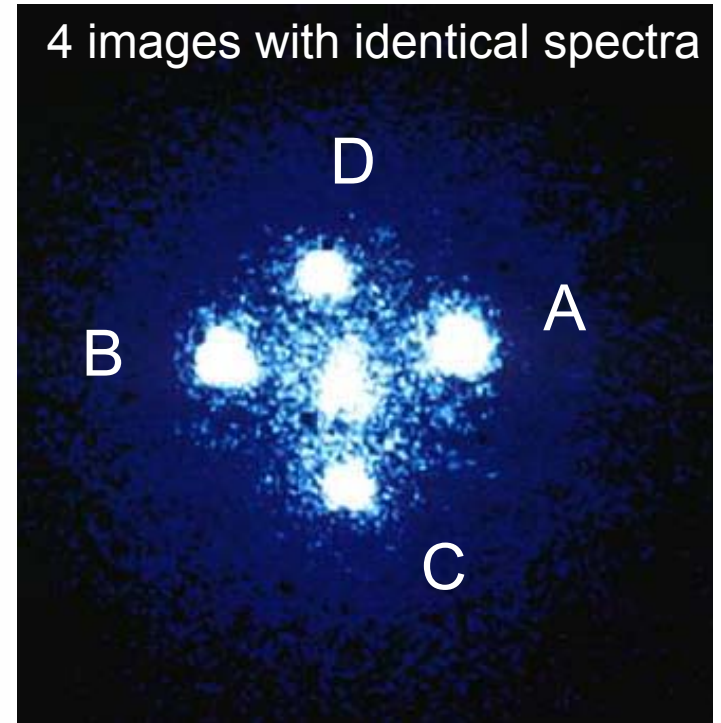
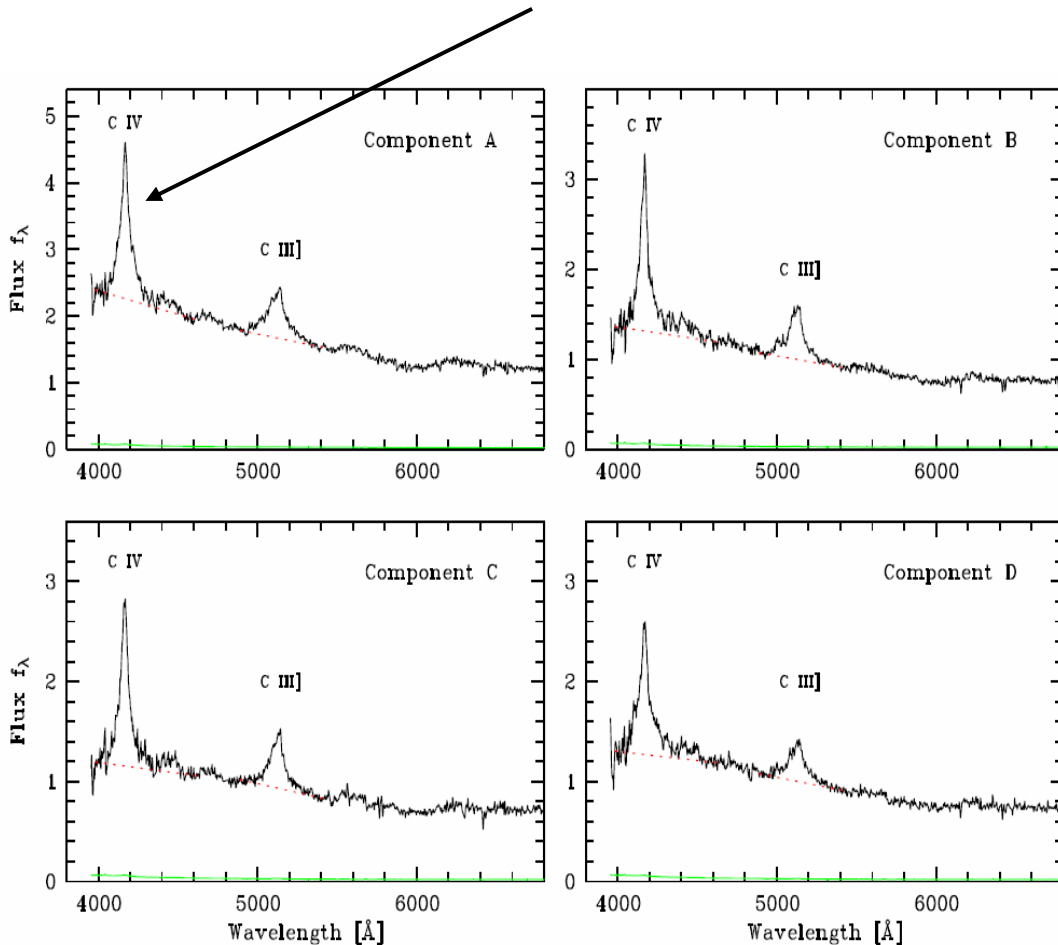
4 images of the same quasar

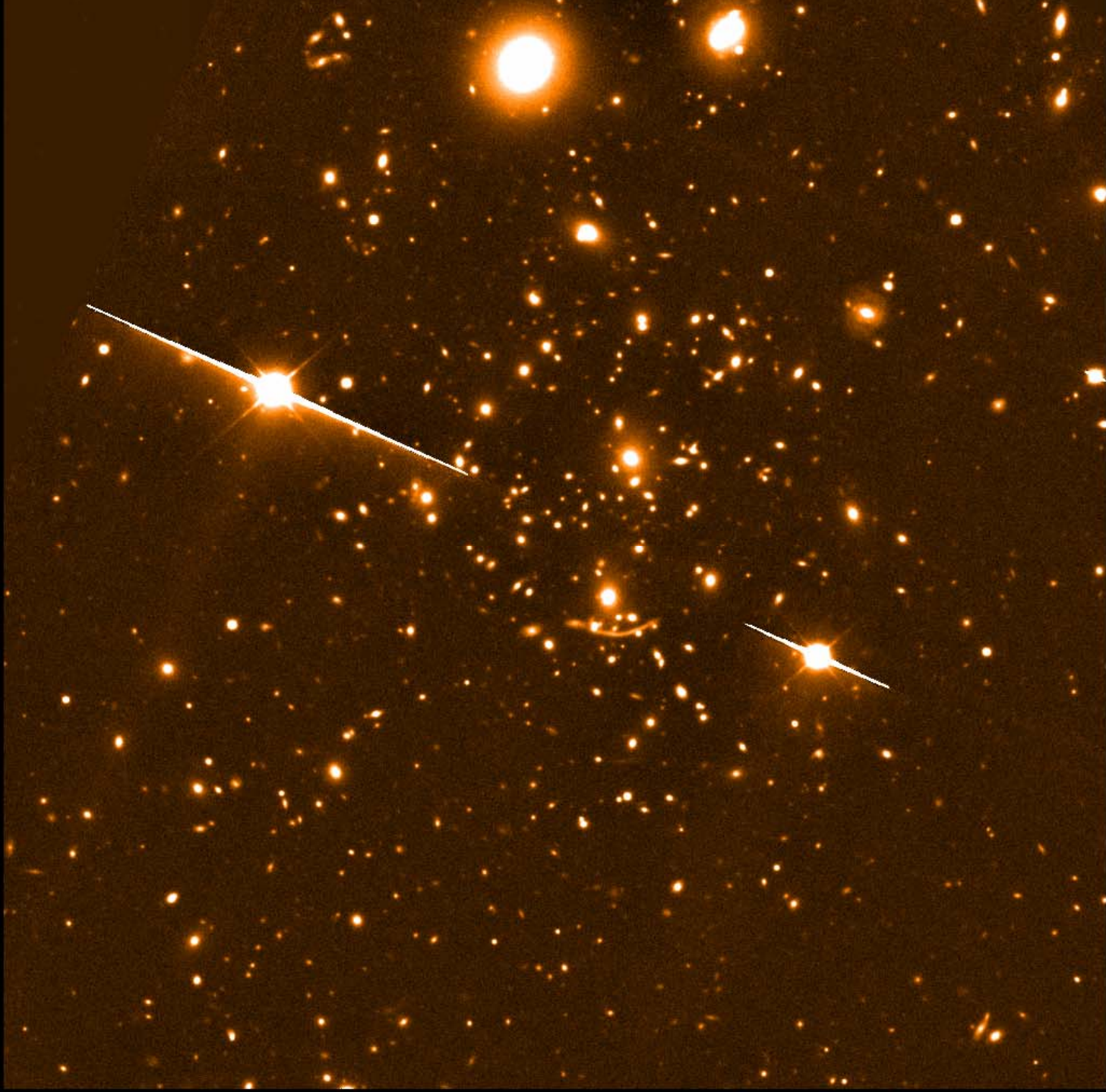
D
A
B
C

A blue-tinted astronomical image showing four distinct, bright, circular spots of light arranged in a cross pattern. The spots are labeled with white capital letters: 'D' at the top, 'A' on the right, 'B' on the left, and 'C' at the bottom. The background is a dark, grainy blue.

The « Einstein Cross »

CIV emission line at 154.9 nm observed 417.6 nm : $z = 1.695$

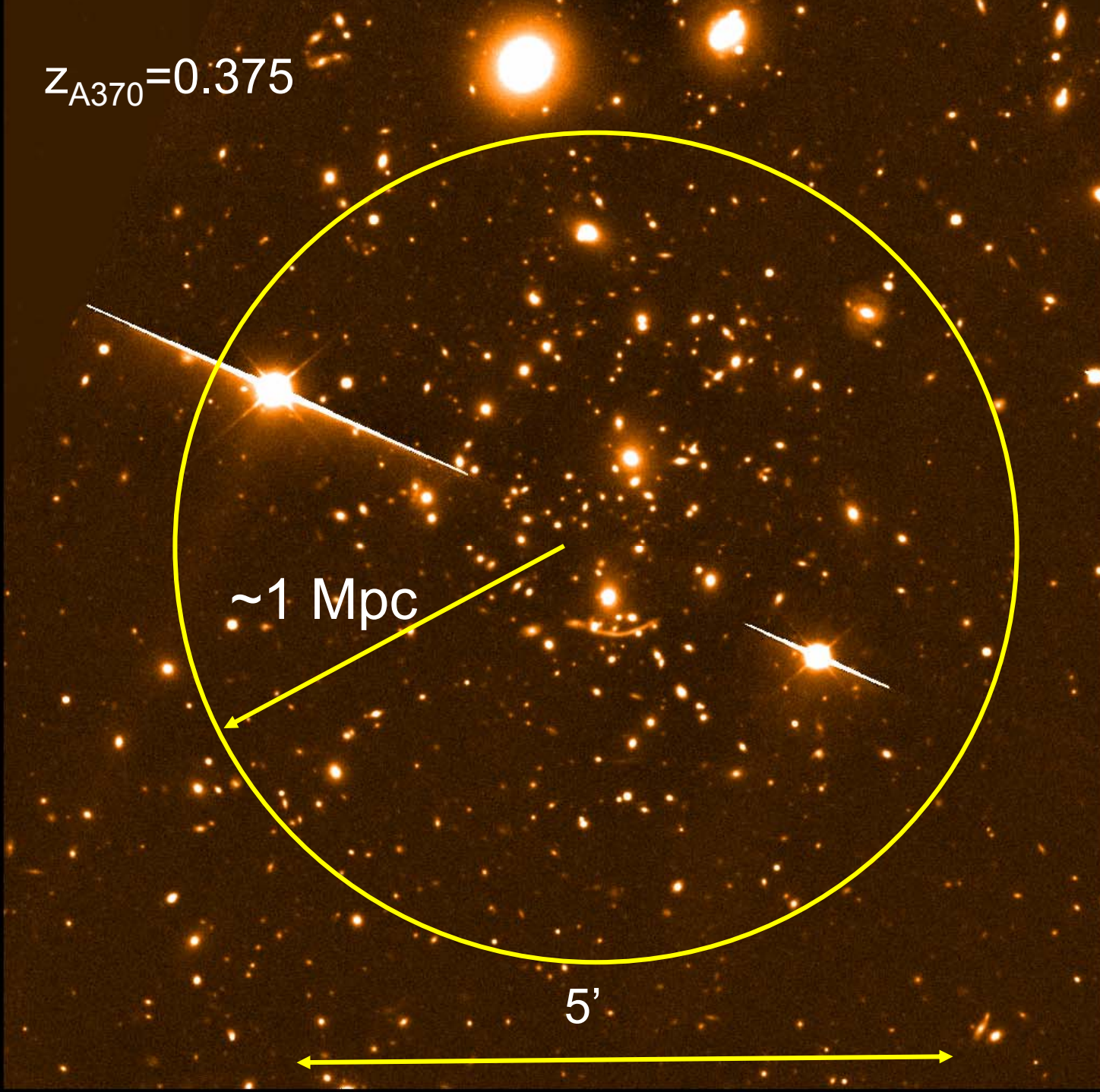




$z_{A370} = 0.375$

~ 1 Mpc

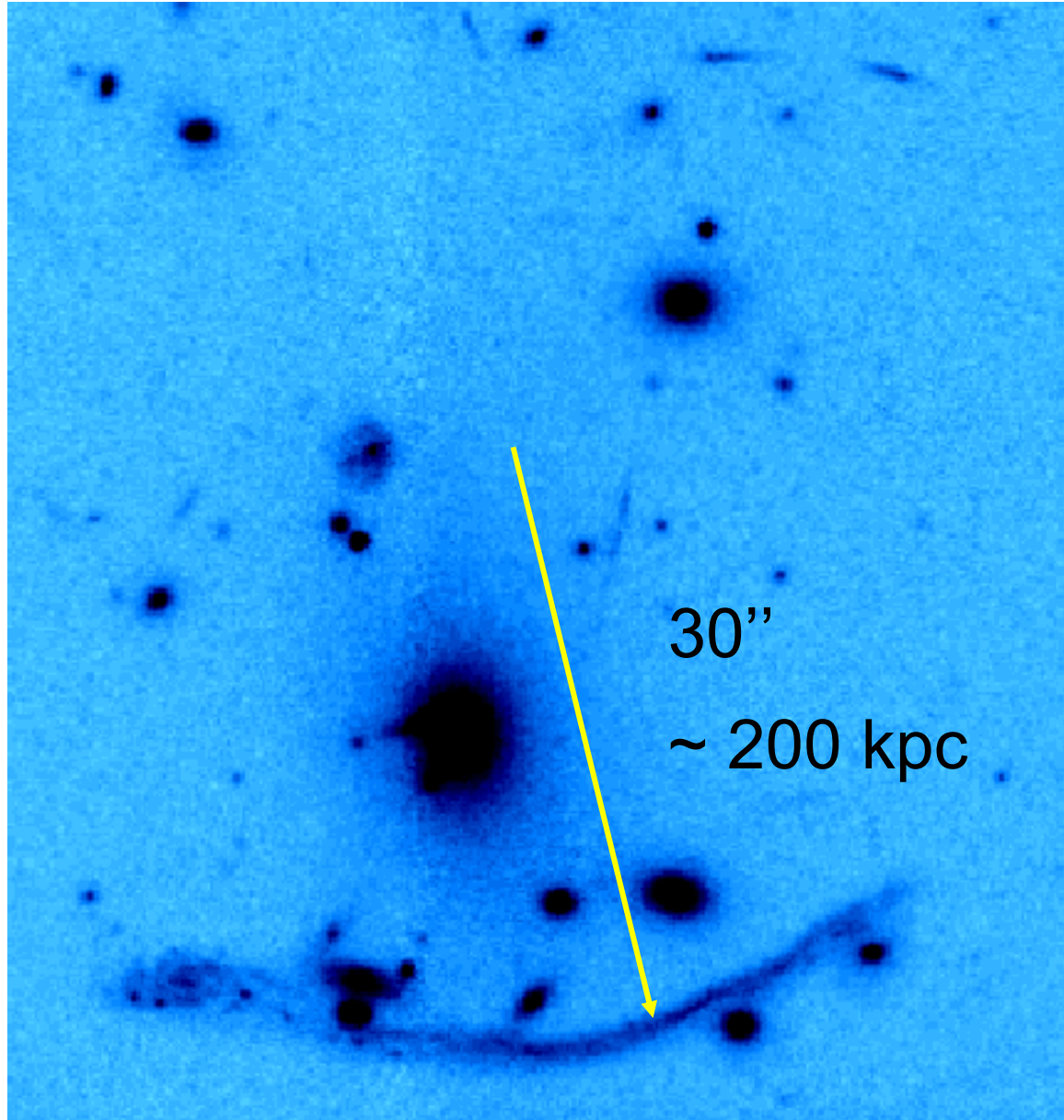
5'



First giant arc discovered in Abell 370

Soucail et al
1987, 1988

$Z_{\text{cluster}} = 0.375$
 $Z_{\text{arc}} = 0.720$



The discovery of « arclets »

Fort et al 1988: arclets

Tyson et al 1990: first weak
Lensing mass reconstruction

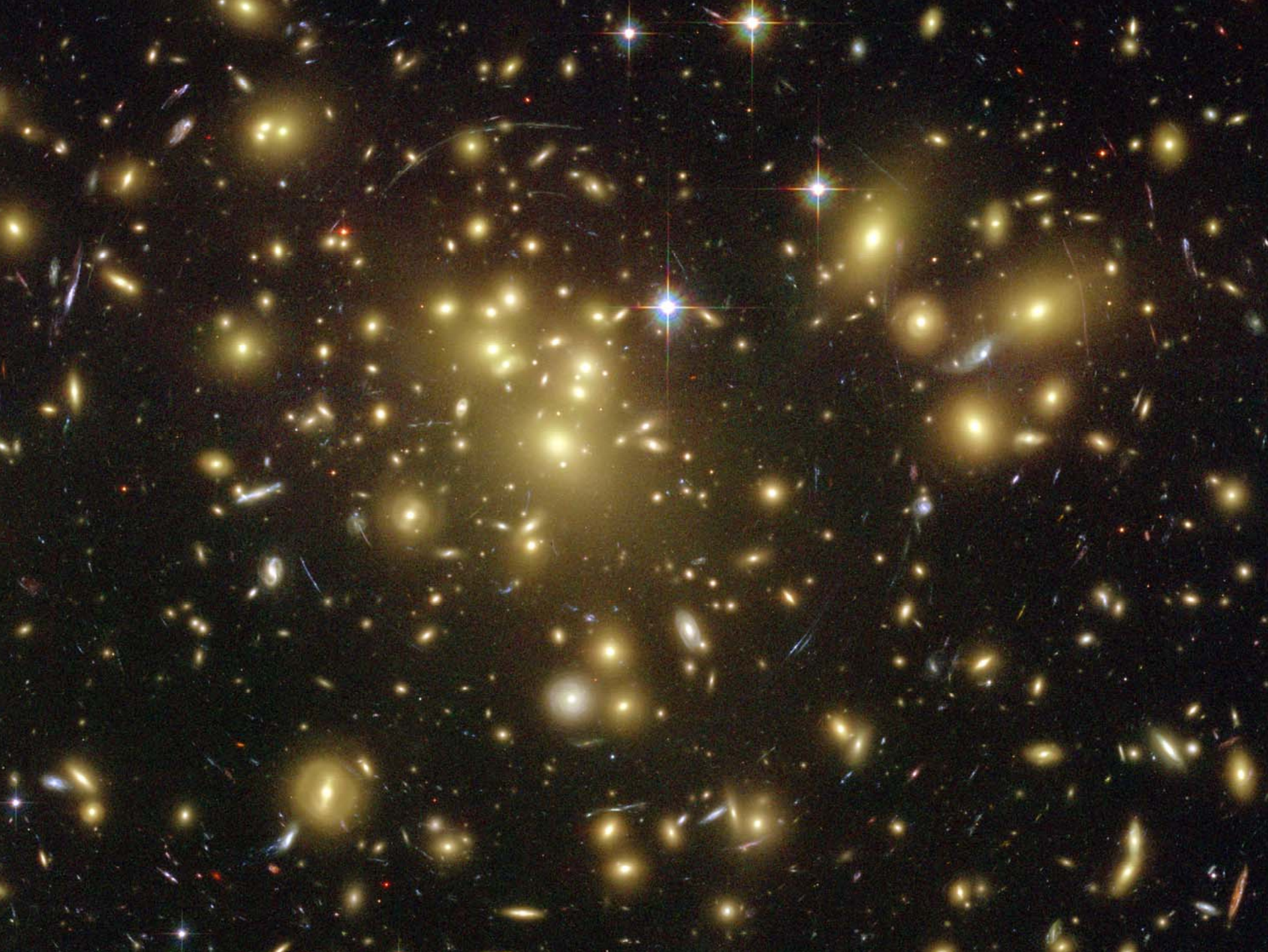


The discovery of « arclets »

Fort et al 1988: arclets

Tyson et al 1990: first weak
Lensing mass reconstruction





Gravitational Lensing

- Fundamental assumptions over the lecture
 - Weak field limit v^2/c^2
 - Stationnary field $t_{\text{dyn}} / t_{\text{cross of photons}}$
 - Thin lens approximation $L_{\text{lens}}/L_{\text{bench}}$
 - Transparent lens
 - Small deflection angle

Lens configuration and deflection angle

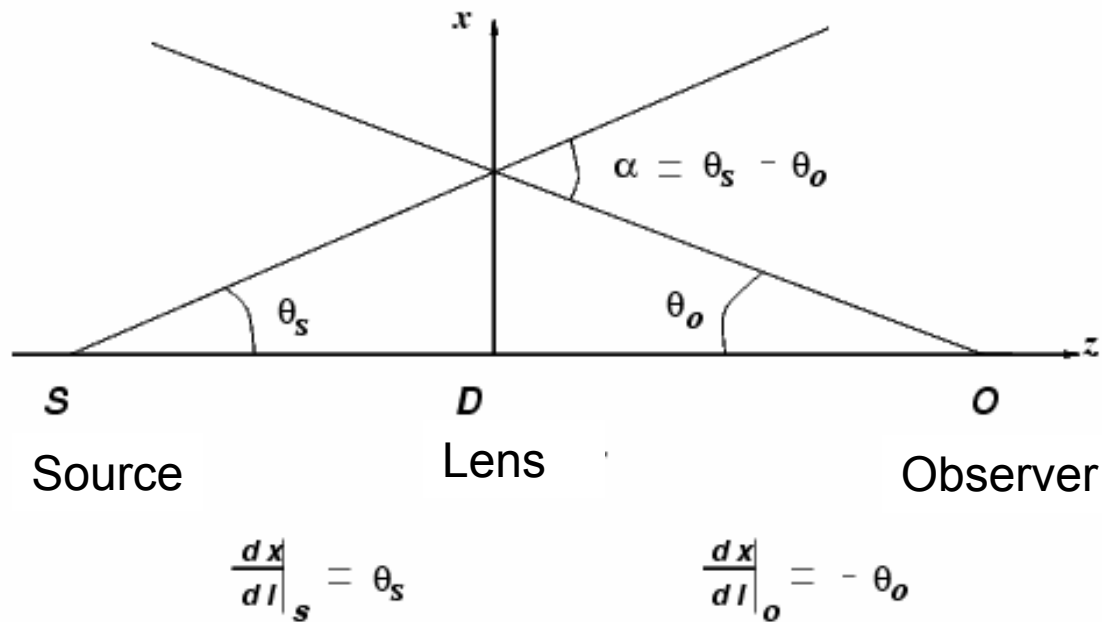


Figure 1: Configuration of the gravitational optical bench.

Deflection angle

In the weak field approximation, the metric writes

$$ds^2 = c^2 \left(1 + \frac{2\Phi}{c^2} \right) dt^2 - \left(1 - \frac{2\Phi}{c^2} \right) dl^2 .$$

For a photon $ds^2 = 0$:

$$dt = \frac{1}{c} \left(\frac{1 - \frac{2\Phi}{c^2}}{1 + \frac{2\Phi}{c^2}} \right)^{1/2} dl \approx \frac{1}{c} \left(1 - \frac{2\Phi}{c^2} \right) dl .$$

Configuration: see Fig.1 .

$$dl^2 = dx^2 + dy^2 + dz^2 .$$

Deflection angle

Fermat principle: photons only follow optical paths with extrema propagation time

→The paths are those stationary with respect to a small variation δt .

Since:
$$ct = \int \left(1 - \frac{2\Phi}{c^2} \right) dl \quad (3)$$

$$ct = \int \left(1 - \frac{2\Phi}{c^2} \right) \left[\left(\frac{dx}{dz} \right)^2 + \left(\frac{dy}{dz} \right)^2 + 1 \right]^{1/2} dz .$$

Equation (3) corresponds to a light beam propagating in a transparent medium with refraction index :

$$n = \left(1 - \frac{2\Phi}{c^2} \right) .$$

Deflection angle

That is, taking into account the relation between n and Φ :

$$\alpha = -\frac{2}{c^2} \int_S^O \nabla_{\perp} \Phi \, dl .$$

(16)

- This is the general expression of a deflection angle for thin lenses in the weak field limit.
- Valid for stars, galaxies, groups and clusters of galaxies and large-scale structures of the universe.

Relation with the Projected Mass Density

The gravitational force produced by the mass inside the lens is

$$\vec{F} = G \int \frac{\vec{x}' - \vec{x}}{|\vec{x}' - \vec{x}|^3} \rho(\vec{x}') d\vec{x}' .$$

Let us define the gravitational potential as $\Phi(\vec{x})$

$$\Phi(\vec{x}) = -G \int \frac{\rho(\vec{x}')}{|\vec{x}' - \vec{x}|} d\vec{x}' ,$$

so that

$$\vec{F} = -\vec{\nabla}\Phi ,$$

Relation with the Projected Mass Density

By substituting in Eq. (16) \rightarrow express the deflection angle as function of the mass density field:

$$\vec{\alpha} = -\frac{2G}{c^2} \int_S^O dl \int d\vec{x}' \nabla_{\perp \vec{x}} \frac{\rho(\vec{x}')}{|\vec{x}' - \vec{x}|}$$

$$\vec{\alpha} = -\frac{2G}{c^2} \int \rho(\vec{x}') d\vec{x}' \int_S^O \frac{(\vec{x}' - \vec{x})_{\perp}}{|\vec{x}' - \vec{x}|^3} dl$$

Relation with the Projected Mass Density

In the *thin lens approximation*, we have

$$\int \rho(\vec{x}') d\vec{x}' = \int \rho(\vec{\xi}', z) d\vec{\xi}' dz = \Sigma(\vec{\xi}')$$

The relation between the deflection angle and the projected mass density is therefore

$$\alpha(\xi) = \frac{4G}{c^2} \int \frac{(\xi - \xi') \Sigma(\xi')}{|\xi - \xi'|^2} d\xi'$$

where

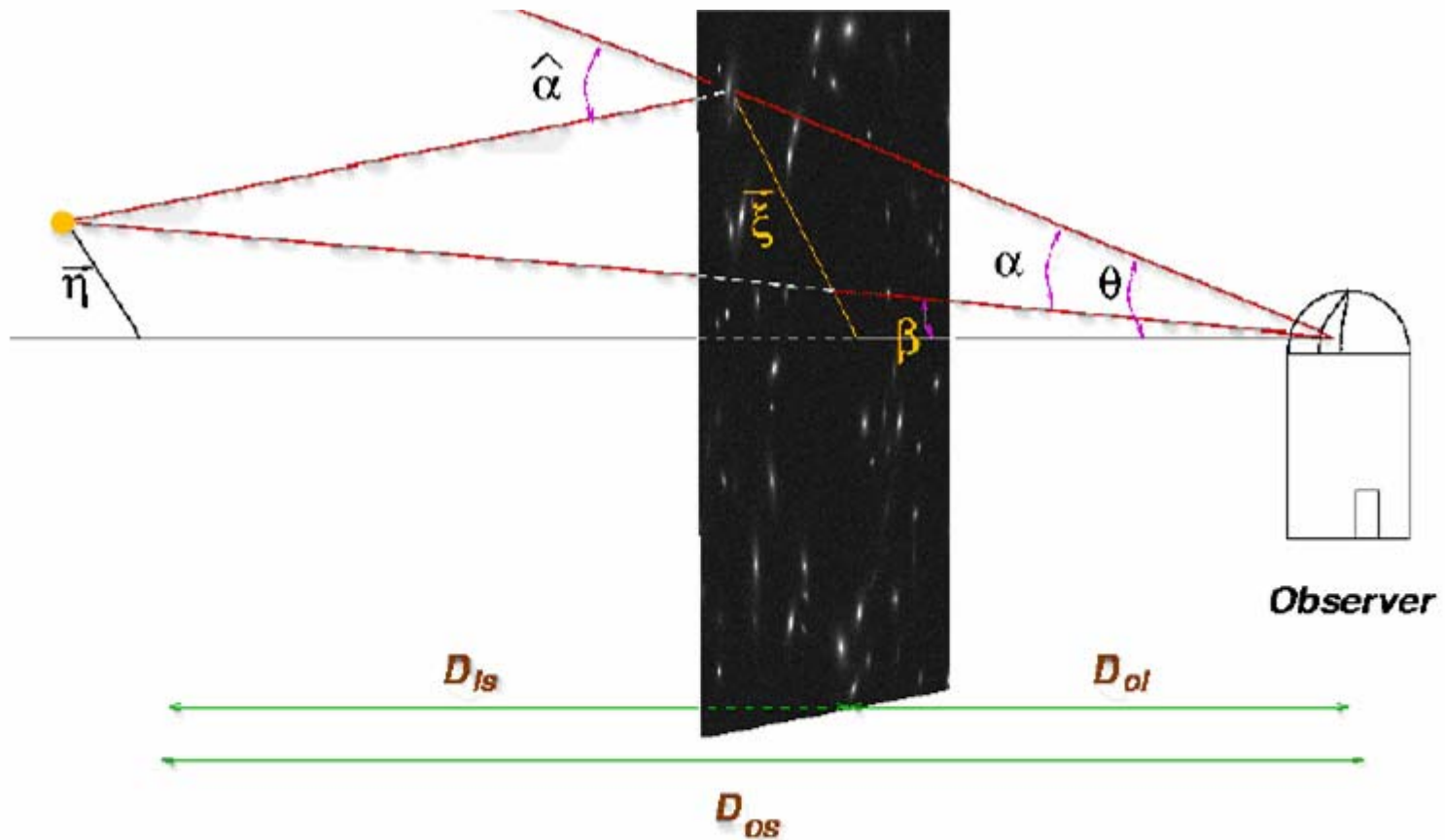
- $\Sigma(\xi)$ is the projected mass density,
- ξ is a 2-dimensional vector in the lens plane and
- the integration is done over the lens plane.

Relation with the Projected Mass Density

For a point mass of mass M : $\Sigma(\xi) = M\delta(\xi)$, then

$$\alpha(\xi) = \frac{4GM}{c^2} \frac{\xi}{|\xi'|^2}$$

Useful quantities and terminology



- Lens equation

$$\vec{\eta} = \frac{D_{os}}{D_{ol}} \vec{\xi} - D_{ls} \hat{\alpha} \left(\vec{\xi} \right)$$

Useful quantities and terminology

- Lens equation

$$\vec{\eta} = \frac{D_{os}}{D_{ol}} \vec{\xi} - D_{ls} \hat{\alpha} \left(\vec{\xi} \right)$$

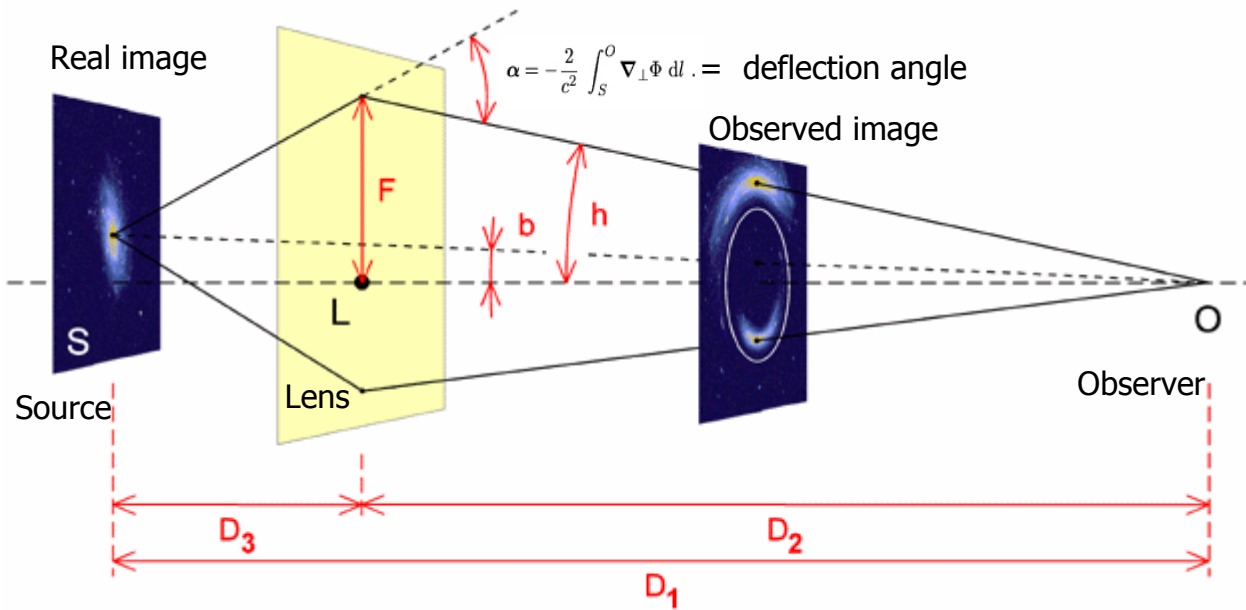
Setting $\vec{\eta} = D_{os} \vec{\beta}$ and $\vec{\xi} = D_{ol} \vec{\theta}$, one can write the lens equation in a simple way, using the scaled deflection angle:

$$\vec{\beta} = \vec{\theta} - \vec{\alpha} \left(\vec{\theta} \right)$$

- Spherically symmetric lens

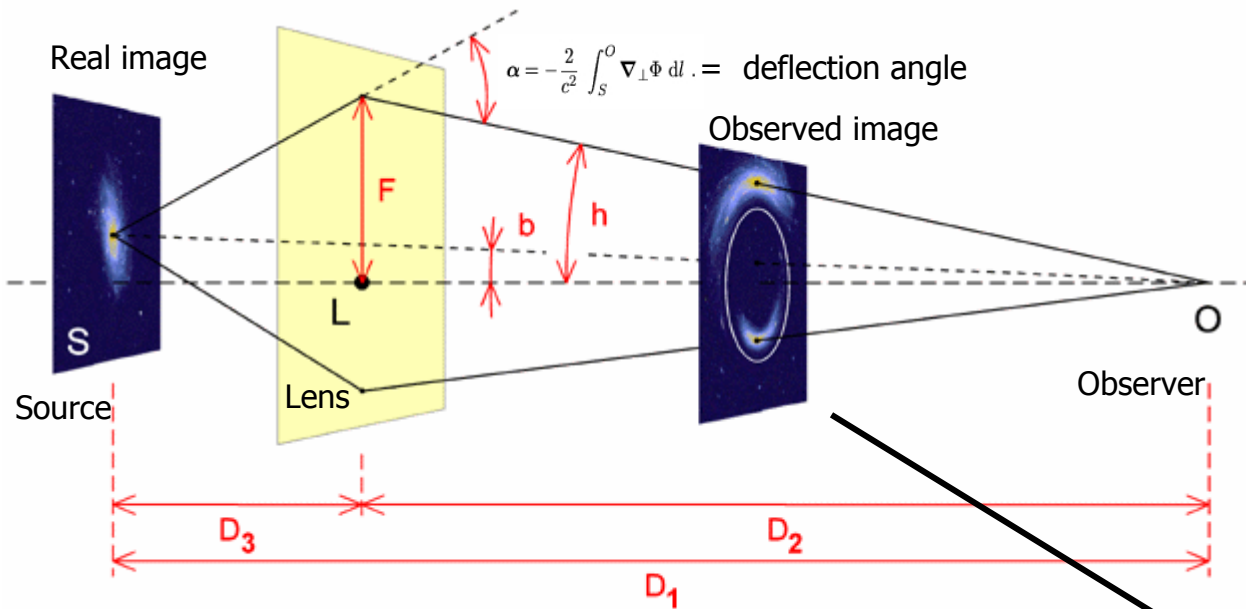
$$\beta = \theta - \frac{D_{ls}}{D_{os} D_{ol}} \frac{4GM(\theta)}{c^2 \theta}$$

Perfect lens configuration



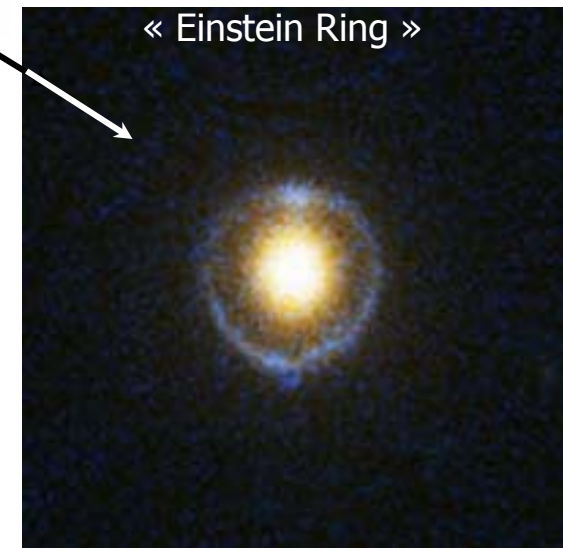
D_1, D_2, D_3 are cosmological distances: depend on the matter-energy content of the Universe

Perfect lens configuration



D_1, D_2, D_3 are cosmological distances: depend on the matter-energy content of the Universe

Source-Lens-Observer perfectly aligned



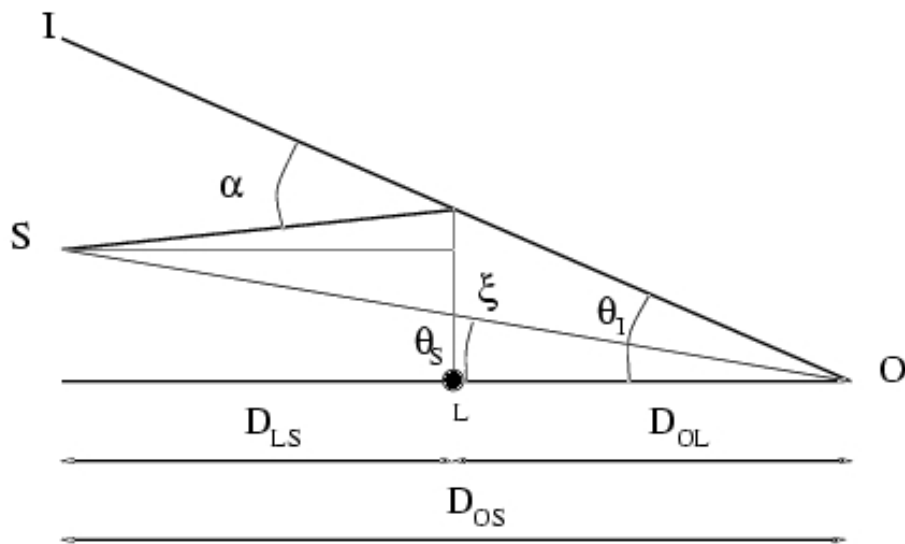
Einstein Rings: perfect alignment

$$\theta_E = \left(\frac{D_{ls}}{D_{os}D_{ol}} \frac{4GM(\theta_E)}{c^2} \right)^{1/2}$$

Typical values:

- For a lens of 1 solar mass located at 1 AU and a source a 1 kpc
 $\theta_E = 0.003$ arc-second
- For a lens of 10^{11} solar masses located at 100kpc and a source at 300 kpc
 $\theta_E = 1$ arc-second
- For a lens of 10^{15} solar masses located at 1Gpc and a source at 3 Gpc
 $\theta_E = 30$ arc-second (sensitive to cosmological parameters)

Image formation, image multiplicity and image shape



Example : a point mass:

Lens Equation

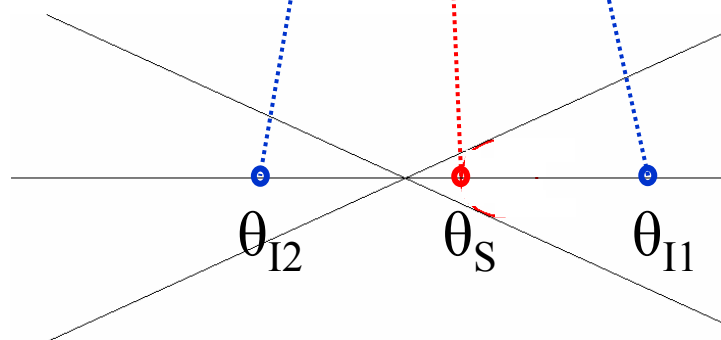
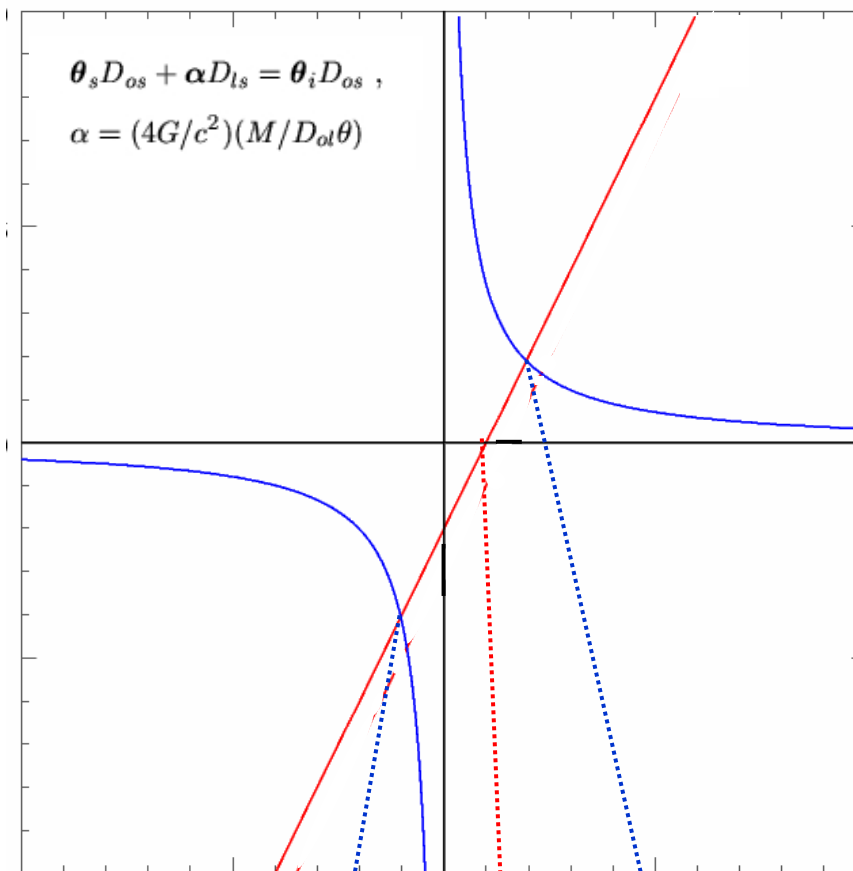
$$\theta_s D_{OS} + \alpha D_{LS} = \theta_l D_{OS} ,$$

Deflection angle

$$\alpha = (4G/c^2)(M/D_{ol}\theta)$$

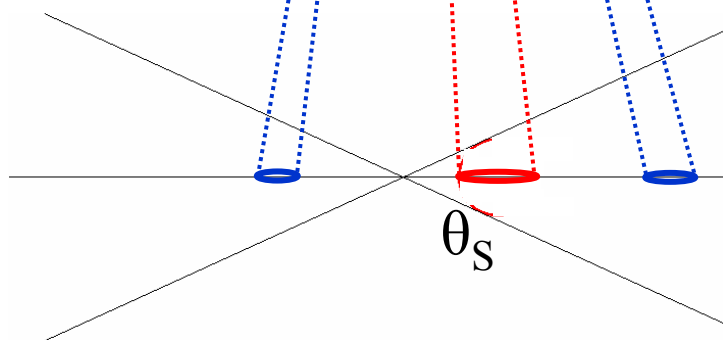
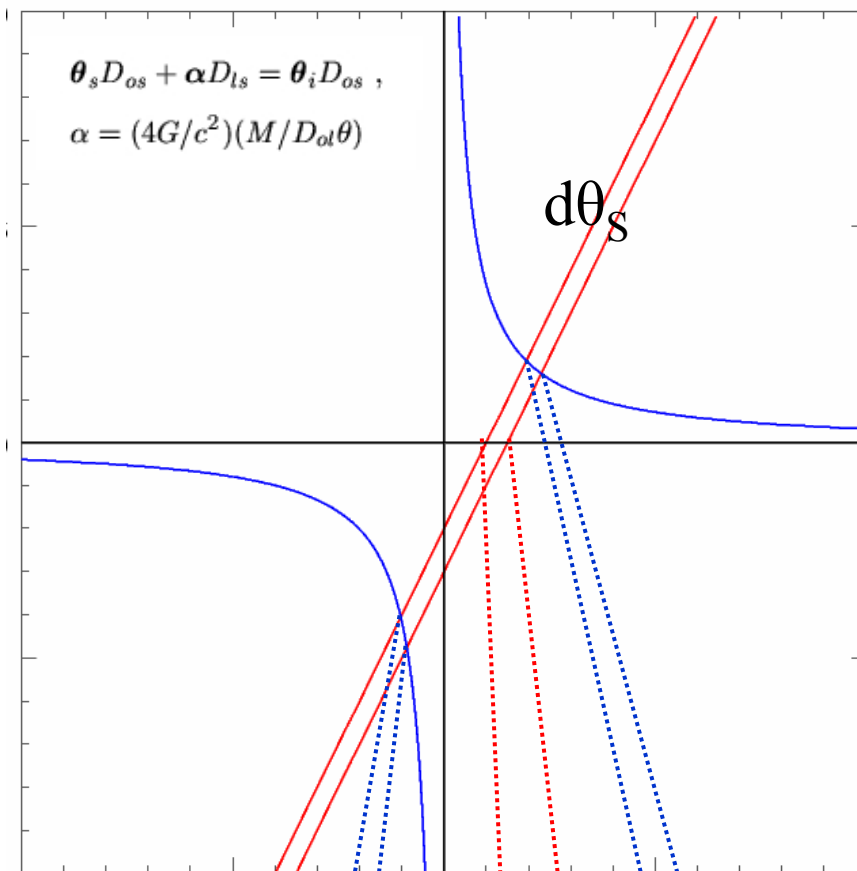
Lens: point mass

Source: point source



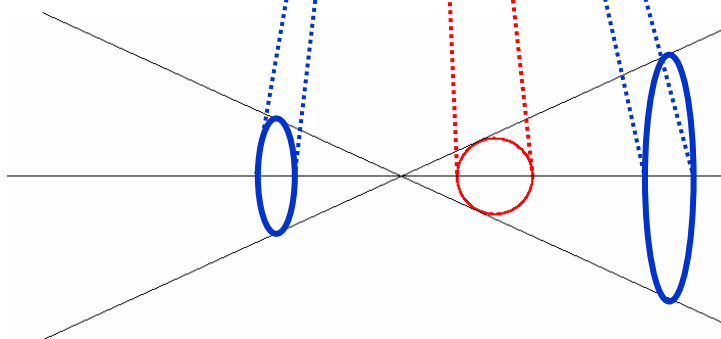
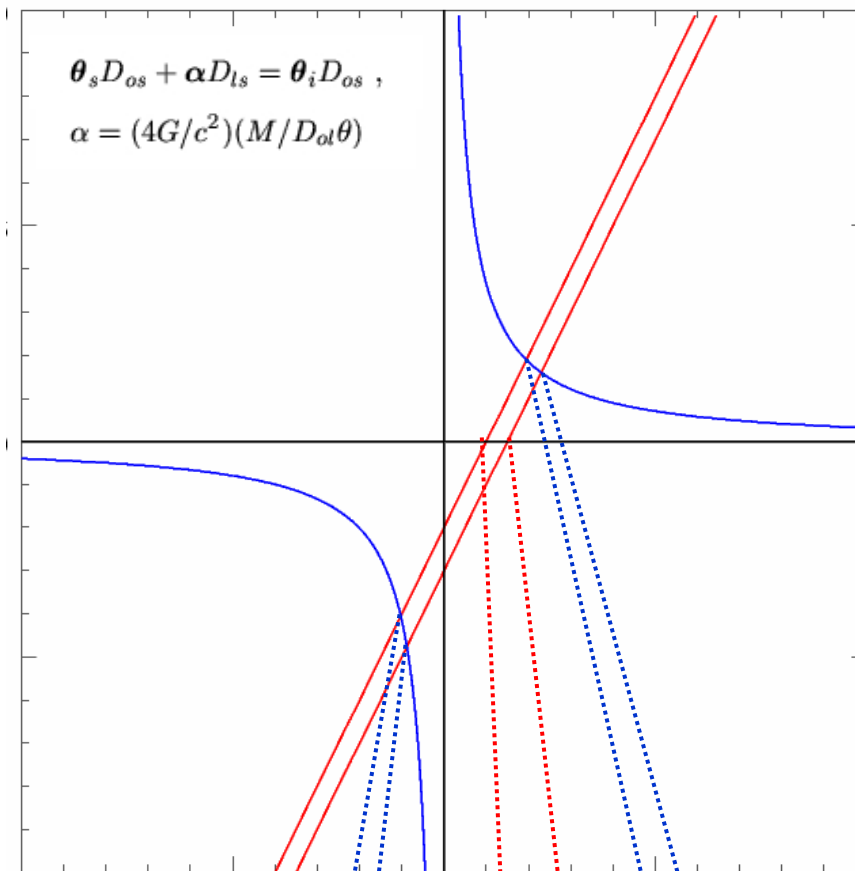
Lens : point
mass

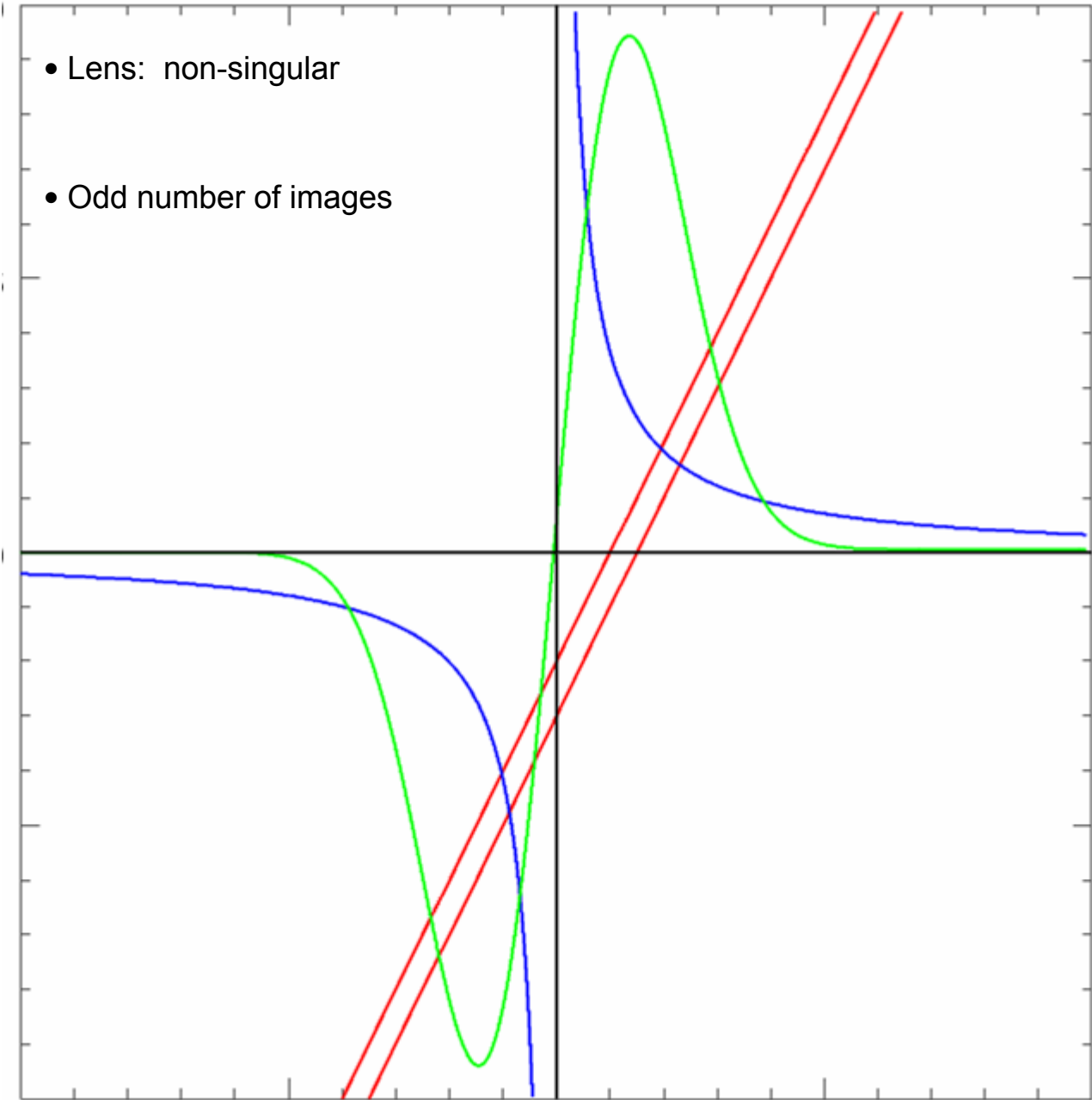
Source: line
(1-D
extended
radially)



Lens: point mass

Source: ellipse (2-D extended)





Convergence and critical density:

The gravitational convergence is a dimensionless surface mass density:

$$\kappa(\vec{\theta}) = \frac{\Sigma(D_{ol}\vec{\theta})}{\Sigma_{cr}}$$

where Σ_{crit} is the *critical surface mass density*.

$$\Sigma_{cr} = \frac{c^2}{4\pi G} \frac{D_{os}}{D_{ol}D_{ls}}$$

that defined a "strength" of the lens. Strong lensing cases have $\Sigma > \Sigma_{cr}$

Convergence and critical density

Example: lensing-cluster

- Typical value: cluster of galaxies of 10^{15} solar masses at 1Gpc and sources at 2 Gpc :

$$\Sigma_{\text{crit}} = 0.5 \text{ g/cm}^2$$

Comparison: typical mass density of a 1Mpc diameter cluster, based on its galaxy light distribution:

$$\Sigma_{\text{''light''}} = 0.02 \text{ g/cm}^2$$

Relations between deflection angle, effective potential and convergence

Since $\kappa = \Sigma / \Sigma_{\text{crit}}$, then

$$\vec{\alpha}(\vec{\theta}) = \frac{1}{\pi} \int \kappa(\vec{\theta}') \frac{\vec{\theta} - \vec{\theta}'}{|\vec{\theta} - \vec{\theta}'|^2} d^2\theta'$$

Using $\nabla \ln|\vec{\theta}| = \vec{\theta}/|\vec{\theta}|^2$, we derive

$$\vec{\alpha} = \vec{\nabla} \psi$$

Relations between deflection angle, effective potential and convergence

$$\vec{\alpha} = \vec{\nabla} \psi$$

$$\psi(\vec{\alpha}) = \frac{1}{\pi} \int \kappa(\vec{\alpha}) \ln |\vec{\theta} - \vec{\theta}'| d^2 \theta'$$

Using $\nabla^2 \ln |\vec{\theta}| = 2\pi \delta_D(\vec{\theta})$, where δ_D is the 2-dimension Dirac delta function:

$$\nabla^2 \psi = 2\kappa$$

= 2-dimension Poisson equation

Magnification and distortion

- Jacobian of the lens mapping. Differentiating the lens equation

$$A(\vec{\theta}) = \frac{\partial \vec{\beta}}{\partial \theta} = \left(\delta_{ij} - \frac{\partial^2 \psi(\vec{\theta})}{\partial \theta_i \partial \theta_j} \right) = M^{-1}$$

- Convergence, Shear

$$\begin{cases} \kappa = \frac{1}{2}(\psi_{,11} + \psi_{,22}) \\ \gamma_1(\vec{\theta}) = \frac{1}{2}(\psi_{,11} - \psi_{,22}) = \gamma(\vec{\theta}) \cos[2\varphi(\vec{\theta})] \\ \gamma_2(\vec{\theta}) = \psi_{,12} = \gamma(\vec{\theta}) \sin[2\varphi(\vec{\theta})] \end{cases}$$

Magnification and distortion

- Magnification, Convergence, Shear

$$A = \mathcal{M}^{-1} = \begin{pmatrix} 1 - \kappa - \gamma_1 & -\gamma_2 \\ -\gamma_2 & 1 - \kappa + \gamma_1 \end{pmatrix}$$

$$\mathcal{M}^{-1} = (1 - \kappa) \begin{pmatrix} 1 & 0 \\ 0 & 1 \end{pmatrix} - \gamma \begin{pmatrix} \cos(2\varphi) & \sin(2\varphi) \\ \sin(2\varphi) & -\cos(2\varphi) \end{pmatrix}$$

where $\gamma = \gamma_1 + i\gamma_2 = |\gamma|e^{2i\varphi}$

- Amplification amplitude

$$\mu = (\det A)^{-1} = \frac{1}{\left[(1 - \kappa)^2 - |\gamma|^2 \right]}$$

- Eigenvalues of \mathcal{M}^{-1} :

$$1 - \kappa + \gamma, \quad 1 - \kappa + \gamma$$

Magnification and distortion

- **Image and source** From the magnification matrix,
 - κ expresses an isotropic magnification. It transforms a circle into a larger/smaller circle.
 - γ is an anisotropic magnification. It transforms a circle into an ellipse with minor and major axes :

$$b = (1 - \kappa + \gamma)^{-1} , \quad a = (1 - \kappa - \gamma)^{-1}$$

- **Reduced shear** Let us write the magnification matrix as:

$$A = \mathcal{M}^{-1} = (1 - \kappa) \begin{pmatrix} 1 - g_1 & -g_2 \\ -g_2 & 1 + g_1 \end{pmatrix}$$

From (reduced) shear to ellipticity

where

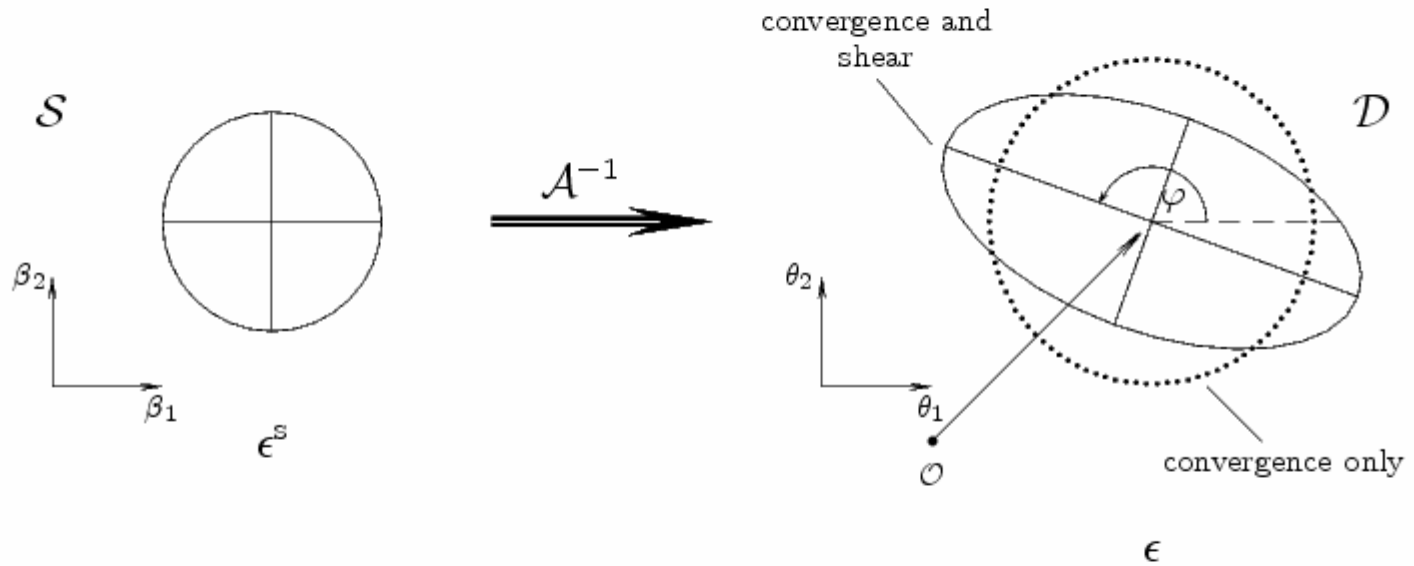
$$g(\vec{\theta}) = \frac{\gamma(\vec{\theta})}{1 - \kappa(\vec{\theta})} = g_1 + \mathbf{i}g_2 = |g|e^{2\mathbf{i}\varphi}$$

is the *reduced shear*. It directly provides the image ellipticity induced by lensing on a circular source:

$$\frac{b}{a} = \frac{1 - |g|}{1 + |g|}$$

as well as the orientation of the major axis, φ .

From shear to ellipticity



Transformation of a circular source into an ellipse by the gravitational convergence and shear terms of the magnification matrix

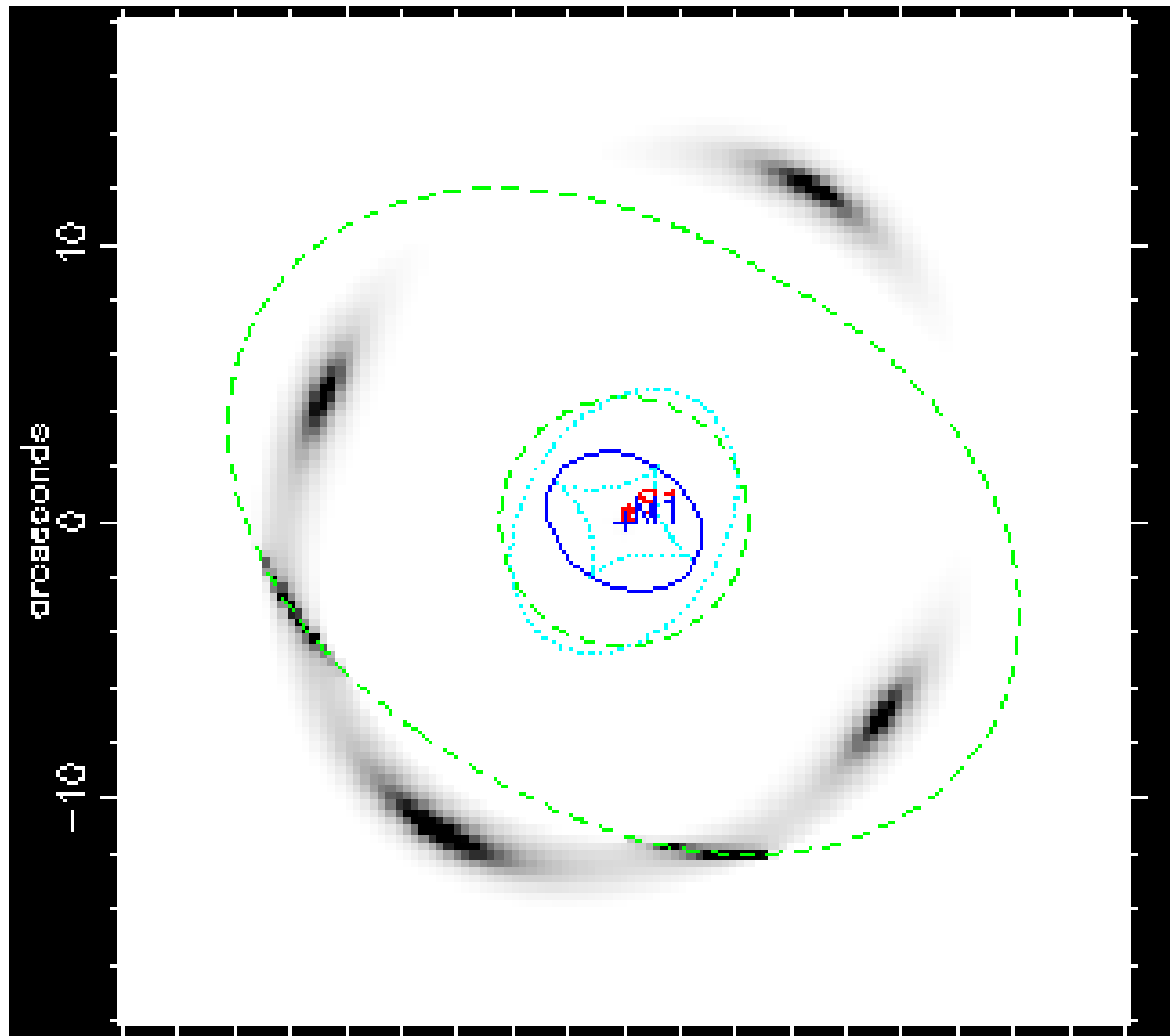
Caustic and Critical Lines

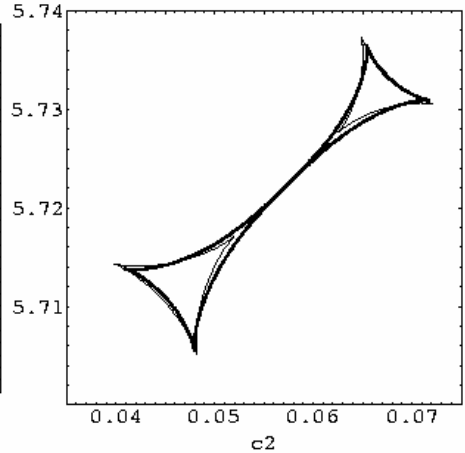
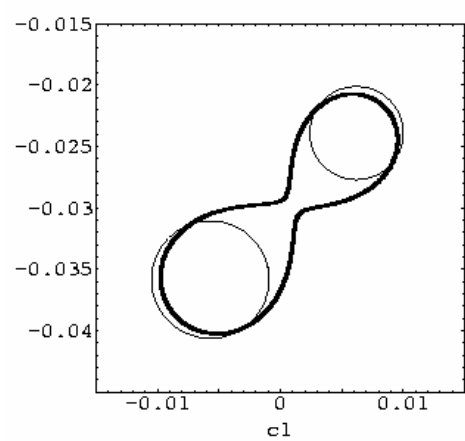
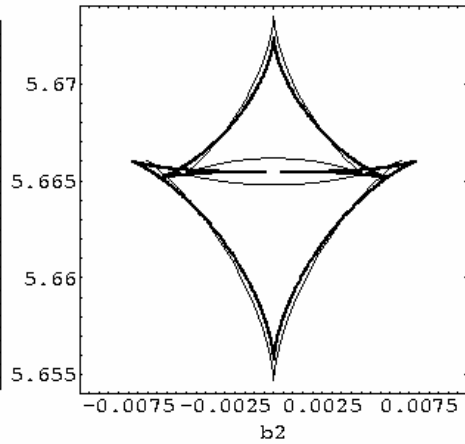
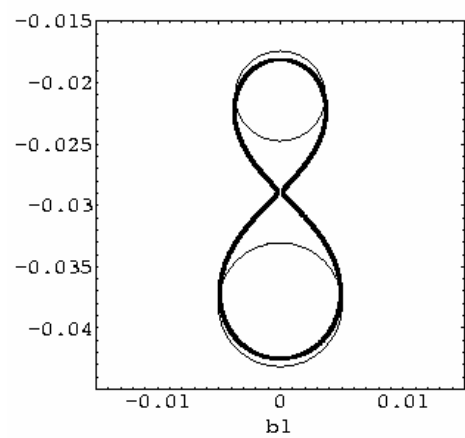
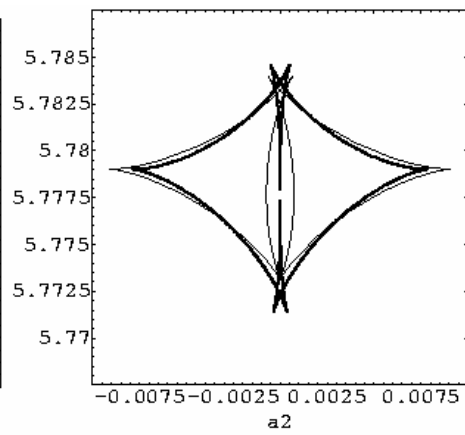
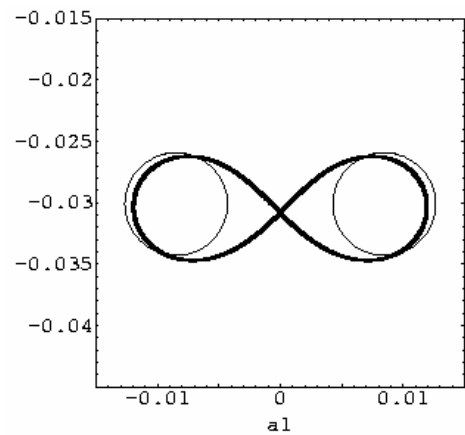
- Amplification amplitude

$$\mu = (\det A)^{-1} = \frac{1}{\left[(1 - \kappa)^2 - |\gamma|^2 \right]}$$

- critical lines corresponds to positions in the lens plane with $\det A = 0$
- the corresponding positions on the source plane are the caustic lines
- the positions of source points with respect to a caustic lines define the number of image multiplication and the source magnification
- when a source crosses a caustic line, its amplification is almost infinity, and image pairs are formed

Caustic and Critical Lines





Caustic and Critical Lines

The image shows a field of galaxies, likely a cluster, with a prominent bright yellowish-white central region. The background is a dark reddish-brown color. Several curved, thin lines are visible, representing caustic and critical lines. These lines are most prominent in the lower-left quadrant, where they form a large, sweeping arc. Other smaller, more linear features are scattered throughout the field, particularly in the upper-right and lower-right areas. The overall appearance is that of a complex gravitational well with various lensing effects.

MS2137-23

MS2137-23

A

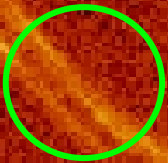
B

A

B

A

A

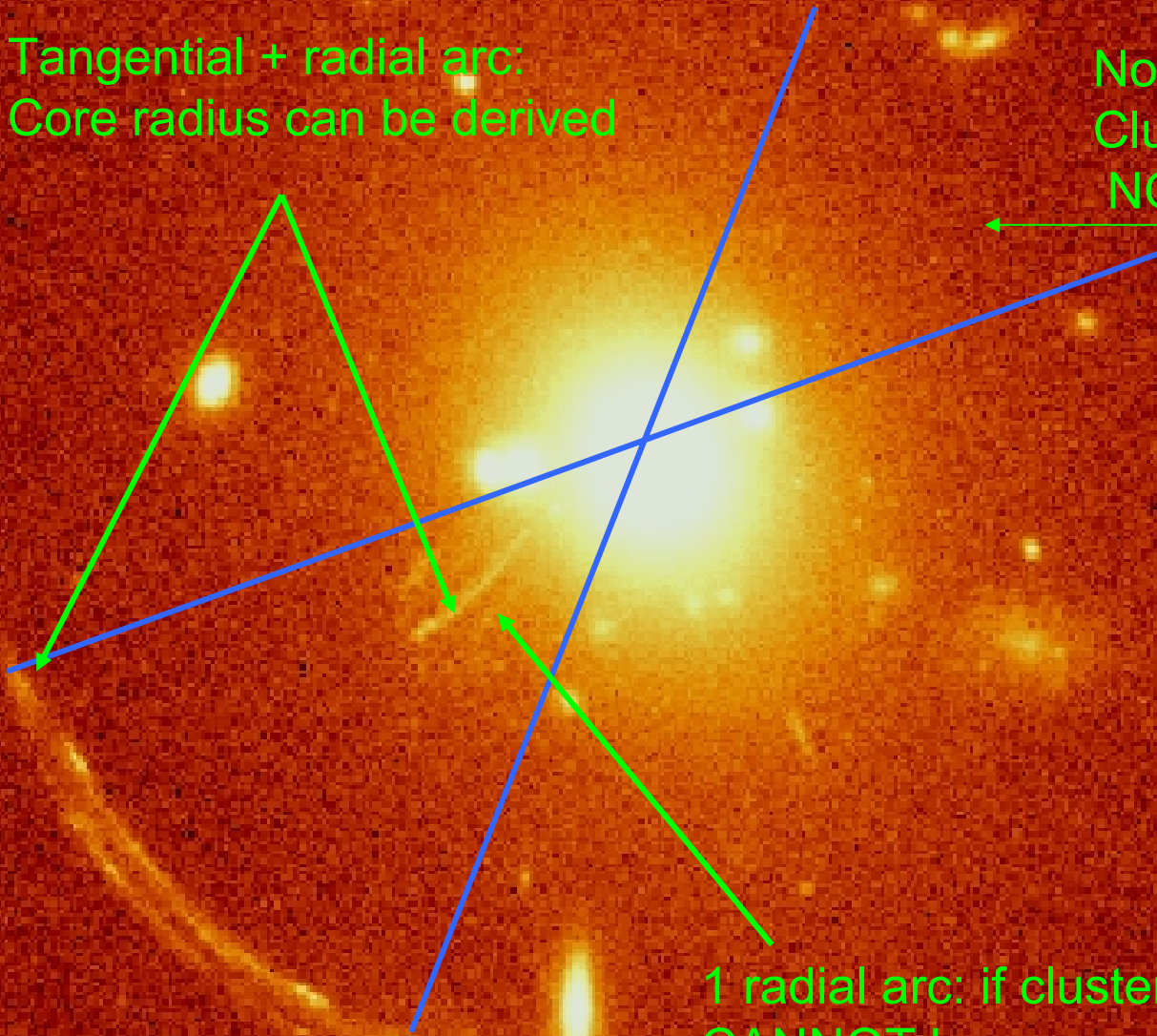


MS2137-23

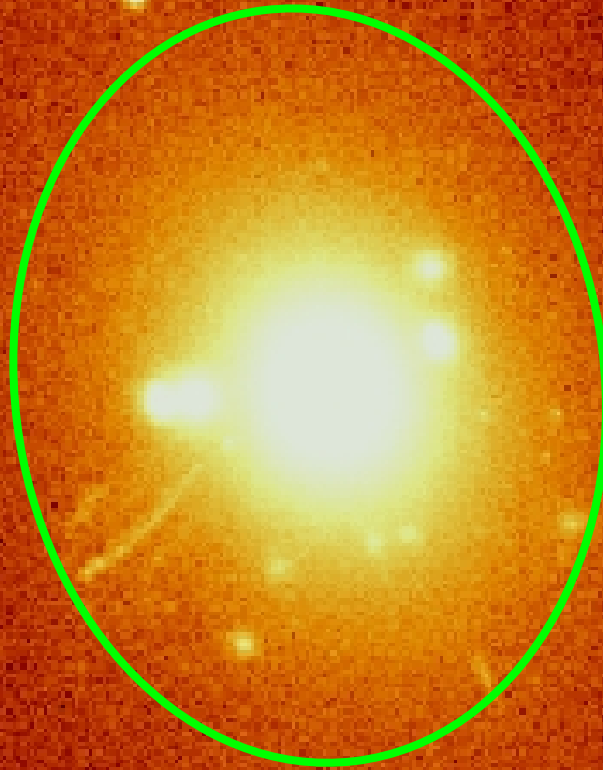
Tangential + radial arc:
Core radius can be derived

No counter arc:
Cluster mass distribution
NOT circular

1 radial arc: if clusters are IS, core radius
CANNOT be zero.

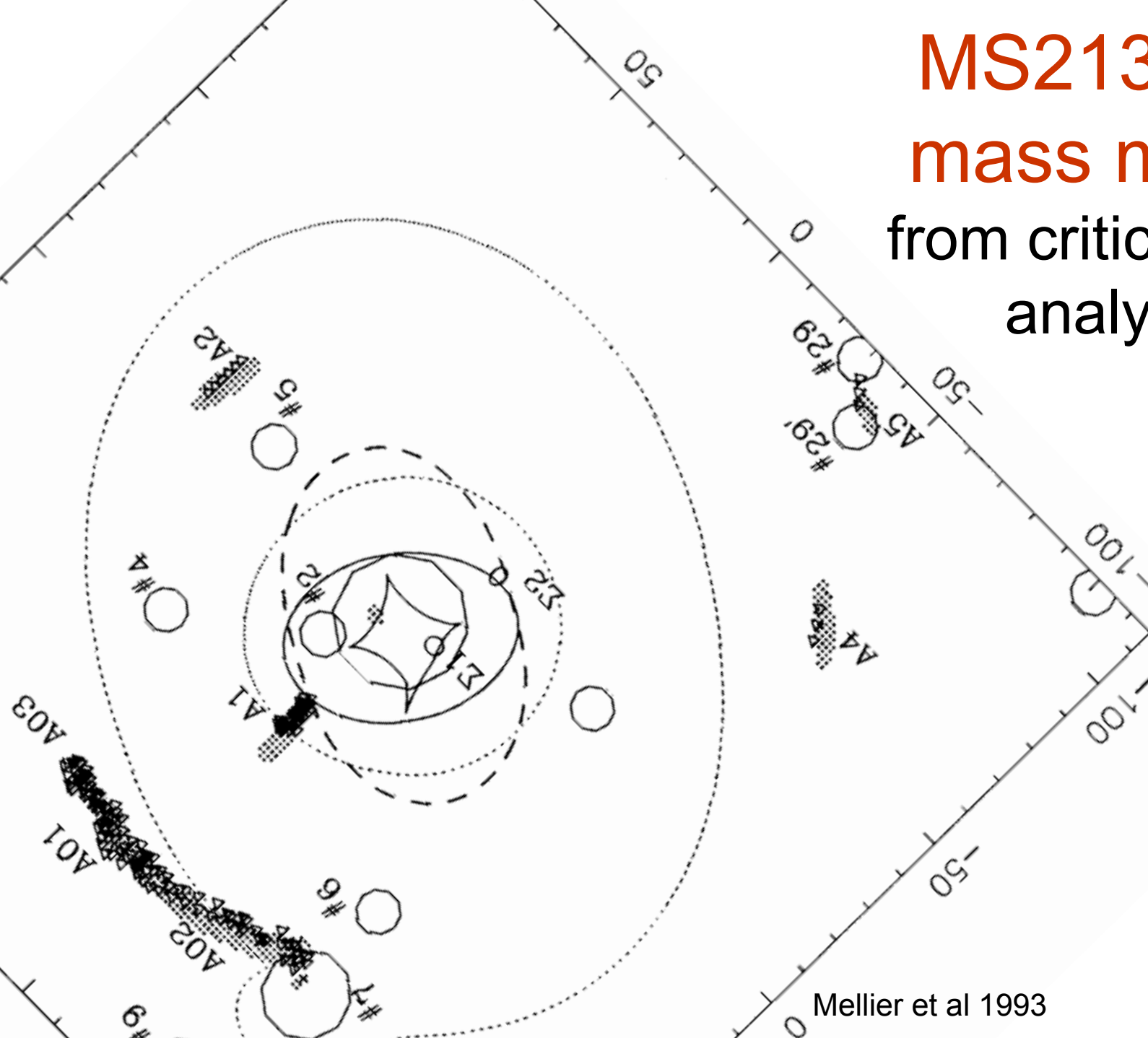


MS2137-23



Ellipticity potential=1/3 ellipticity light
Orientation potential = orientation light

MS2137-23 mass model from critical lines analysis

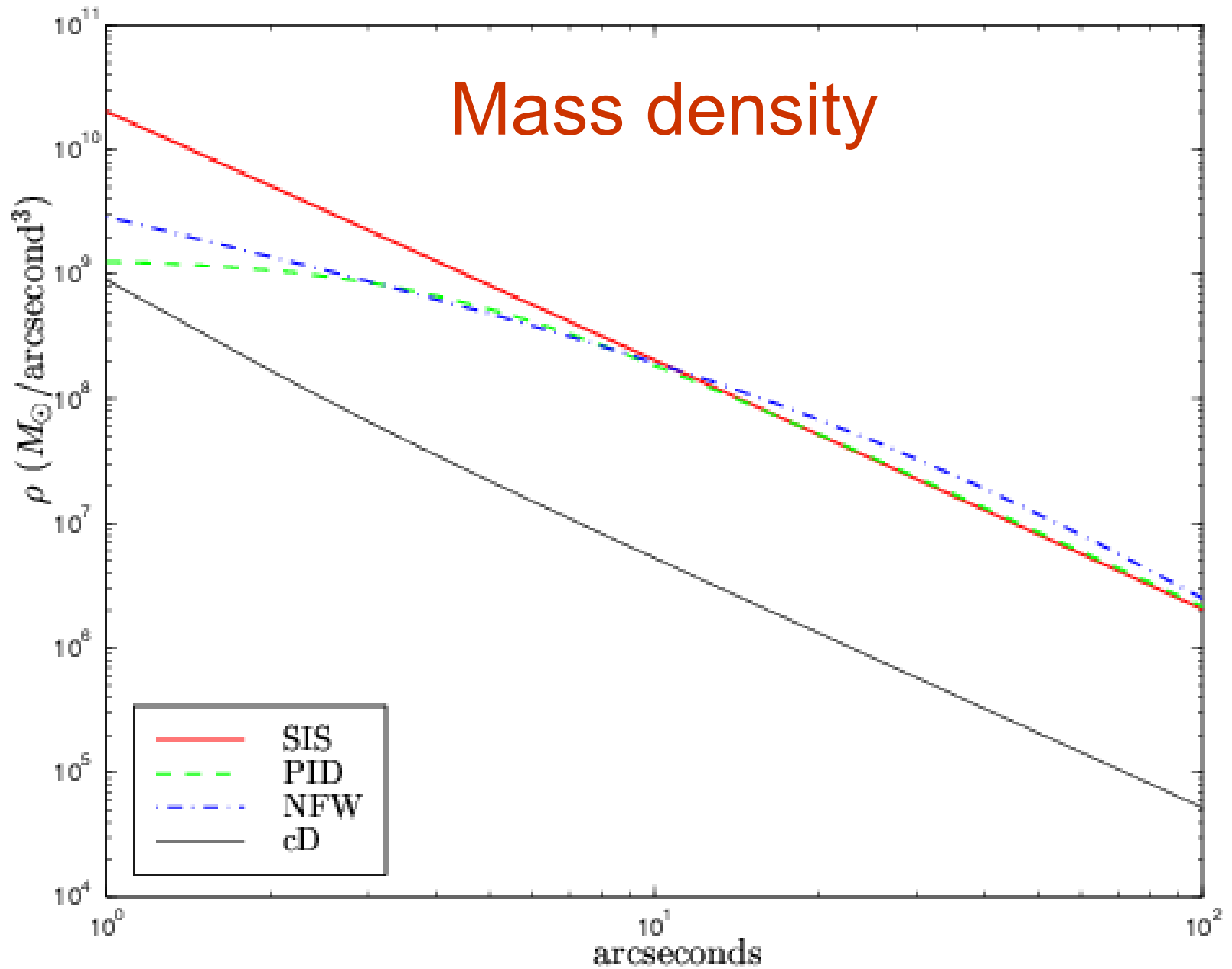


Mellier et al 1993

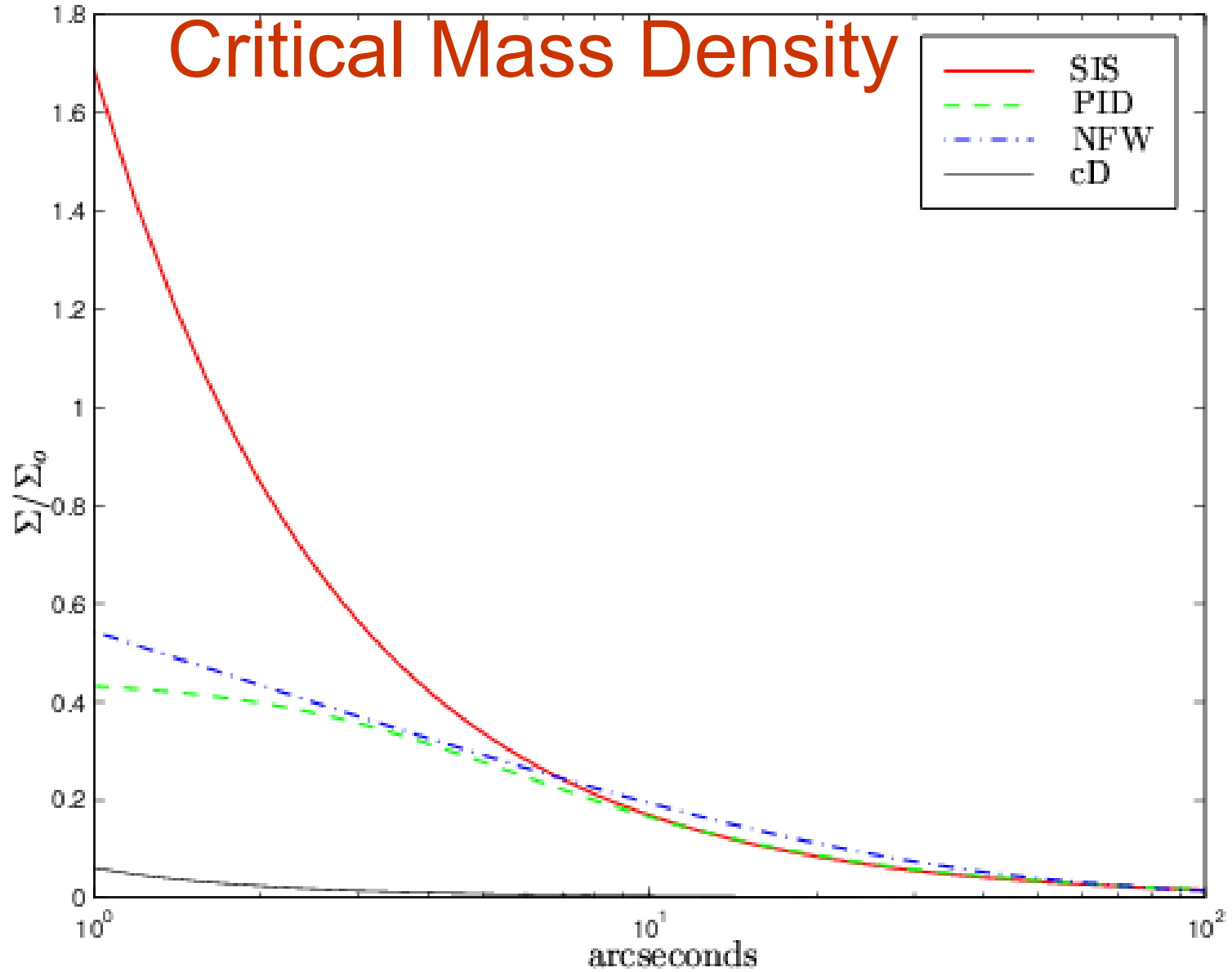
Lensing properties of different mass density profiles

$$\begin{aligned}\bar{\rho}_{SIS}(r) &= \frac{1}{r^2} \\ \bar{\rho}_{PID}(r; r_c) &= \frac{1}{r_c^2} \frac{1}{1 + \left(\frac{r}{r_c}\right)^2} \\ \bar{\rho}_{NFW}(r; r_s) &= \frac{1}{r_s^2} \frac{1}{\frac{r}{r_s} \left(1 + \frac{r}{r_s}\right)^2} \\ \bar{\rho}_{cD}(r; r_c, r_h) &= \frac{1}{r_c^2} \frac{1 + \left(\frac{r}{r_c}\right)^2}{\left(1 + \left(\frac{r}{r_h}\right)^2\right)^2}\end{aligned}$$

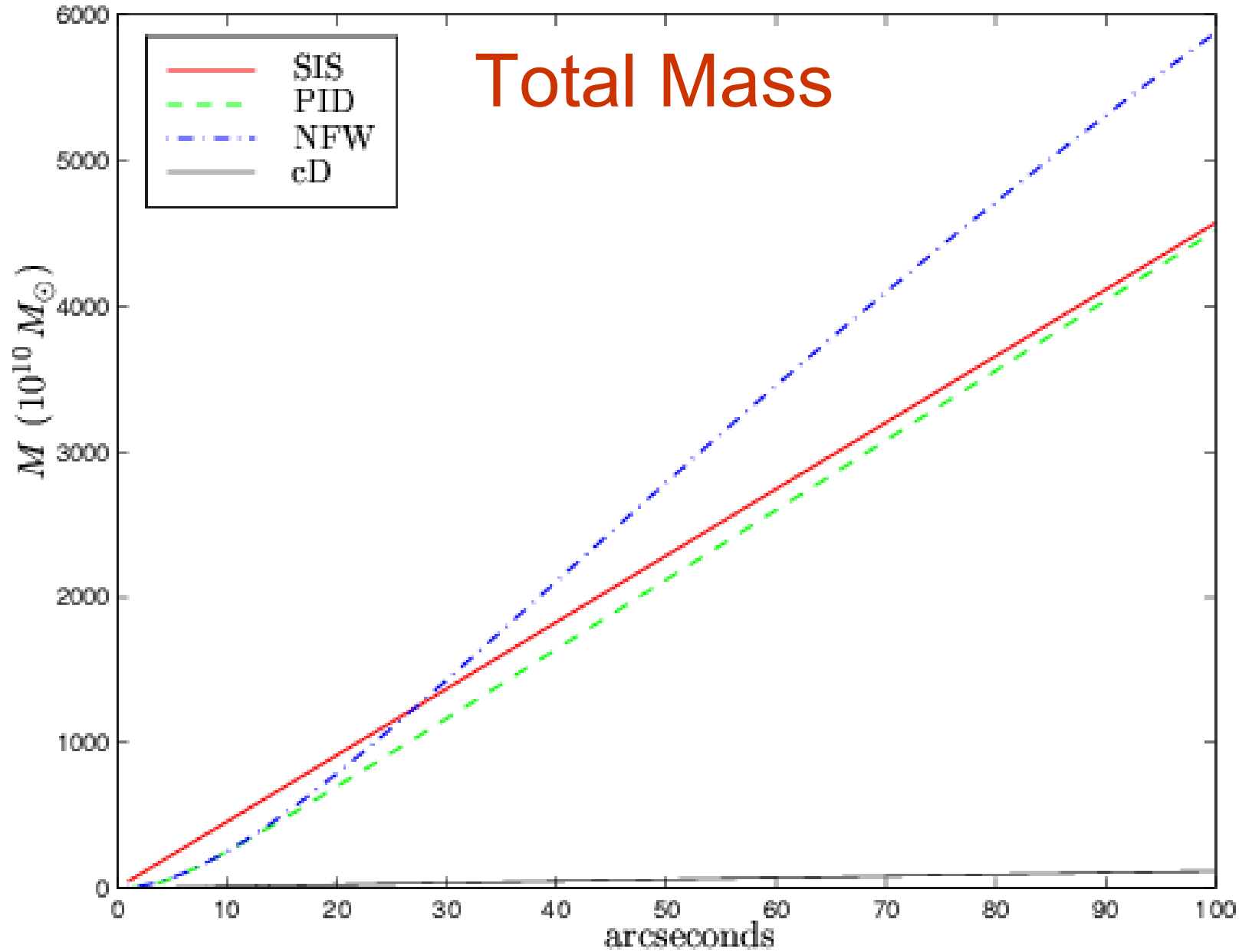
Mass density



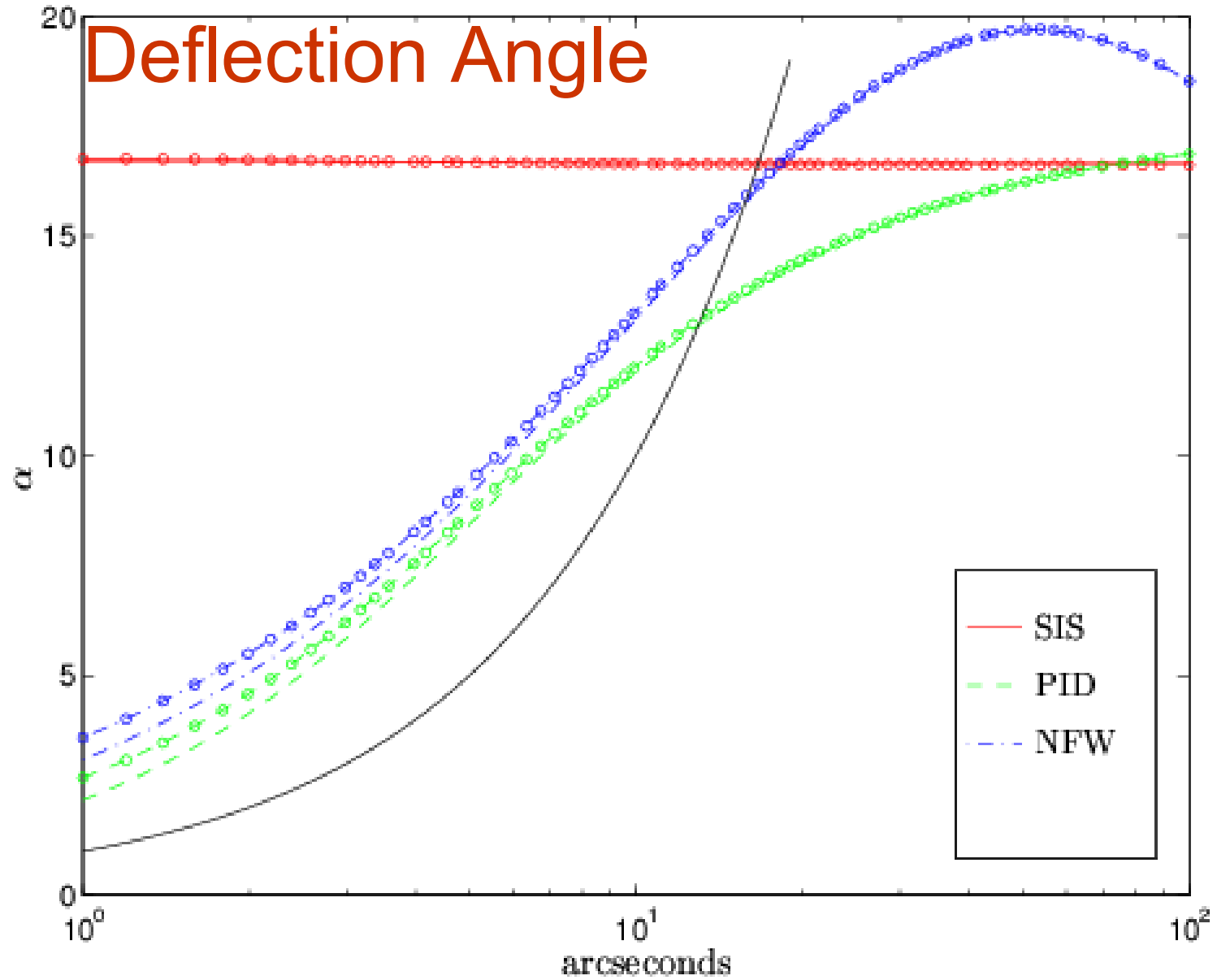
Critical Mass Density



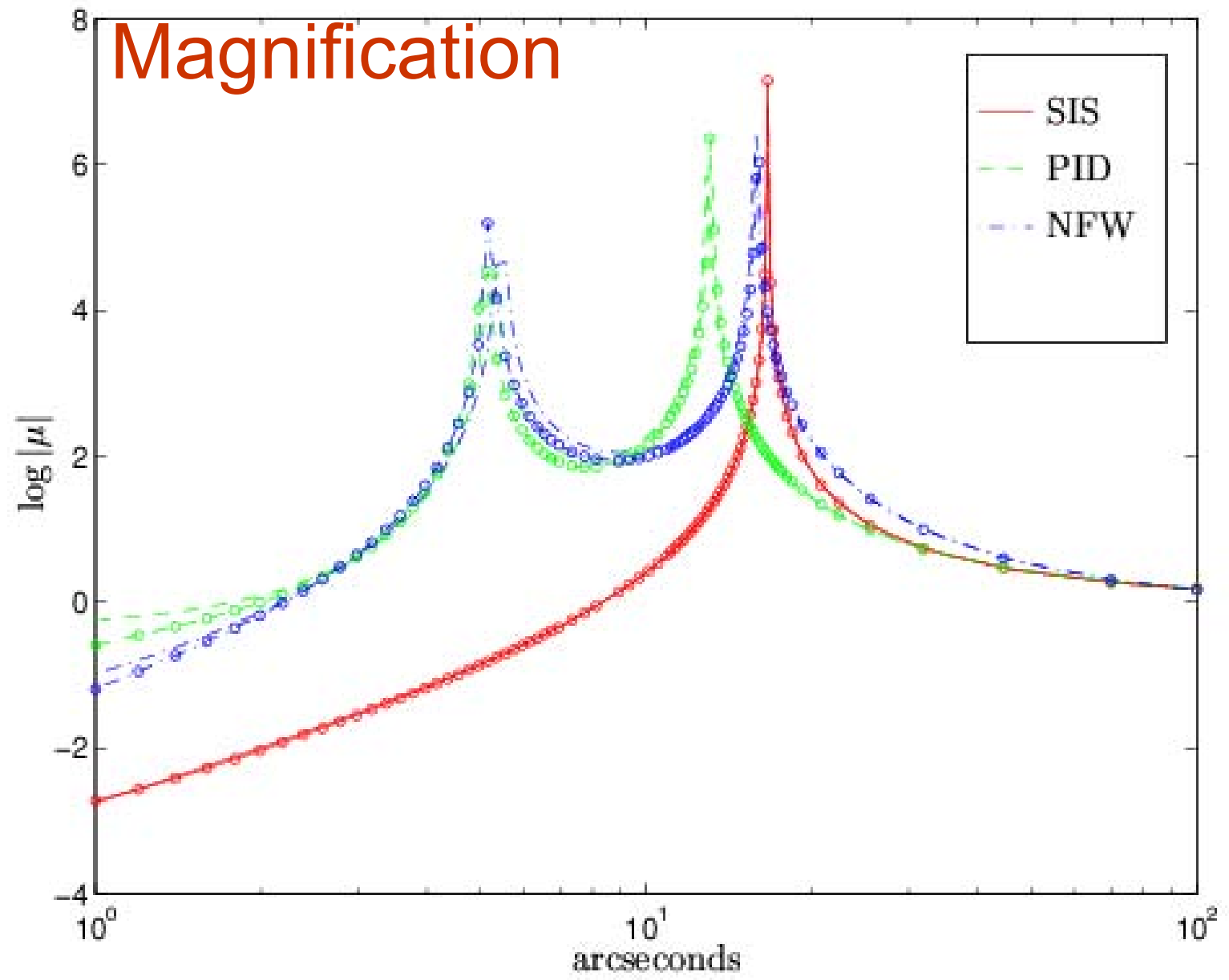
Total Mass



Deflection Angle



Magnification



The locally linearised lens equation

Consequence of the Liouville Theorem:

Etherington theorem:

Gravitational lensing effect conserves the surface brightness of lensed objects

The locally linearised lens equation

Expression of surface brightness conservation for a lensed source:

$$I(\vec{\theta}) = I^s [\vec{\beta}(\vec{\theta})]$$

Assumption of the locally linearised lensing Source vs. Length scale of the Lens: the typical size of the lensed source is smaller than the scale of variation of magnification

The locally linearised lens equation

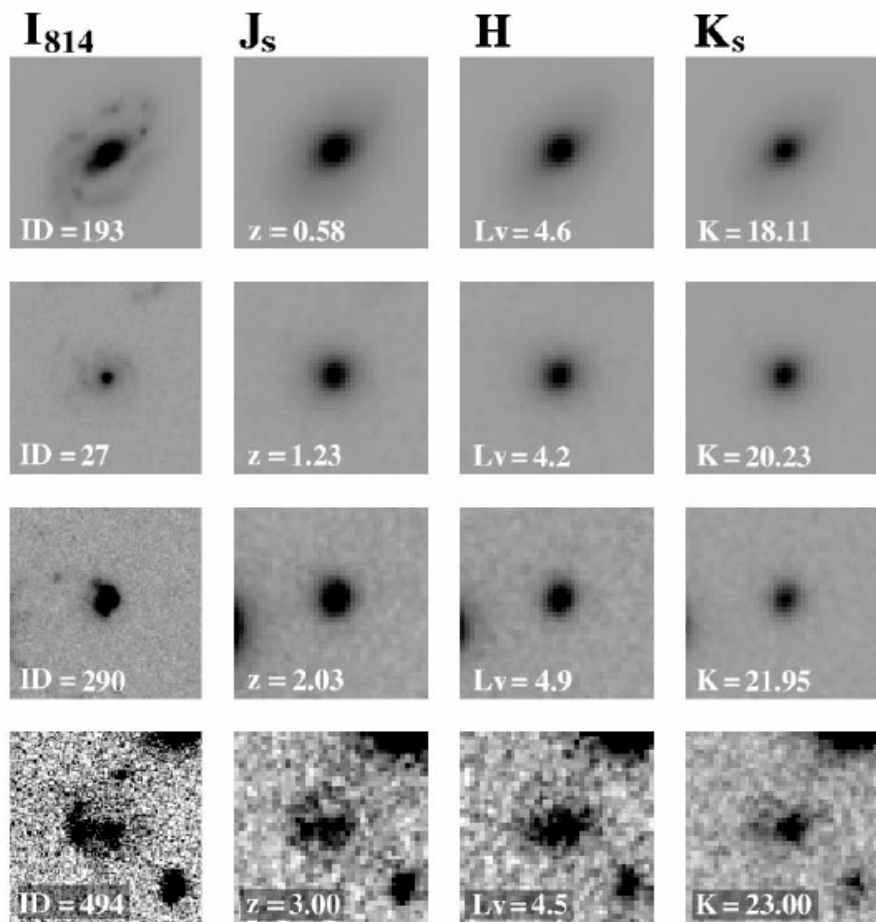
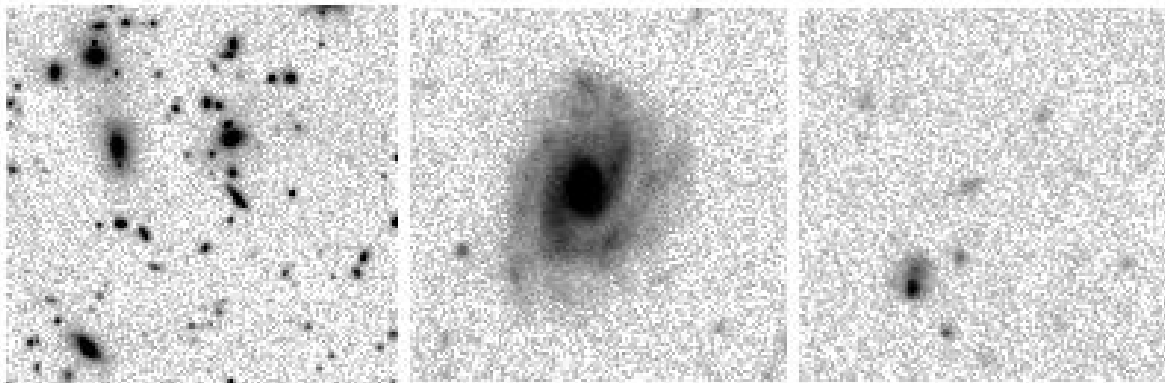
- \implies Linearisation:

$$I(\vec{\theta}) = I^s \left[\vec{\beta}(\vec{\theta}_0) + A(\vec{\theta}_0) (\vec{\theta} - \vec{\theta}_0) \right]$$

- \implies an elliptical image of a source is transformed into an ellipse. A circular source is transformed into an ellipse with major axis $(1 - \kappa - \gamma)^{-1}$ and minor axis $(1 - \kappa + \gamma)^{-1}$.

We can relate lensing effect to shapes of lensed objects

The shape of galaxies



5"

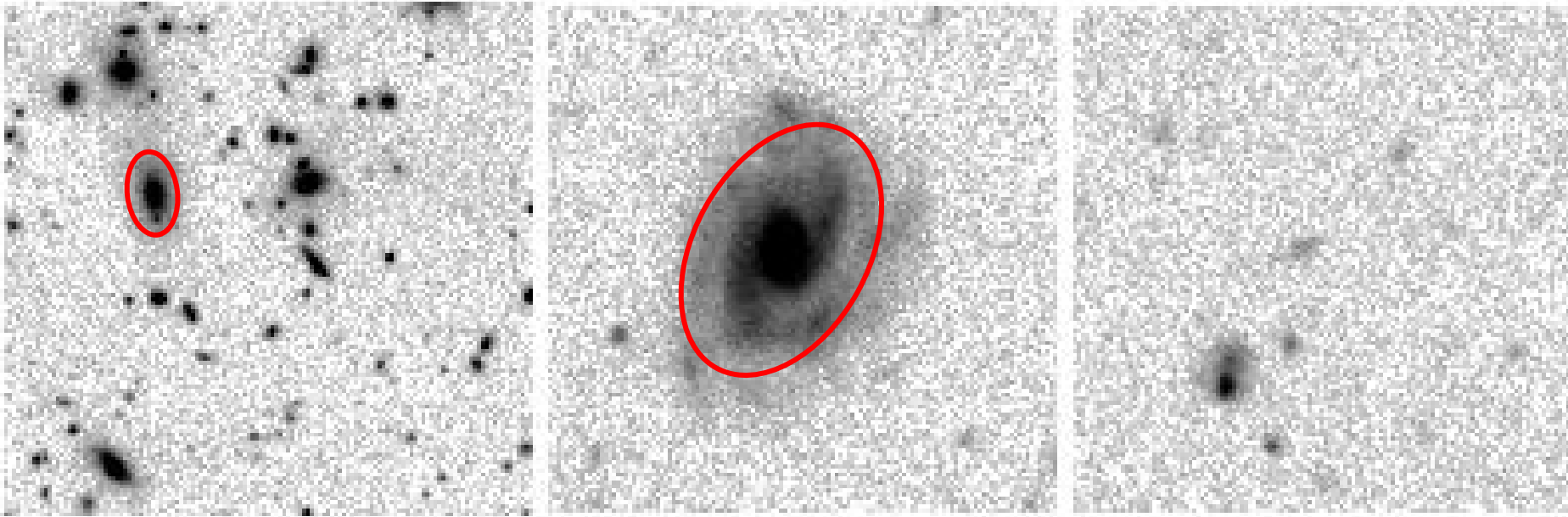
Change with

- PSF
- image sampling
- optical aberrations
- filter
- morphological type
- redshift (shift+evolution)
- signal-to-noise ratio

The shape of galaxies

To first order: all galaxies are ellipses, more or less noisy

Can be characterised by their second moments



The shape is weighted by the galaxy surface brightness

The shape of galaxies

Assume $I(\vec{\theta})$ is the surface brightness in an image. The centroid of the image can be defined as

- Centroid of a galaxy:

$$\vec{\theta}_0 = \frac{\int d^2\theta \vec{\theta} I(\vec{\theta}) q_I [I(\vec{\theta})]}{\int d^2\theta I(\vec{\theta}) q_I [I(\vec{\theta})]}$$

where q_I is a weight function (e.g. the Heaviside function).

The shape of galaxies

- **Second moments** One can then define the second brightness moment tensor

$$Q_{ij} = \frac{\int d^2\theta (\theta_i - \theta_{0,i}) (\theta_j - \theta_{0,j}) I(\vec{\theta}) q_I [I(\vec{\theta})]}{\int d^2\theta I(\vec{\theta}) q_I [I(\vec{\theta})]}$$

So, a circular object has

$$Q_{11} = Q_{22} \text{ and } Q_{12} = 0$$

Likewise, for the source, taking into account the surface

The shape of galaxies

Surface brightness conservation:

$$Q_{ij}^S = \frac{\int d^2\beta (\beta_i - \beta_{0,i}) (\beta_j - \beta_{0,j}) I^S(\vec{\theta}) q_I [I^S(\vec{\beta})]}{\int d^2\beta I^S(\vec{\theta}) q_I [I^S(\vec{\beta})]}$$

using lensing equation and the locally linearised lens equation, we have

$$d^2\beta = \det A d^2\theta \quad \text{and} \quad \vec{\beta} - \vec{\beta}_0 = A (\vec{\theta} - \vec{\theta}_0)$$

we then find the

- Relation between source and image shapes

$$Q^S = A(\vec{\theta}_0) Q A^T(\vec{\theta}_0)$$

Definition(s) of ellipticity

- Current definition(s) of ellipticities:

$$\varepsilon = \frac{1 - \frac{b}{a}}{1 + \frac{b}{a}} e^{2i\phi} \quad ; \quad \chi = \frac{1 - \left(\frac{b}{a}\right)^2}{1 + \left(\frac{b}{a}\right)^2} e^{2i\phi}$$

with

$$a = (1 - \kappa - \gamma)^{-1} \quad \text{and} \quad b = (1 - \kappa + \gamma)^{-1}$$

ε is directly the reduced shear

$$|g| = |\varepsilon| = \frac{|\gamma|}{1 - \kappa}$$

Ellipticity

- Relations with second moments:

$$\varepsilon = \frac{Q_{11} - Q_{22} + 2iQ_{12}}{Q_{11} + Q_{22} + 2(Q_{11}Q_{22} - Q_{12}^2)^{1/2}}$$

$$\chi = \frac{Q_{11} - Q_{22} + 2iQ_{12}}{Q_{11} + Q_{22}}$$

so,

$$\varepsilon = \frac{\chi}{1 + (1 - |\chi|^2)^{1/2}} \quad \text{and} \quad \chi = \frac{2\varepsilon}{1 + |\varepsilon|^2}$$

From ellipticity to shear

$$Q^S = A Q A$$

$$Q^S = [1 - \kappa]^2 \begin{pmatrix} 1 - g_1 & -g_2 \\ -g_2 & 1 + g_1 \end{pmatrix} \times \begin{pmatrix} Q_{11} & Q_{12} \\ Q_{12} & Q_{22} \end{pmatrix} \times \begin{pmatrix} 1 - g_1 & -g_2 \\ -g_2 & 1 + g_1 \end{pmatrix}$$

Hence

$$\frac{Q_{11}^S}{(1 - \kappa)^2} = (1 - g_1)^2 Q_{11} - 2g_2(1 - g_1) Q_{12} + g_2^2 Q_{22}$$

$$\frac{Q_{22}^S}{(1 - \kappa)^2} = g_2^2 Q_{11} - 2g_2(1 + g_1) Q_{12} + (1 + g_1)^2 Q_{22}$$

From ellipticity to shear

$$\frac{Q_{11}^S + Q_{22}^S}{(1 - \kappa)^2} = (Q_{11} + Q_{22}) \times (1 + |g|^2 - 2g_1\chi_1 - 2g_2\chi_2)$$

We can now express the ellipticity of the source as function of the ellipticity of the image and the gravitational shear:

$$\chi^S = \frac{-2g + \chi + g^2\chi^*}{1 + |g|^2 - 2\Re(g\chi^*)}$$

From ellipticity to shear

and since

$$\varepsilon = \frac{\chi}{1 + (1 - |\chi|^2)^{1/2}}$$

we have

$$\left\{ \varepsilon^s = \begin{cases} \frac{\varepsilon^i - g}{1 - g^* \varepsilon^i} & \text{for } |g| < 1 \\ \frac{1 - g(\varepsilon^i)^*}{(\varepsilon^i)^* - g^*} & \text{for } |g| > 1 \end{cases} \right.$$

Two shapes: tangential/radial shape

The weak lensing regime

- From ellipticity to shear

$$\varepsilon^s = \begin{cases} \frac{\varepsilon^i - g}{1 - g^* \varepsilon^i} & \text{for } |g| < 1 \\ \frac{1 - g(\varepsilon)^*}{(\varepsilon)^* - g^*} & \text{for } |g| > 1 \end{cases}$$

- Weak Lensing regime : $\kappa \ll 1, |\gamma| \ll 1, |g|^2 \simeq 0$ Therefore

$$g = \frac{\gamma}{1 - \kappa} \simeq \gamma$$

In that case

$$\chi \simeq \chi^s + 2(g - \chi^s \Re(g\chi^*))$$

The weak lensing regime

In we decompose one component , for example

$$\chi_1 = \chi_1^S + 2g_1 (1 - \chi_i^S \chi_1) - 2g_2 \chi_1^S \chi_2$$

So, we can write the relation as follow:

$$\chi_i = \chi_i^S + 2 (\delta_{ij} - \chi_i^S \chi_j) \gamma_j$$

- Sources orientation is isotropically distributed ←

$$\langle \chi^S \rangle \simeq 0$$

which implies!

$$\langle \chi \rangle \simeq 2\gamma = 2g$$

Therefore, the image ellipticity of galaxies provide an unbiased estimate of the gravitational shear.

Definitions:

tangential and cross shear components

- Cartesian coordinates:

$$\gamma = \gamma_1 + i\gamma_2 = |\gamma|e^{2i\varphi}$$

Tangential and Cross components

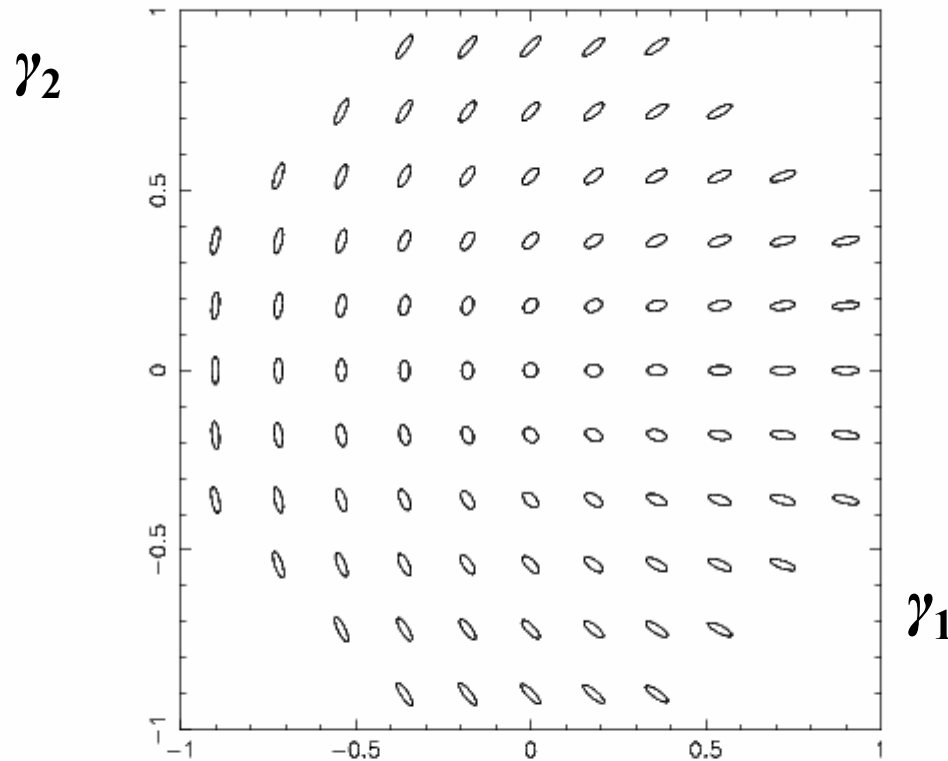


Figure 4: Orientation of the ellipses given by the Cartesian coordinates γ_1 (x-axis) and γ_2 (y-axis), with the polar angle ranging from 0 to 2π .

Definitions:

tangential and cross shear components

- Cartesian coordinates:

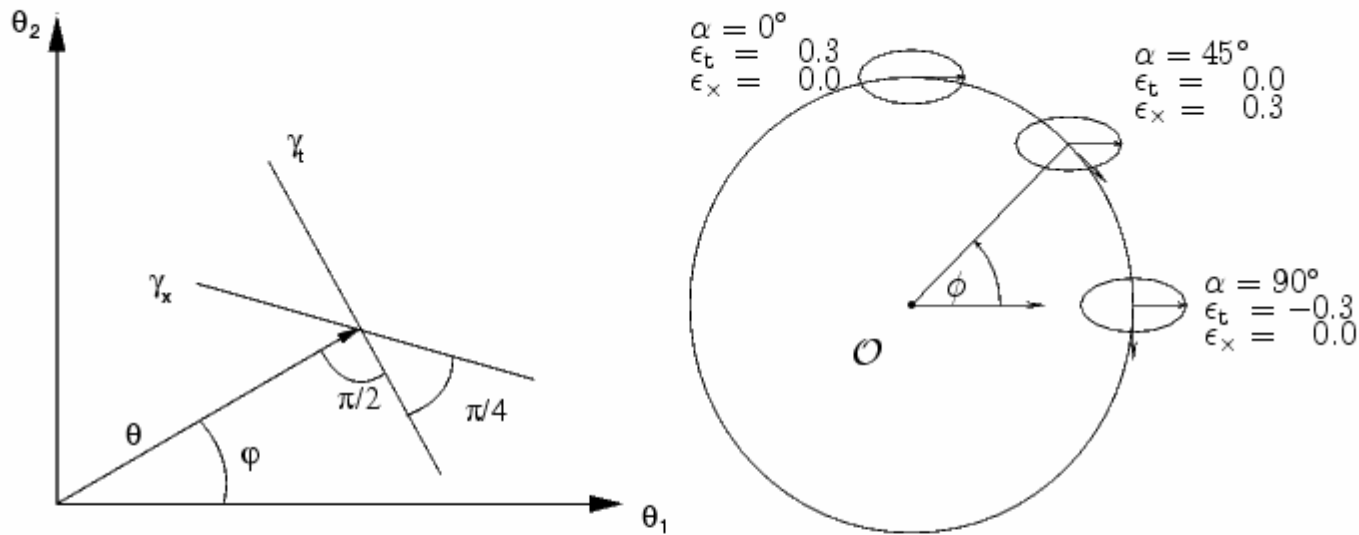
$$\gamma = \gamma_1 + i\gamma_2 = |\gamma|e^{2i\phi}$$

The tangential and cross components of the shear with respect to a direction ϕ is

$$\gamma_t = -\Re [\gamma e^{-2i\phi}] \quad ; \quad \gamma_x = -\text{Im} [\gamma e^{-2i\phi}]$$

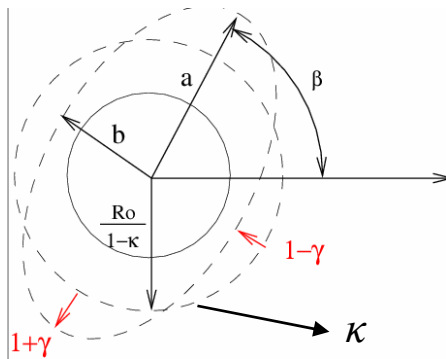
Likewise, one can define the tangential and cross image ellipticity components, ε_t and ε_x .

Tangential and Cross components



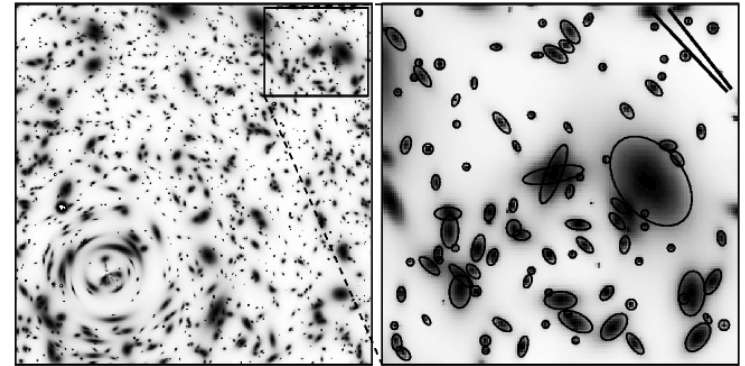
With these definition, for a spherical mass overdensity, the shear will be tangential with $\gamma_t > 0$ and $\gamma_x = 0$.

Summary: from shear to galaxy ellipticity



$$\delta = \frac{2\gamma(1-\kappa)}{(1-\kappa)^2 + |\gamma|^2} = \frac{a^2 - b^2}{a^2 + b^2}$$

$$\delta \sim 2\gamma \quad (\text{weak lensing regime})$$



$$M_{ij} = \frac{\int I(\theta) \theta_i \theta_j d^2\theta}{\int I(\theta) d^2\theta}$$

$$\frac{a^2 - b^2}{a^2 + b^2}$$

$$= \epsilon_s + \epsilon_i + \text{noise} + \text{systematics} \dots$$

Reliability of results: depends on PSF analysis

Assume sources orientation is isotropic:

Weak lensing regime : $\delta \sim 2\gamma = \langle \epsilon_{\text{Shear}} \rangle_{\theta} + \text{noise}$

Mass reconstruction from weak lensing

We have shown that

$$\alpha(\theta) = \frac{1}{\pi} \int \kappa(\theta') \frac{\theta - \theta'}{|\theta - \theta'|^2} d\theta^2$$

that is

$$\psi(\theta) = \frac{1}{\pi} \int \kappa(\theta') \ln|\theta - \theta'| d\theta^2$$

where the amplification matrix writes

$$A(\theta) = \frac{\partial \beta}{\partial \theta} = \left(\delta_{ij} - \frac{\partial^2 \psi(\theta)}{\partial \theta_i \partial \theta_j} \right)$$

Mass reconstruction from weak lensing

or, as function of the convergence and shear components

$$\begin{pmatrix} 1 - \kappa - \gamma_1 & -\gamma_2 \\ -\gamma_2 & 1 - \kappa + \gamma_1 \end{pmatrix}$$

Let set

$$\begin{cases} \gamma = \gamma_1 + i\gamma_2 = |\gamma|e^{2i\psi} \\ \gamma_1 = \frac{1}{2}(\psi_{,11} + \psi_{,22}) \\ \gamma_2 = \psi_{,12} \end{cases}$$

then

$$\gamma = \left(\frac{\partial_1^2 - \partial_2^2}{2} + i\partial_1\partial_2 \right) \psi(\theta)$$

Mass reconstruction from weak lensing

So, we can express γ as function of κ as follows :

$$\gamma(\theta) = \frac{1}{\pi} \int \kappa(\theta') F(\theta - \theta') d\theta^2 \quad (98)$$

with

$$F(\theta) = \frac{\theta_1^2 - \theta_2^2 + 2i\theta_1\theta_2}{|\theta|^4} = F_1(\theta) + iF_2(\theta)$$

Let write this relation in Fourier space:

$$\kappa(\theta) = \frac{1}{(2\pi)^2} \int \hat{\kappa}(\mathbf{k}) e^{i\mathbf{k}\cdot\theta} d^2k$$

Eq. (98)= convolution \rightarrow

$$\hat{\gamma}(\mathbf{k}) = \frac{1}{\pi} \hat{\kappa}(\mathbf{k}) \hat{F}(\hat{k})$$

--

Mass reconstruction from weak lensing

By inverting this relation, one can then reconstruct the κ field:

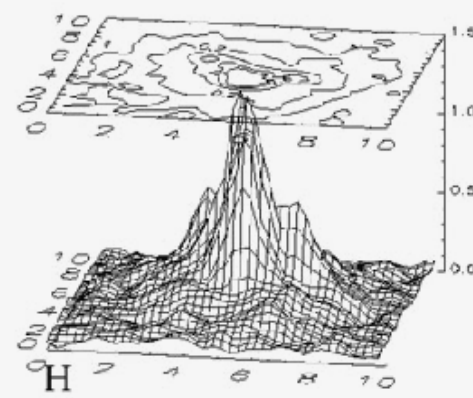
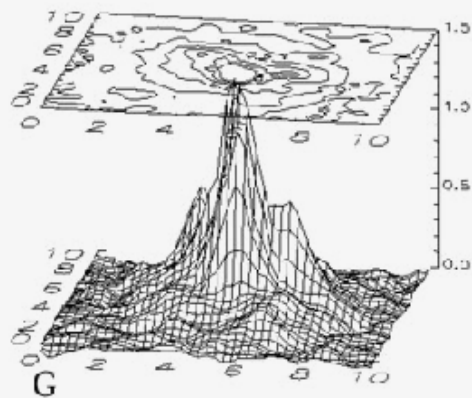
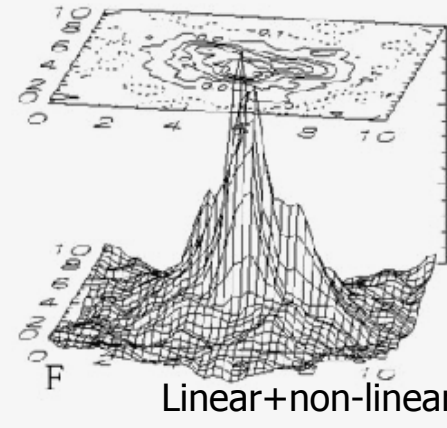
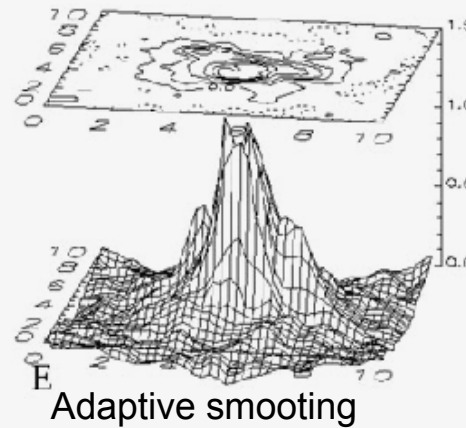
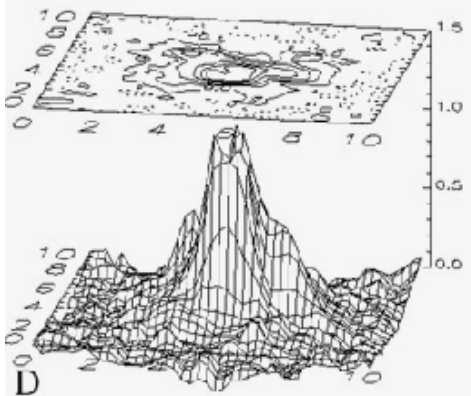
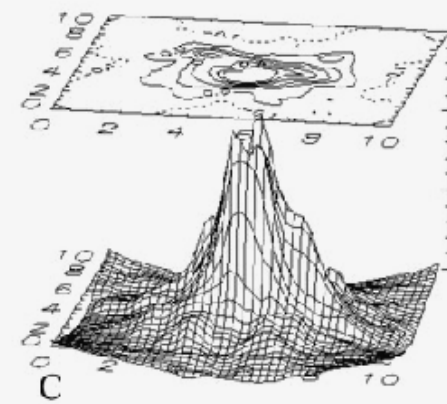
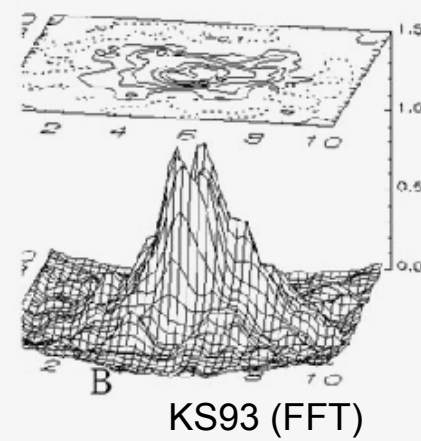
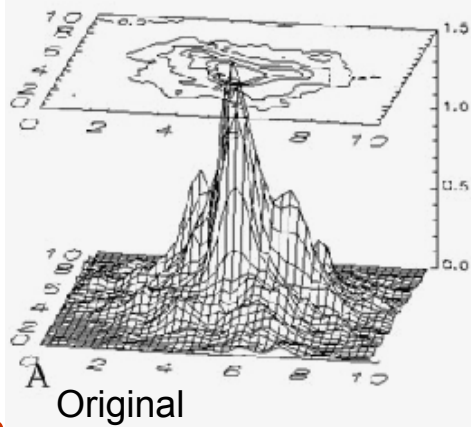
$$\kappa(\boldsymbol{\theta}) = \frac{1}{\pi} \int \hat{F}^*(\boldsymbol{\theta} - \boldsymbol{\theta}') \gamma(\boldsymbol{\theta}') d\boldsymbol{\theta}' + \kappa_0$$

where the real part is the matter field. *Application:*

$$\Sigma(\boldsymbol{\theta}) - \Sigma_0 = \Sigma_{critic} \frac{1}{\pi} a^2 \sum_{i,j} \Re(\hat{F}^*(\boldsymbol{\theta} - \boldsymbol{\theta}_{i,j}) \bar{\boldsymbol{\epsilon}}(\boldsymbol{\theta}_{i,j}))$$

where a is the distance between grid points

Mass reconstruction algorithms



=F + mass=0 a the boundaries

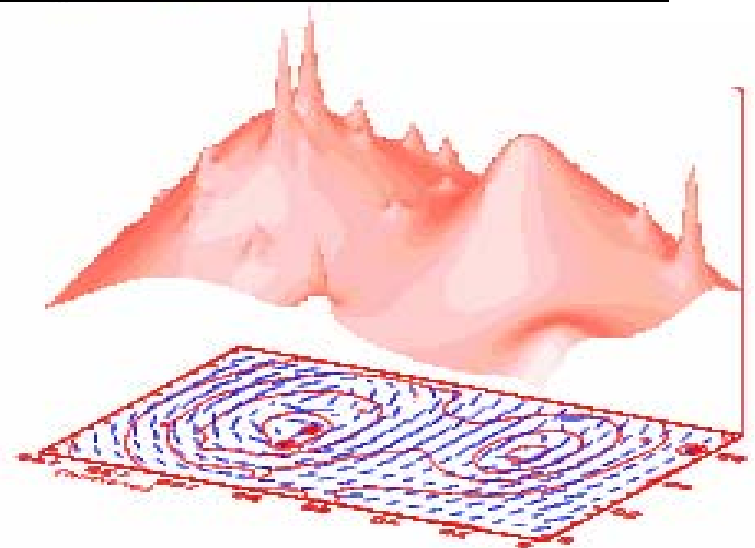


Galaxy Cluster Abell 2218

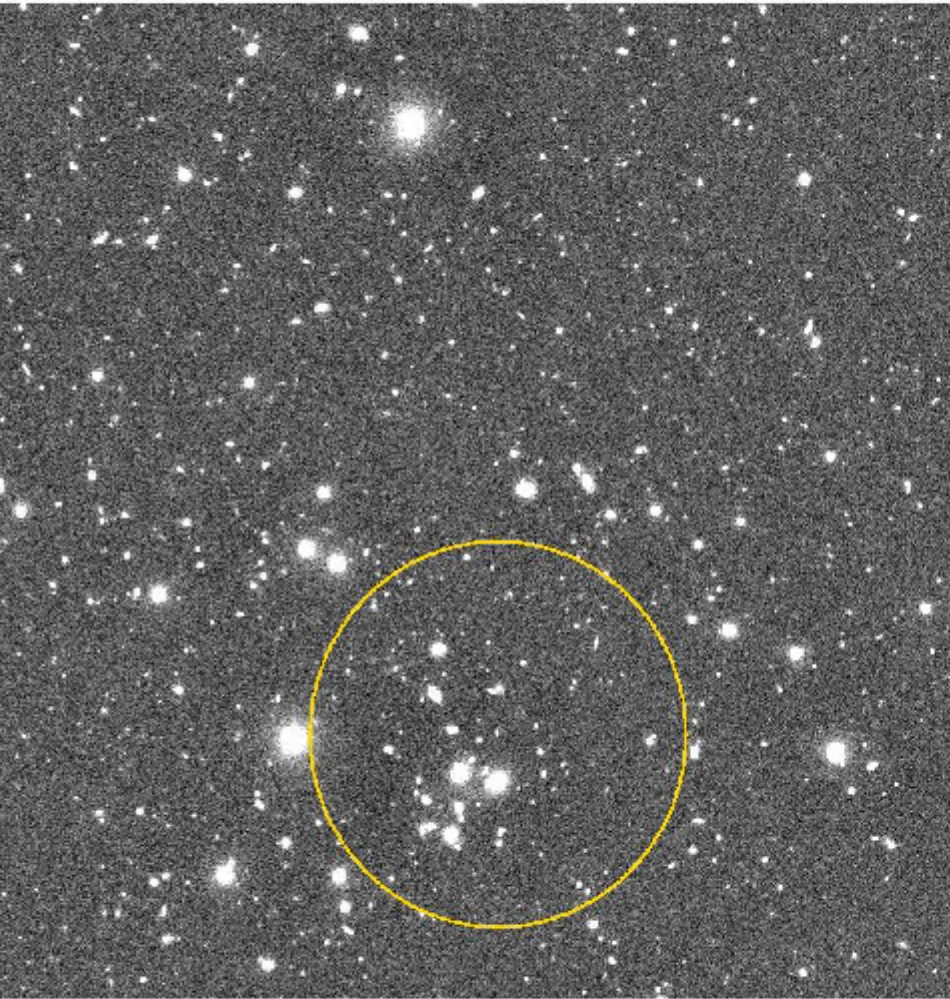
HST • WFPC2

NASA, A. Fruchter and the ERO Team (STScI) • STScI-PRC00-08

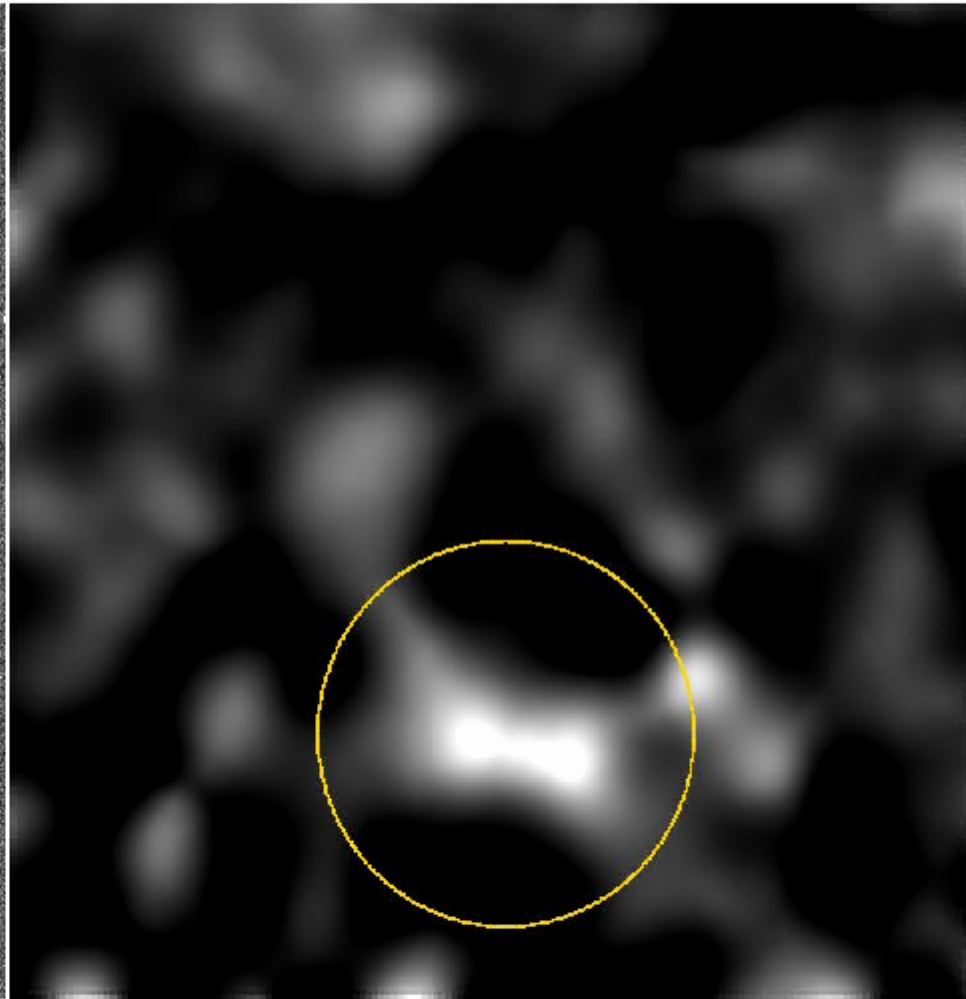
Mass reconstruction of the
Lensing cluster Abell 2218
($z=0.18$)



Finding clusters from dark matter detection only:



VLT I-band Image: 36 mn exposure



Dark Matter reconstruction

Getting the absolute mass

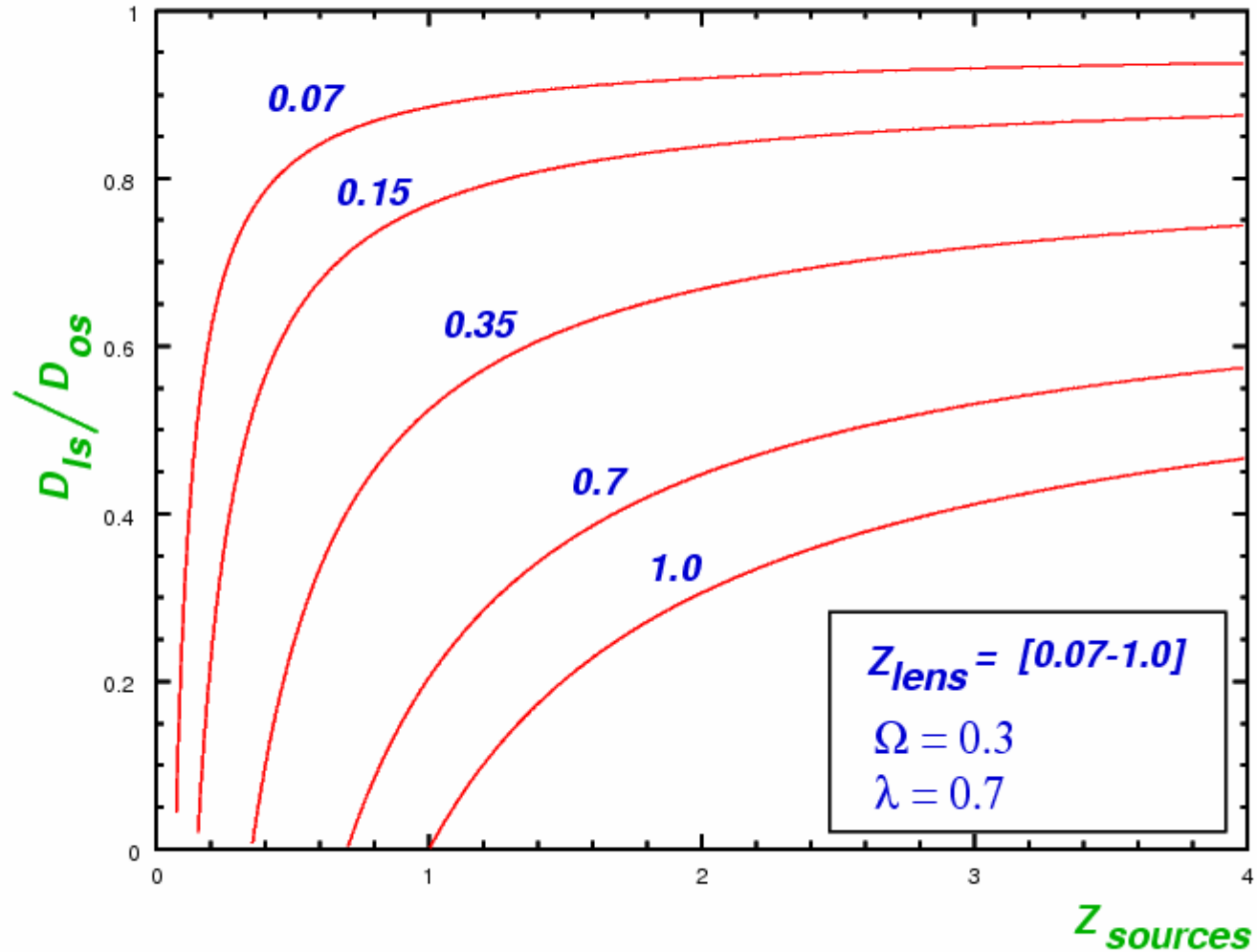
- The mass reconstruction provides the shape of the projected mass distribution but not the absolute scale.
- Need the redshift of the sources:

$$\kappa(\vec{\theta}, z) = \frac{\Sigma(\vec{\theta})}{\Sigma_{critic}(z)} = \Sigma(\vec{\theta}) \frac{4\pi G}{c^2} D_{ol} \left[\frac{D_{ls}}{D_{os}} \right]$$

$$\gamma(\vec{\theta}, z) = \frac{4\pi G}{c^2} D_{ol} \left[\frac{D_{ls}}{D_{os}} \right] \gamma(\vec{\theta})$$

- Very sensitive to the redshift distribution for high- z lenses

Getting the absolute mass



Example: the Singular Isothermal Sphere (SIS)

- Mass density:

$$\rho(r) = \frac{\sigma_v^2}{2\pi G r^2} \quad (111)$$

- Projected mass density:

$$\Sigma(\xi) = \frac{\sigma_v^2}{2G \xi} \quad (112)$$

- Mass inside ξ

$$M(\xi) = \int_0^\xi 2\pi \xi' \Sigma(\xi') d\xi' \quad (113)$$

The Singular Isothermal Sphere

- Angular Einstein radius

$$\theta_E = 4\pi \left(\frac{\sigma_v}{c} \right)^2 \frac{D_{ls}}{D_{os}}$$

- Lensing equation

$$\vec{\beta} = \vec{\theta} - \theta_E \frac{\vec{\theta}}{|\vec{\theta}|}$$

- Lensing properties

$$\kappa(\theta) = \frac{\theta_E}{2\theta}; \quad |\gamma(\theta)| = \frac{\theta_E}{2\theta}; \quad \alpha(\vec{\theta}) = \theta_E \frac{\vec{\theta}}{|\vec{\theta}|}$$

The Singular Isothermal Sphere:

Expected Signal-to-Noise from weak lensing studies of clusters/groups of galaxies

$$S/N = 10 \left(\frac{n}{30 \text{ arcmin}^2} \right)^{1/2} \left(\frac{\sigma_{\epsilon}}{0.2} \right)^{-1} \left(\frac{\sigma_v}{600 \text{ km/s}} \right)^2 \left(\frac{\ln \left[\frac{\theta_2}{\theta_1} \right]}{\ln 10} \right)^{1/2} \left\langle \frac{D_{ls}}{D_{os}} \right\rangle$$

Therefore to increase the S/N

- Go deep: increase n
- Observe massive clusters: increase σ^2
- Reduce intrinsic ellipticity dispersion: space better

The mass sheet degeneracy

- Changing $a \longrightarrow \lambda a$ and $b \longrightarrow \lambda b$ keeps ε unchanged.
- $\iff \gamma \longrightarrow \lambda \gamma$ and $\kappa \longrightarrow \lambda \kappa$.
- \iff changing $\kappa \longrightarrow \kappa' = \lambda \kappa + (1 - \lambda)$: rescaling κ and adding a constant mass density.
- This mass sheet degeneracy results from the fact that the gravitational distortion is sensitive to the gradient of the projected mass density.
- We are only measuring ellipticity modification, no size modification of galaxies

Solve the mass sheet degeneracy using magnification

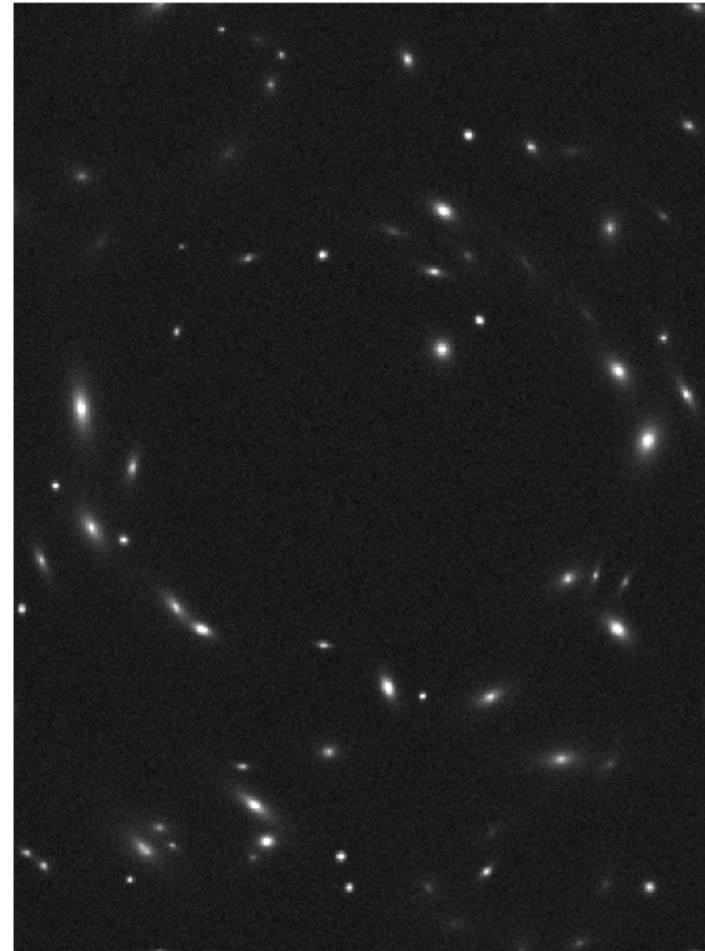
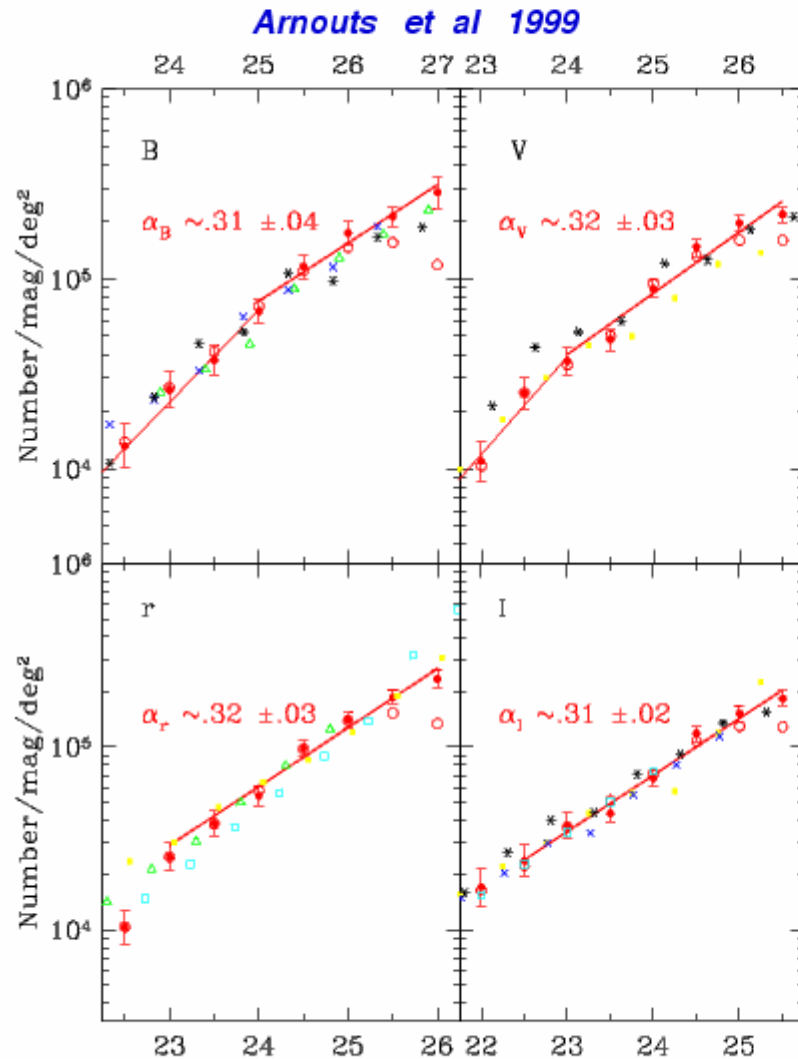
- Magnification: increases the flux received from galaxies \longrightarrow more galaxies visible and ALSO magnifies by the same amount the area of the projected lensed sky \longrightarrow decreases the galaxy number density (Broadhurst 1995):

$$N(< m, r) = N_0(< m) \mu(r)^{2.5\alpha-1} \approx N_0 (1 + 2\kappa)^{2.5\alpha-1} \quad (127)$$

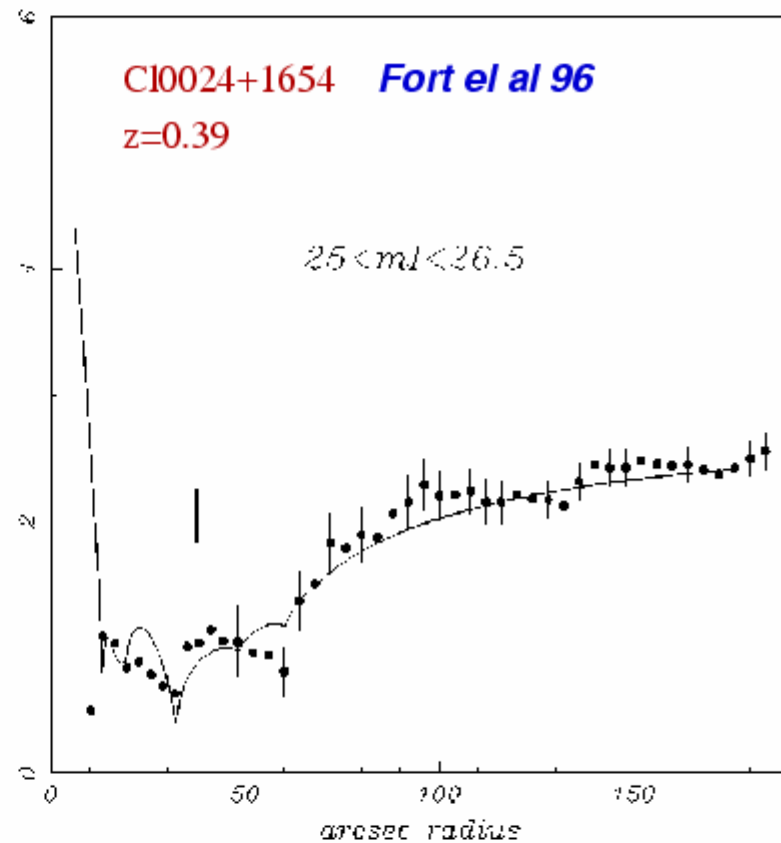
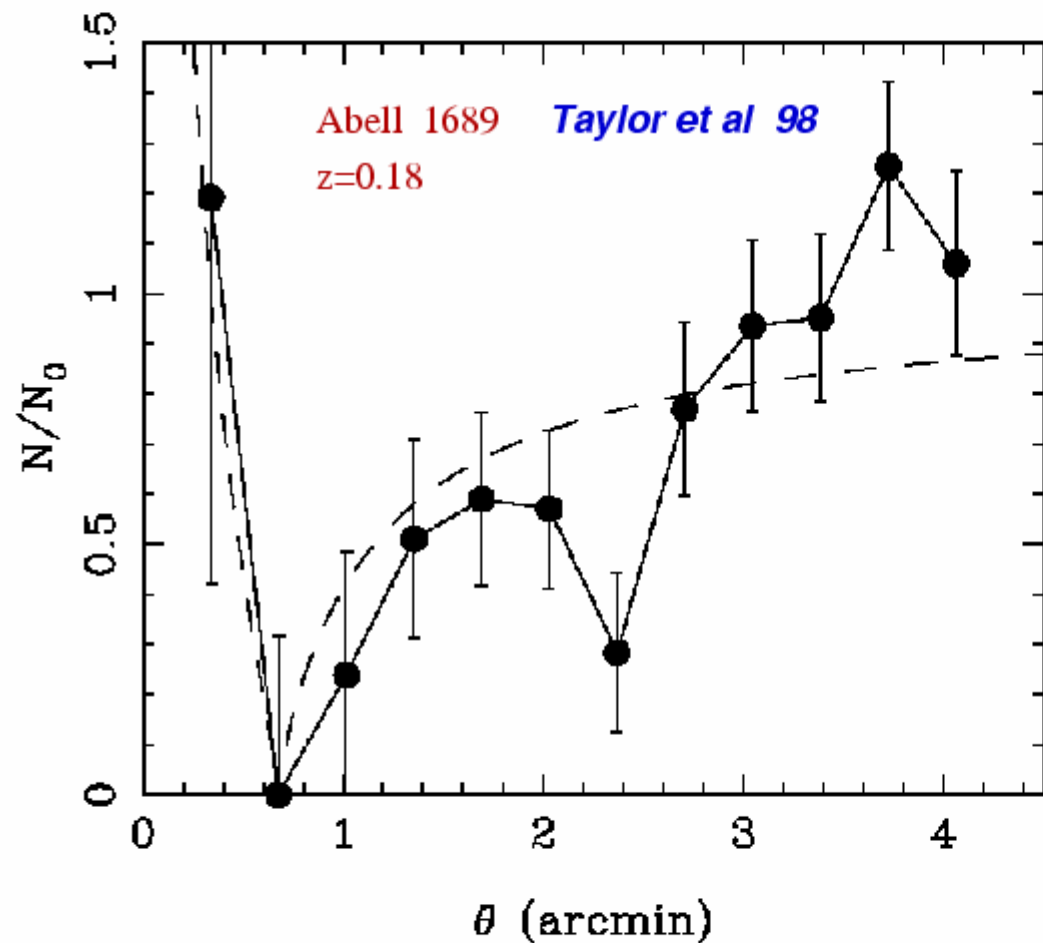
$\mu(r)$ is the magnification, $N_0(< m)$ the intrinsic (unlensed) number density, and

$$\alpha = \frac{d \log N(< m)}{dm} \quad (128)$$

Magnification and galaxy depletion



Magnification and galaxy depletion



II. Gravitational Lensing:

applications to clusters of
galaxies

From cluster galaxy observation to cluster mass map

MS1054
HST

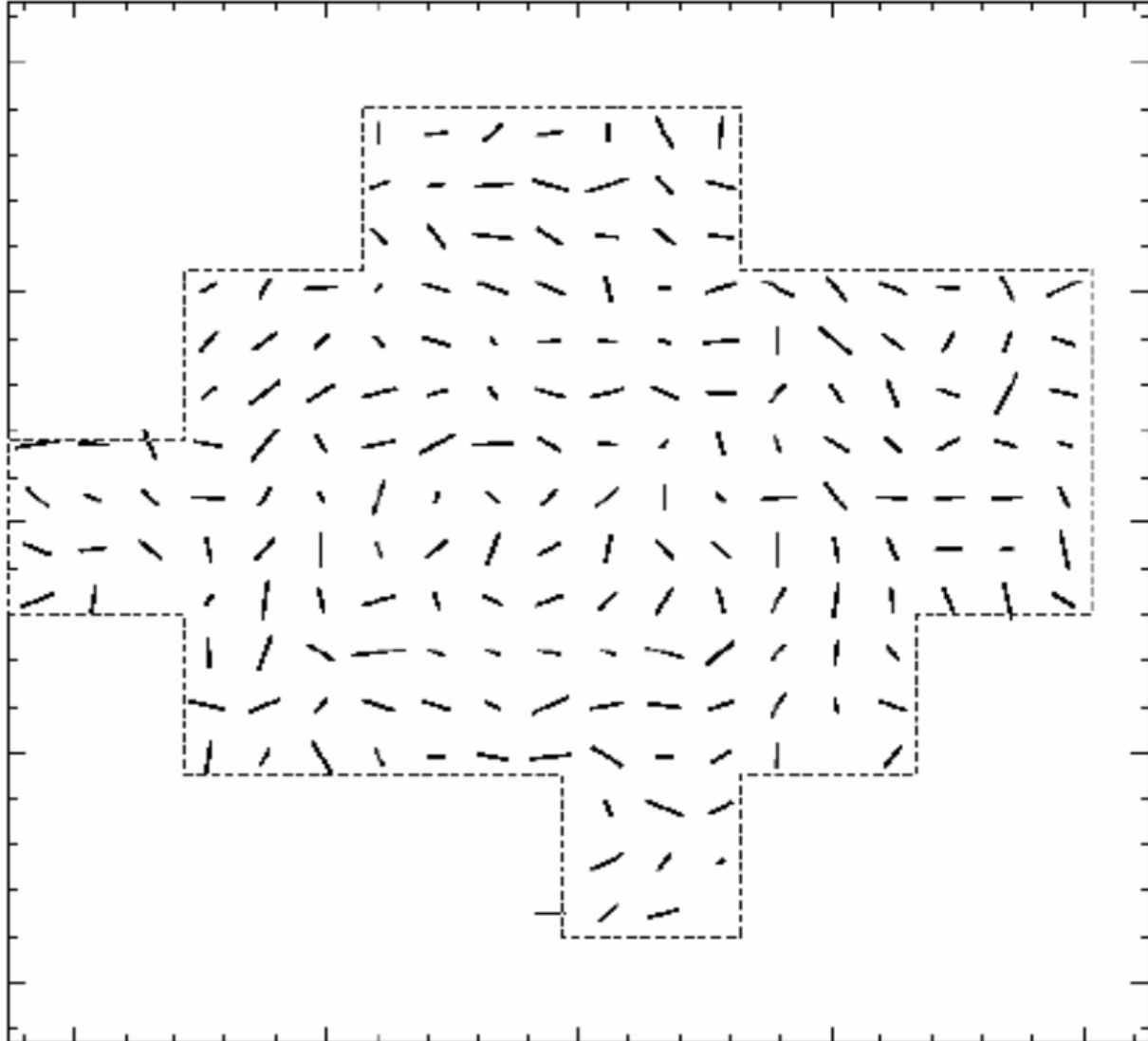
Hoekstra
et al 1998



From cluster galaxy observation to cluster mass map

MS1054
HST

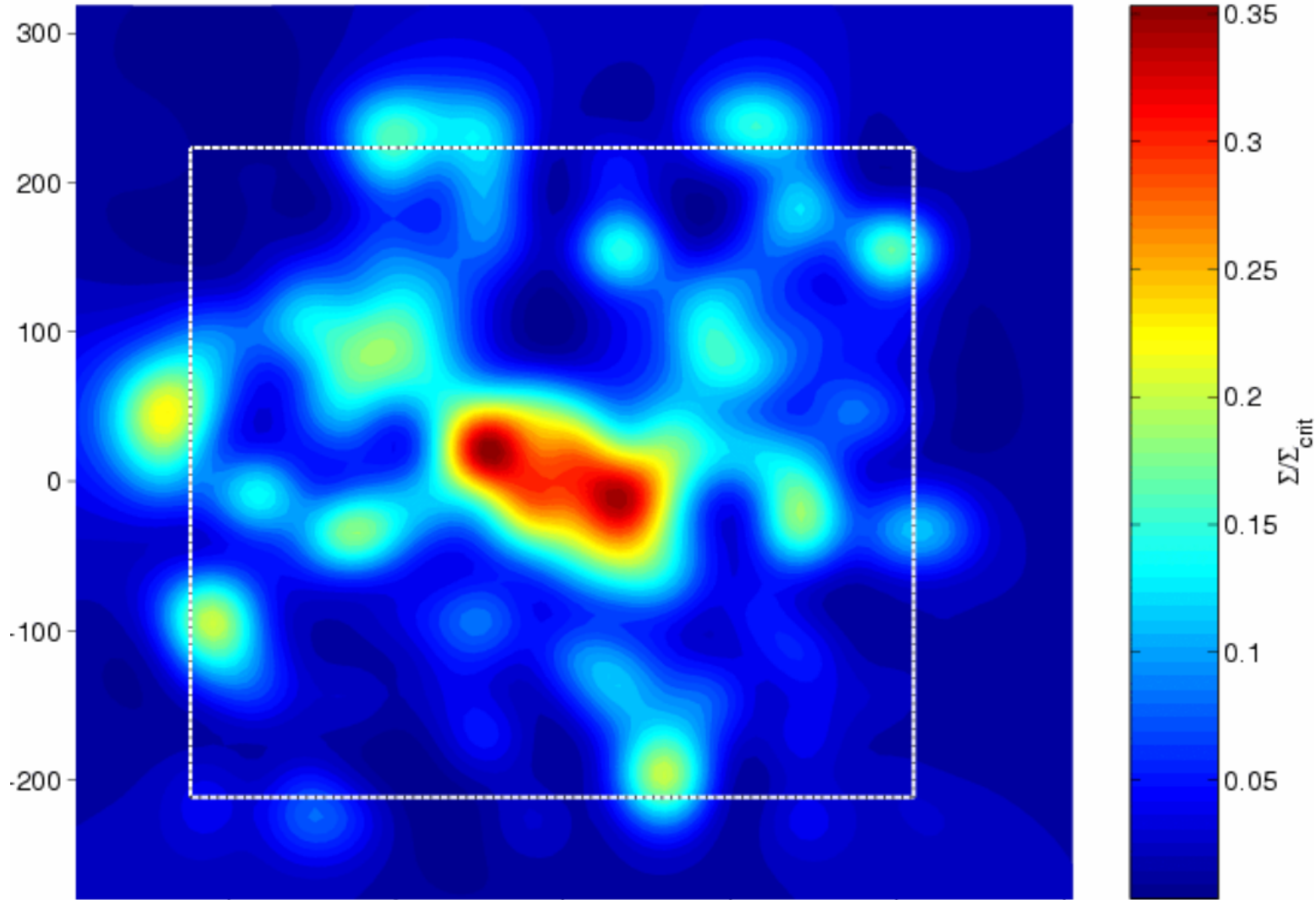
Hoekstra et al
1998

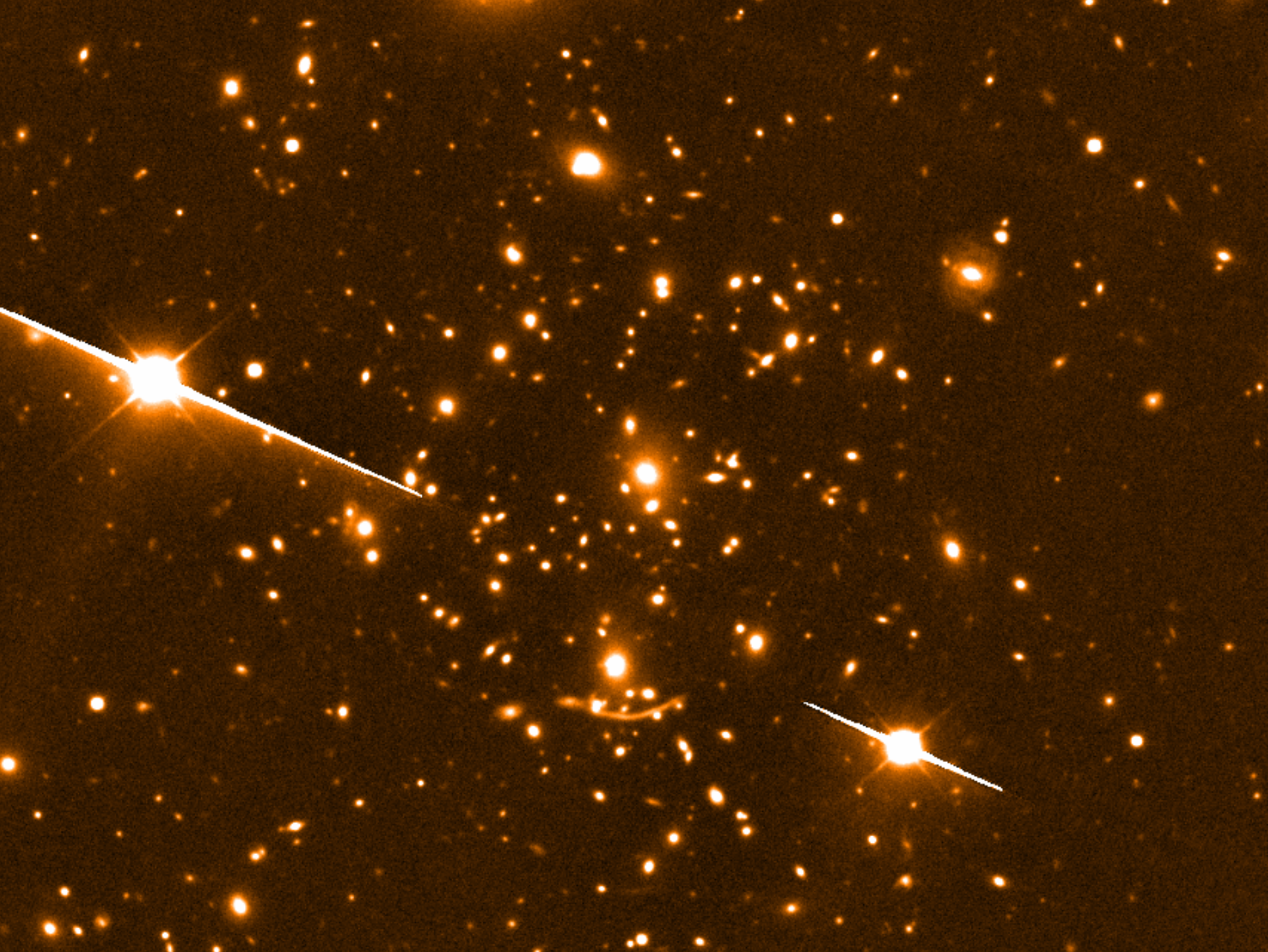


From cluster galaxy observation to cluster mass map

MS1054
HST

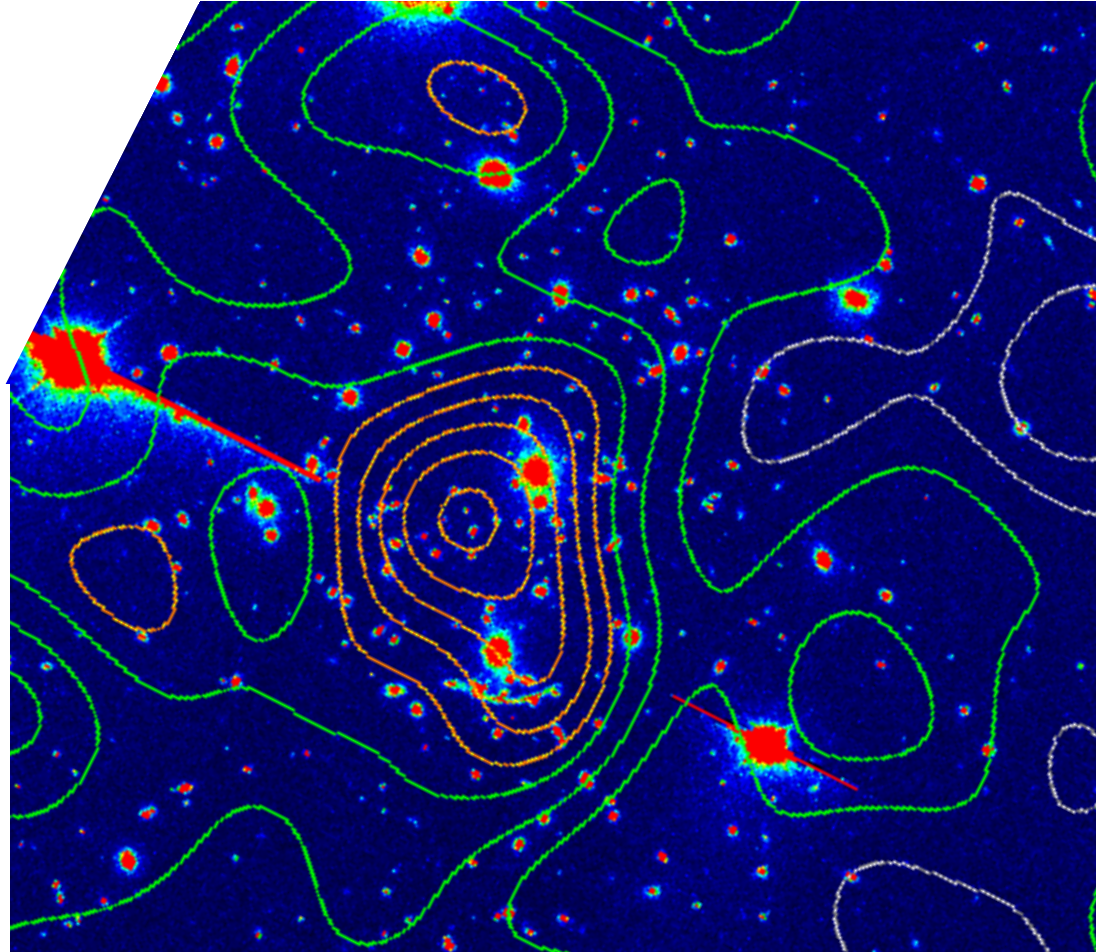
Hoekstra
et al 1998





First giant
arc
discovered
in Abell
370

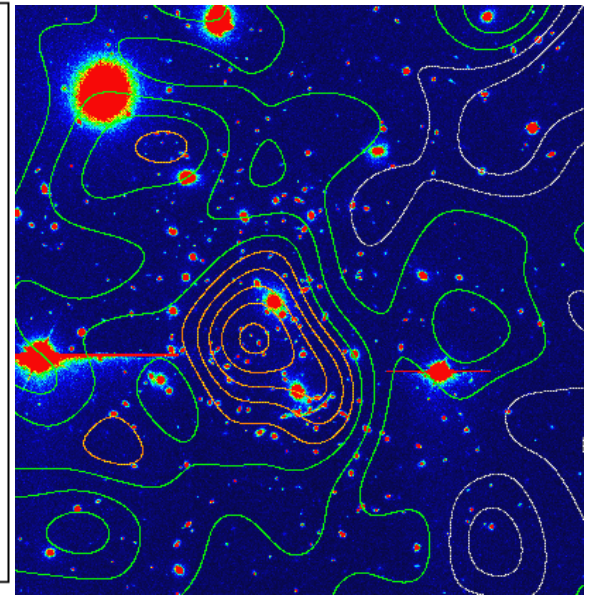
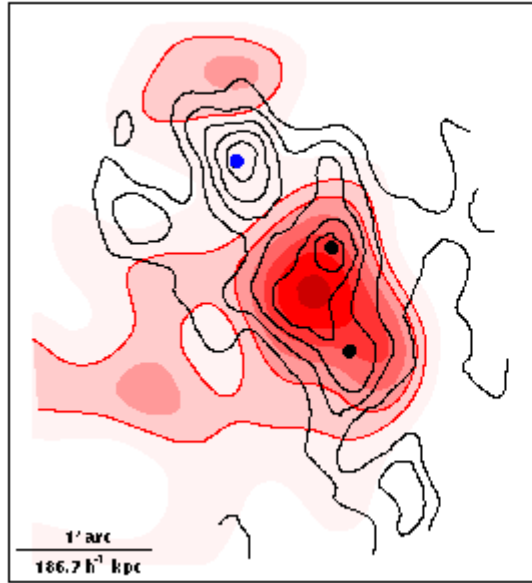
$$Z_{\text{cluster}} = 0.374 ,$$
$$Z_{\text{arc}} = 0.720$$



Abell 370

$Z_{\text{cluster}} = 0.374$, $Z_{\text{arc}} = 0.720$

X-ray luminosity contours (black)

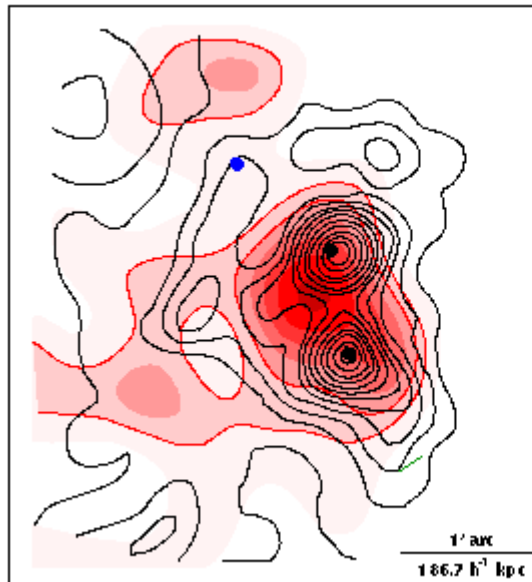


Does light trace mass?

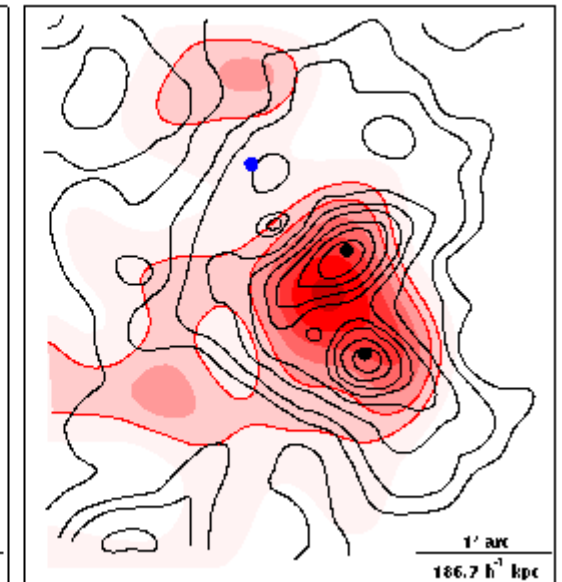
X-ray vs. Mass : yes

Red galaxies vs. Mass: yes

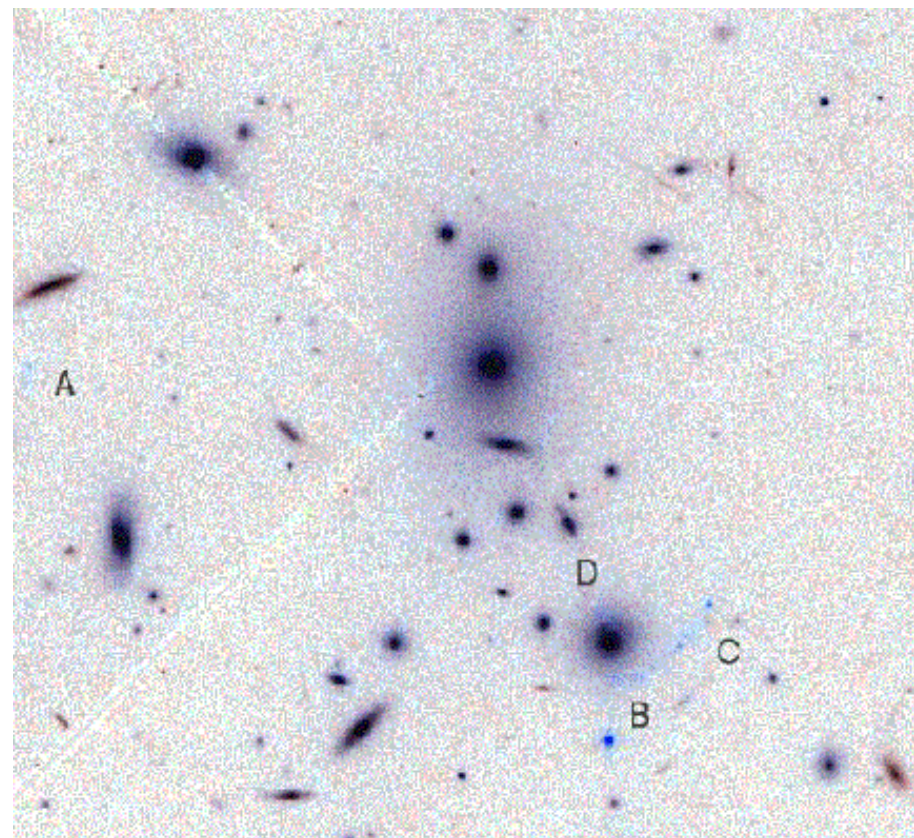
Cluster optical luminosity contours (black)



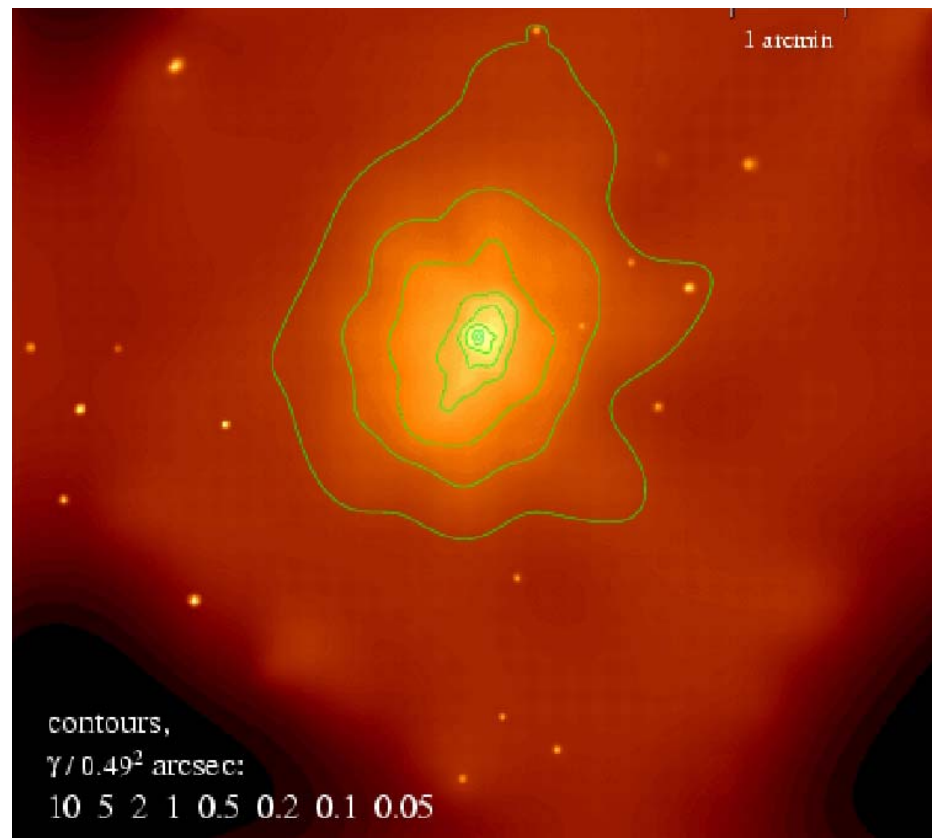
Cluster galaxy number density contours (black)



MS1358+6245



HST

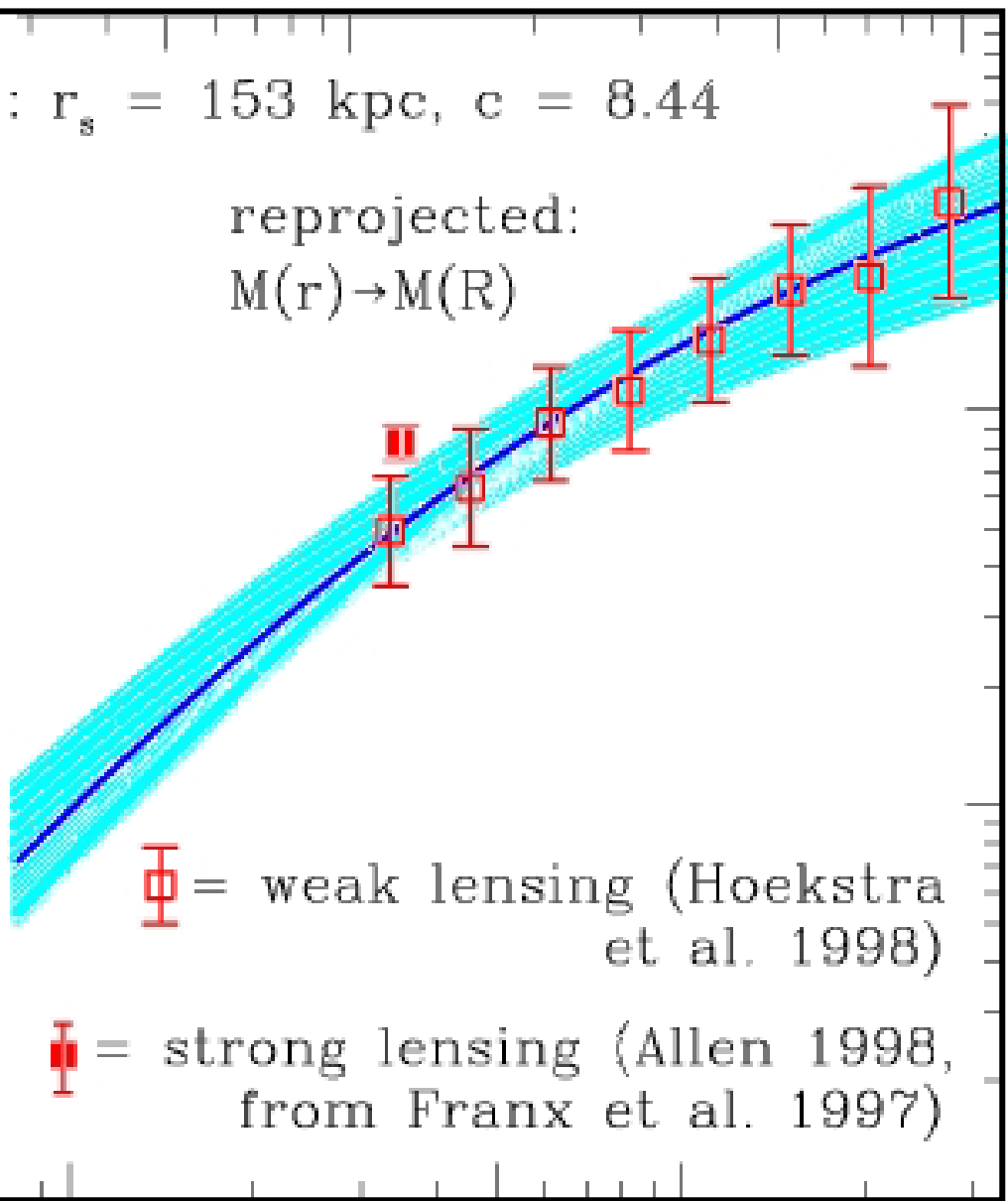


Chandra

50 100 500 10^3

$r_s = 153$ kpc, $c = 8.44$

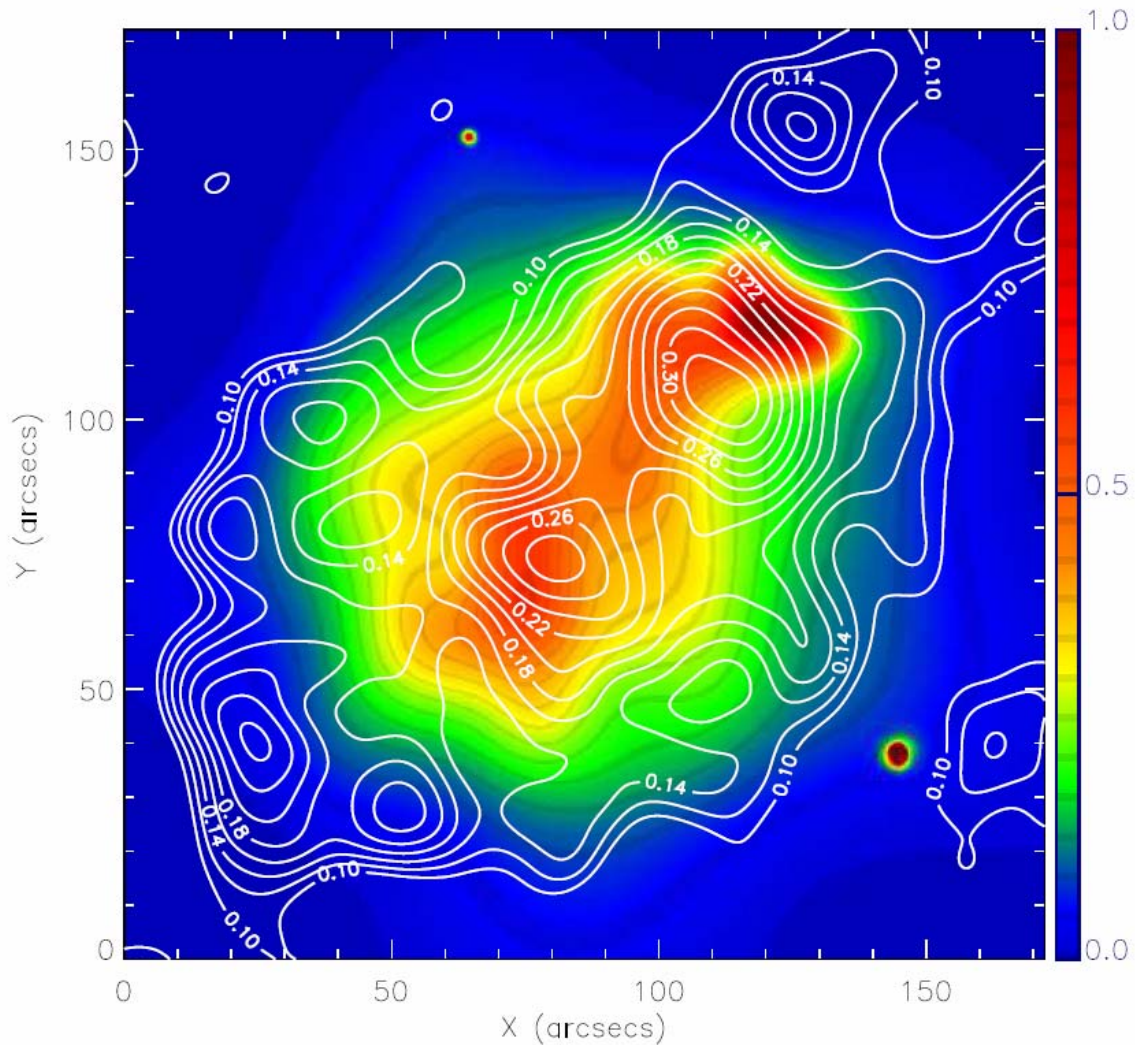
reprojected:
 $M(r) \rightarrow M(R)$



X-ray Chandra:
baryonic versus
dark matter
from strong /
weak lensing

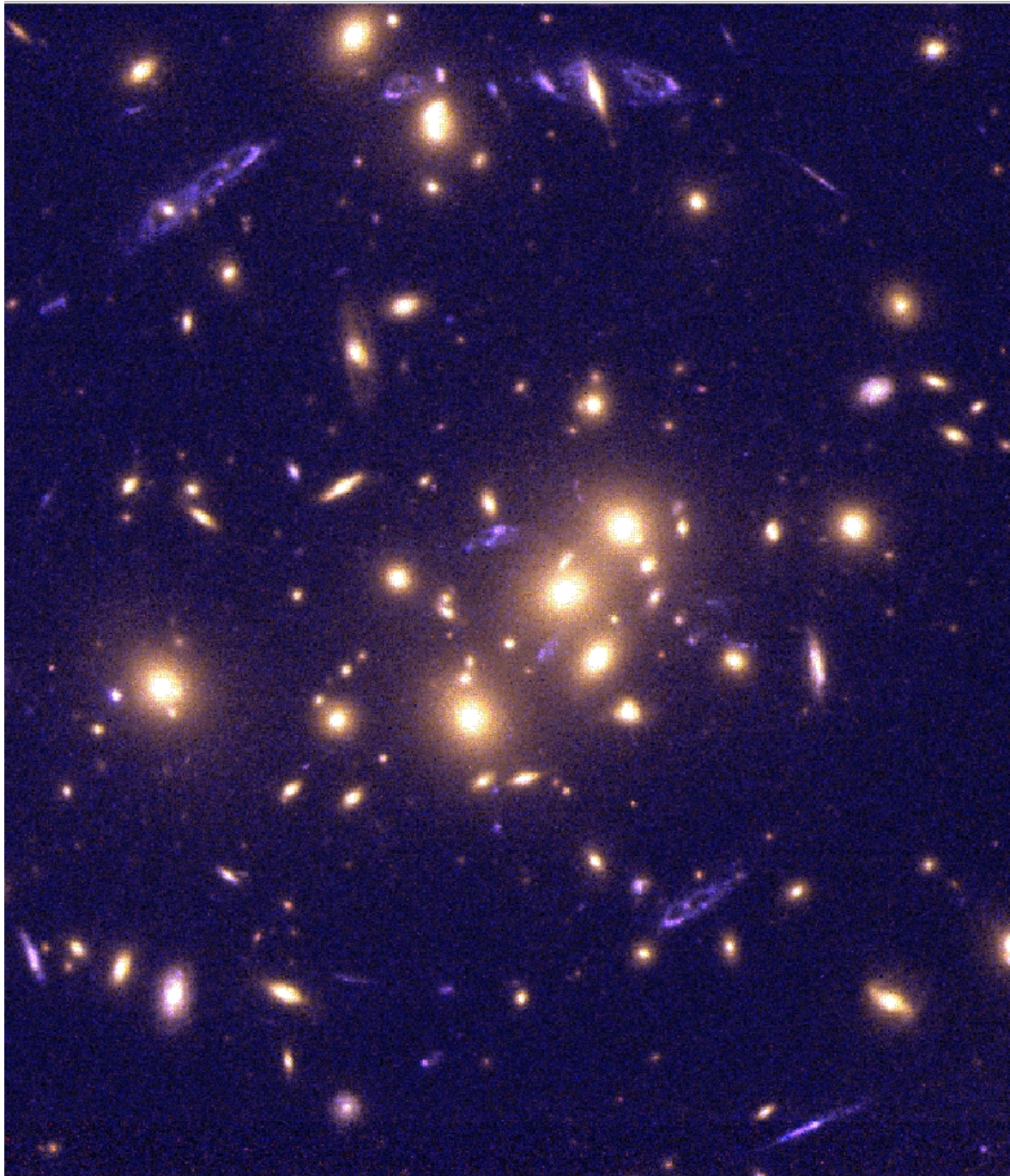
Cluster of galaxies
MS1358+6254

MS1054: Chandra and weak lensing

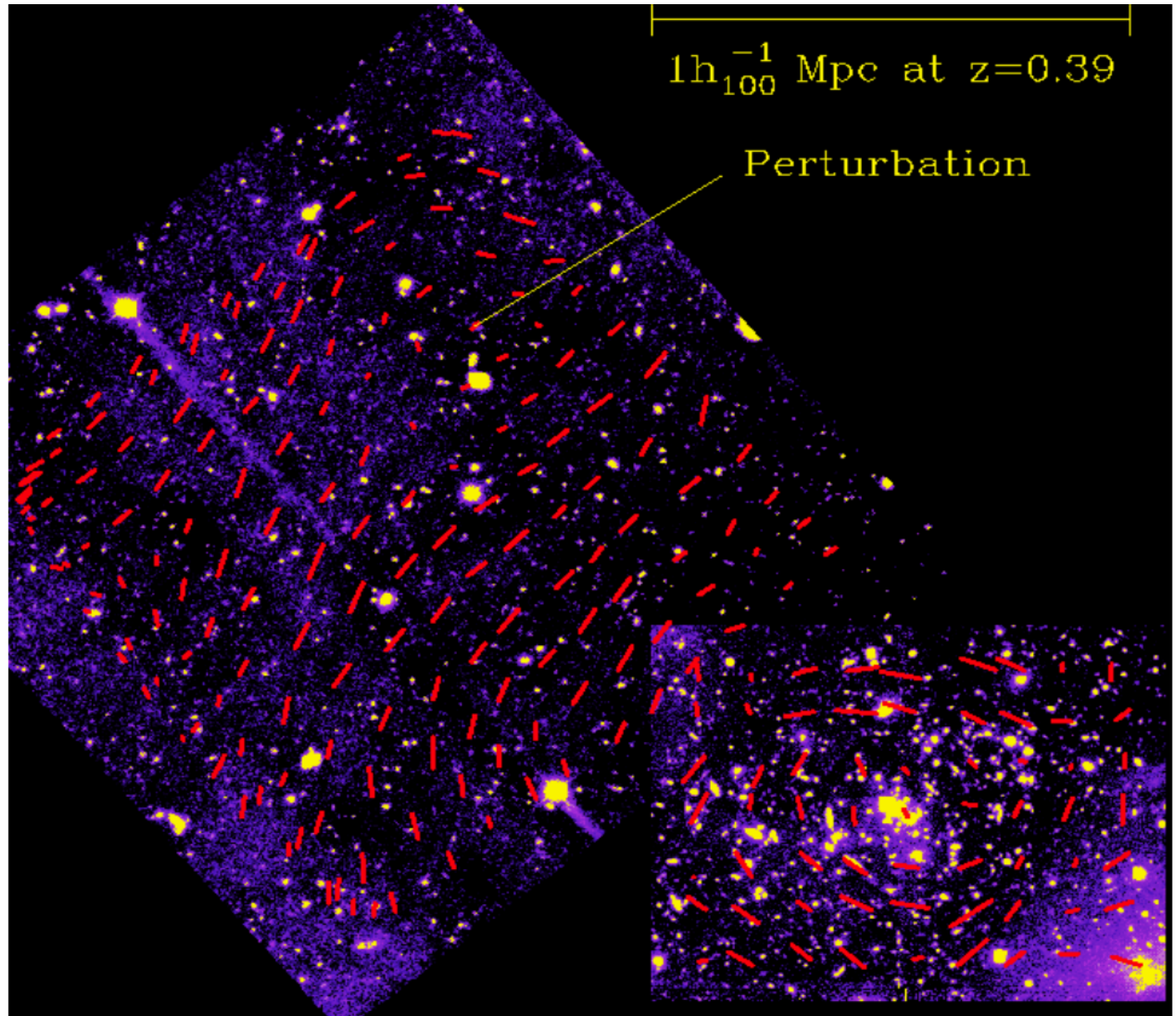


baryonic and
dark matter
distribution
maps

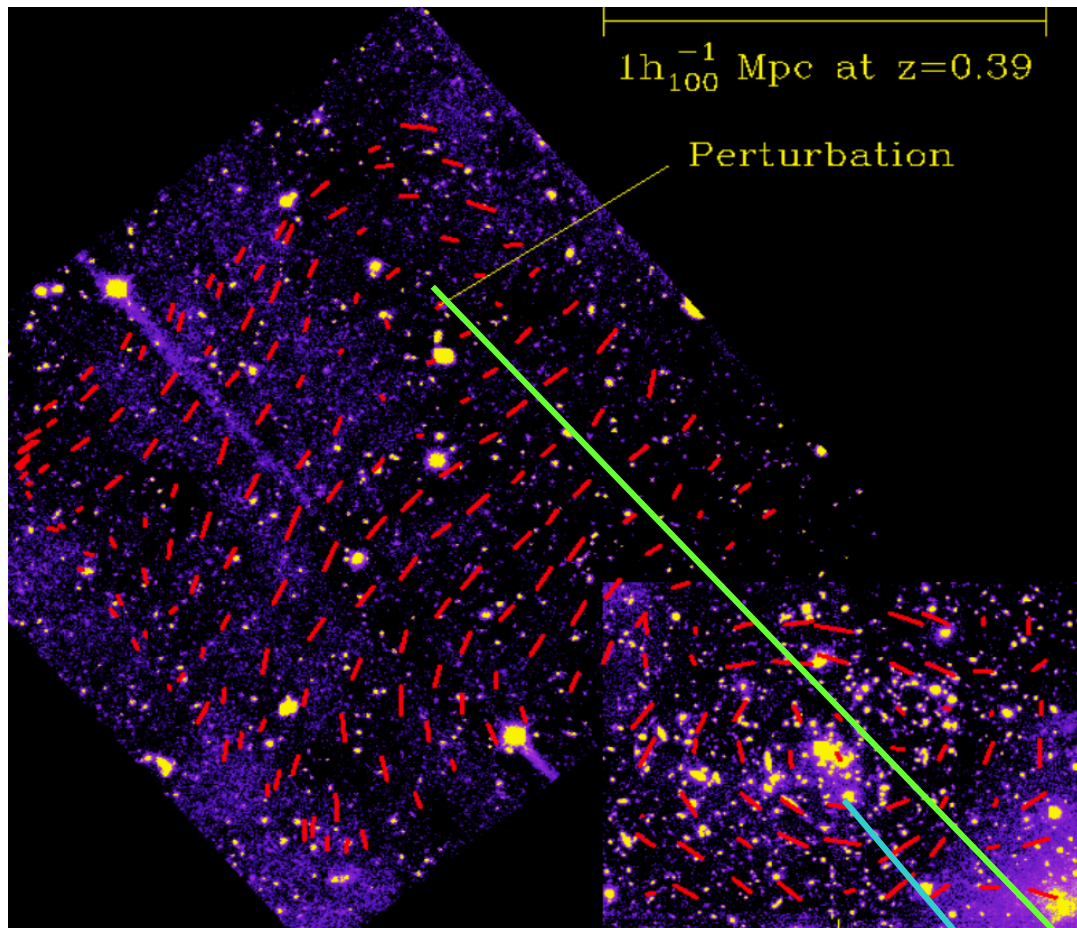
Jee et al 2007



Cl0024+1654
 $z=0.55$

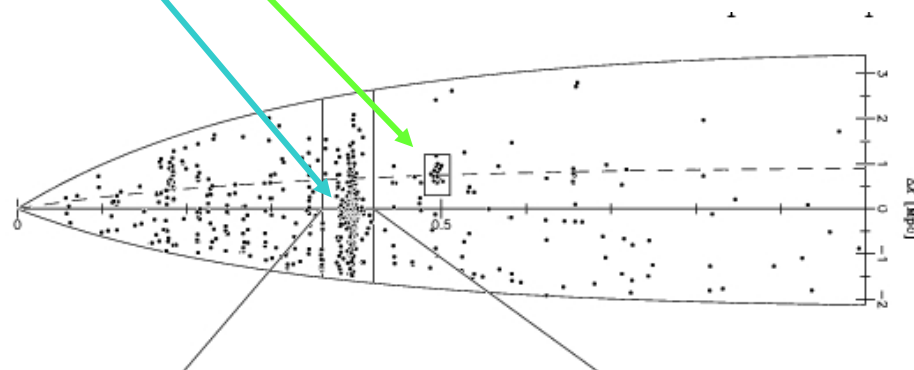


CI0024+1654
z=0.55



CI0024+1654
 $z=0.55$

Spectroscopic
detection of a group at
the location of the WL
perturbation



Summary mass from cluster WL reconstruction

**May 2007:
147 clusters
76 publications
Dahle 2007**

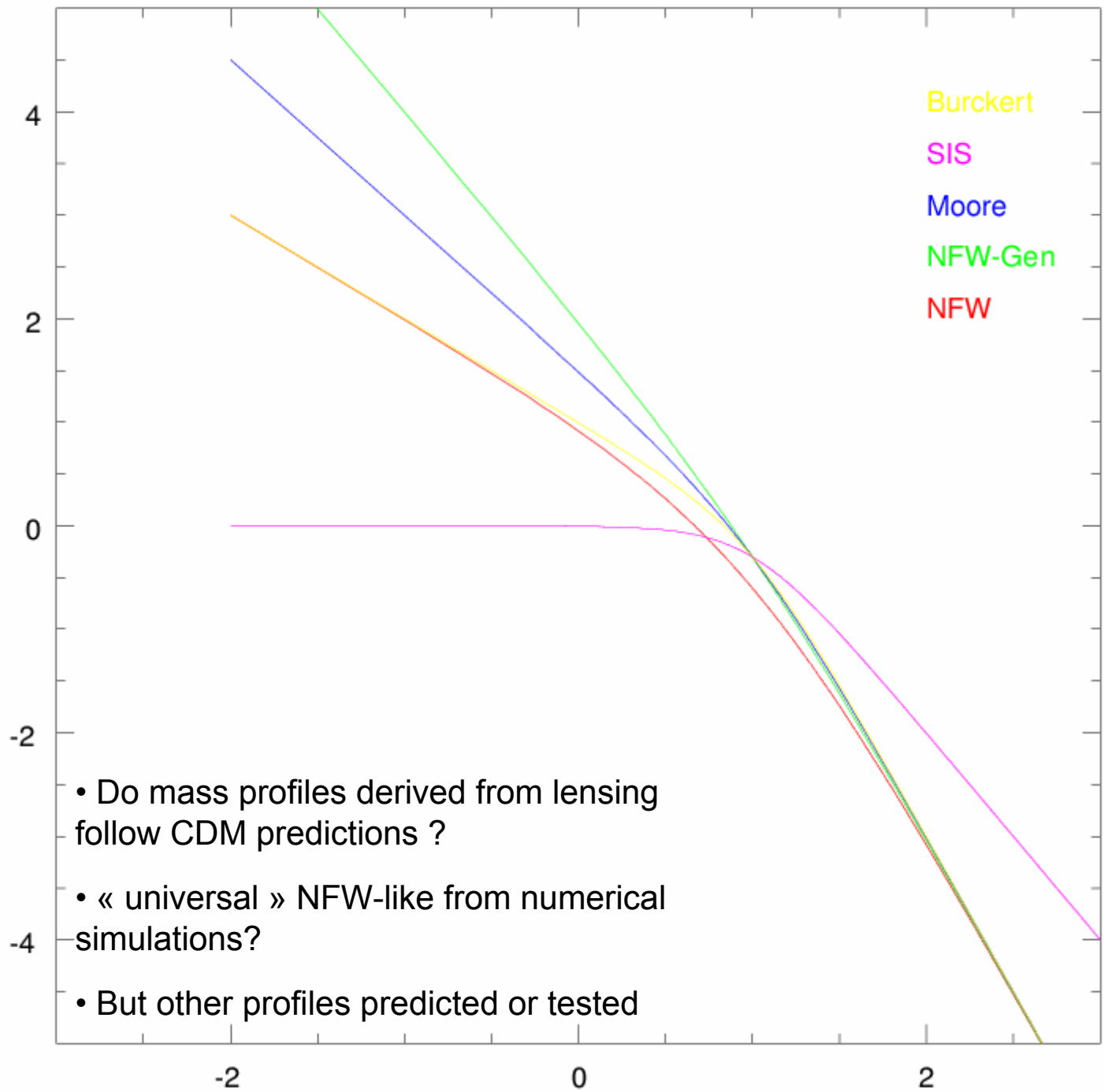
- Median σ_v :
~ 1000 km/sec

- Median M/L :
~ 350 h

| Cluster | z | σ_{obs} (kms^{-1}) | σ_{wl} (kms^{-1}) | M/L (h_{100}) | Scale (h_{100}^{-1} Mpc) | Tel. | Ref. |
|-----------------|-----------|---|--|----------------------|--------------------------------|---------|--------------------------|
| A2218 | 0.17 | 1370 | 1000-1400 | ≈ 300 | 0.5 | CFHT | Squires et al (19) |
| | | | - | 310 | 0.1 | HST | Smail et al (20) |
| A1689 | 0.18 | 2400 | 1200-1500 | - | 0.5 | CTIO | Tyson et al (21) |
| | | | - | 400 | 1.0 | CTIO | Tyson & Fischer (22) |
| | | | 1030 | - | 1.0 | ESO/2.2 | Clowe & Schneider (23) |
| A2163 | 0.20 | 1680 | 740-1000 | 300 | 0.5 | CFHT | Squires et al (25) |
| A2390 | 0.23 | 1090 | ≈ 1000 | 320 | 0.5 | CFHT | Squires et al (24) |
| < 8 clusters > | < 0.2 > | - | - | < 295 > | 1.0 | CTIO | Wittman et al (26) |
| MS1455+22 | 0.26 | 1133 | - | 1080 | 0.4 | WHT | Smail et al (27) |
| AC118 | 0.31 | 1950 | - | 370 | 0.15 | HST | Smail et al (20) |
| MS1008-1224 | 0.31 | 1054 | 940 | 340 | 0.5 | VLT | Athreya et al (28) |
| | | | 850 | ≈ 320 | 0.5 | VLT | Lombardi et al (29) |
| MS2137-23 | 0.31 | - | 950 | 300 | 0.5 | VLT | Gavazzi et al (in prep.) |
| MS1358+62 | 0.33 | 940 | 780 | 180 | 0.75 | HST | Hoekstra et al (30) |
| MS1224+20 | 0.33 | 802 | - | ≈ 800 | 1.0 | CFHT | Fahlman et al (31) |
| | | | 1300 | 890 | 1.0 | MDM2.2 | Fischer (32) |
| Q0957+56 | 0.36 | 715 | - | - | 0.5 | CFHT | Fischer et al (33) |
| Cl0024+17 | 0.39 | 1250 | - | 150 | 0.15 | HST | Smail et al (20) |
| | | | 1300 | ≈ 900 | 1.5 | CFHT | Bonnet et al (10) |
| Cl0939+47 | 0.41 | 1080 | - | 120 | 0.2 | HST | Smail et al (20) |
| | | | - | ≈ 250 | 0.2 | HST | Seitz et al (34) |
| Cl0302+17 | 0.42 | 1080 | - | 80 | 0.2 | HST | Smail et al (20) |
| RXJ1347-11 | 0.45 | - | 1500 | 400 | 1.0 | CTIO | Fischer & Tyson (35) |
| 3C295 | 0.46 | 1670 | 1100-1500 | - | 0.5 | CFHT | Tyson et al (21) |
| | | | - | 330 | 0.2 | HST | Smail et al (20) |
| Cl0412-65 | 0.51 | - | - | 70 | 0.2 | HST | Smail et al (20) |
| Cl1601+43 | 0.54 | 1170 | - | 190 | 0.2 | HST | Smail et al (20) |
| MS0016+16 | 0.55 | 1230 | - | 180 | 0.2 | HST | Smail et al (20) |
| | | | 740 | 740 | 0.6 | WHT | Smail (36) |
| | | | 800 | - | 0.6 | Keck | Clowe et al (6) |
| MS0451 | 0.55 | 1371 | 980 | - | 0.6 | Keck | Clowe et al (6) |
| Cl0054-27 | 0.56 | - | - | 400 | 0.2 | HST | Smail et al (20) |
| MS2053 | 0.59 | 820 | 730 | - | 0.5 | Keck | Clowe et al (6) |
| | | | 886 | 360 | 0.5 | HST | Hoekstra et al (40) |
| MS1137+60 | 0.78 | 884 | 1190 | 270 | 0.5 | Keck | Clowe et al (37,6) |
| RXJ1716+67 | 0.81 | 1522 | - | 190 | 0.5 | Keck | Clowe et al (37) |
| | | | 1030 | - | 0.5 | Keck | Clowe et al (6) |
| MS1054-03 | 0.83 | 1360 | 1100-2200 | 350-1600 | 0.5 | UH2.2 | Luppino & Kaiser (38) |
| | | | 1310 | 250-500 | 0.5 | HST | Hoekstra et al (39) |
| | | | 1080 | - | 0.5 | Keck | Clowe et al (6) |
| < 10 clusters > | < 0.5 > | - | - | - | 1.0 | VLT | White et al (2002) |
| EDICS | - < 0.8 > | - | - | - | - | - | and Clowe et al (2002) |

Mass profile

NFW, SIS, POW, Generalised-
NFW, Moore, Buckert, de
Vaucouleur??



The Navarro-Frenk-White profile

$$\rho(r) = \frac{\delta_c \rho_{rc}(z)}{(r/r_s) (1 + r/r_s)^2}$$

$$\rho_{rc}(z) = \frac{3H(z)^2}{8\pi G}$$

Virial radius r_{200} : radius inside which mass density equals $200 \rho_{rc}(z)$

C = concentration parameter

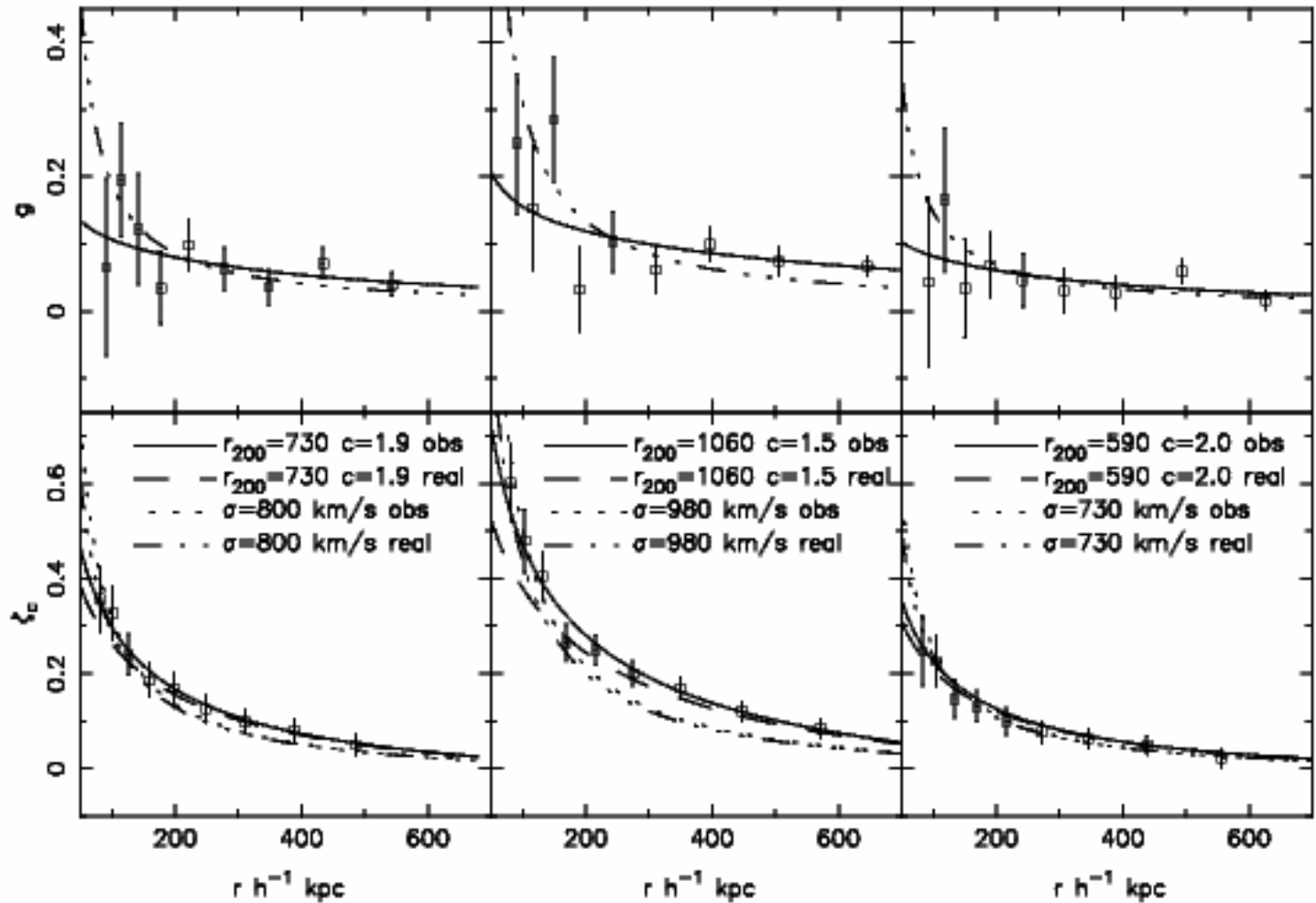
$$\delta_c = \frac{200}{3} \frac{C^3}{\ln(1+C) - C/(1+C)}$$

NFW or SIS ?

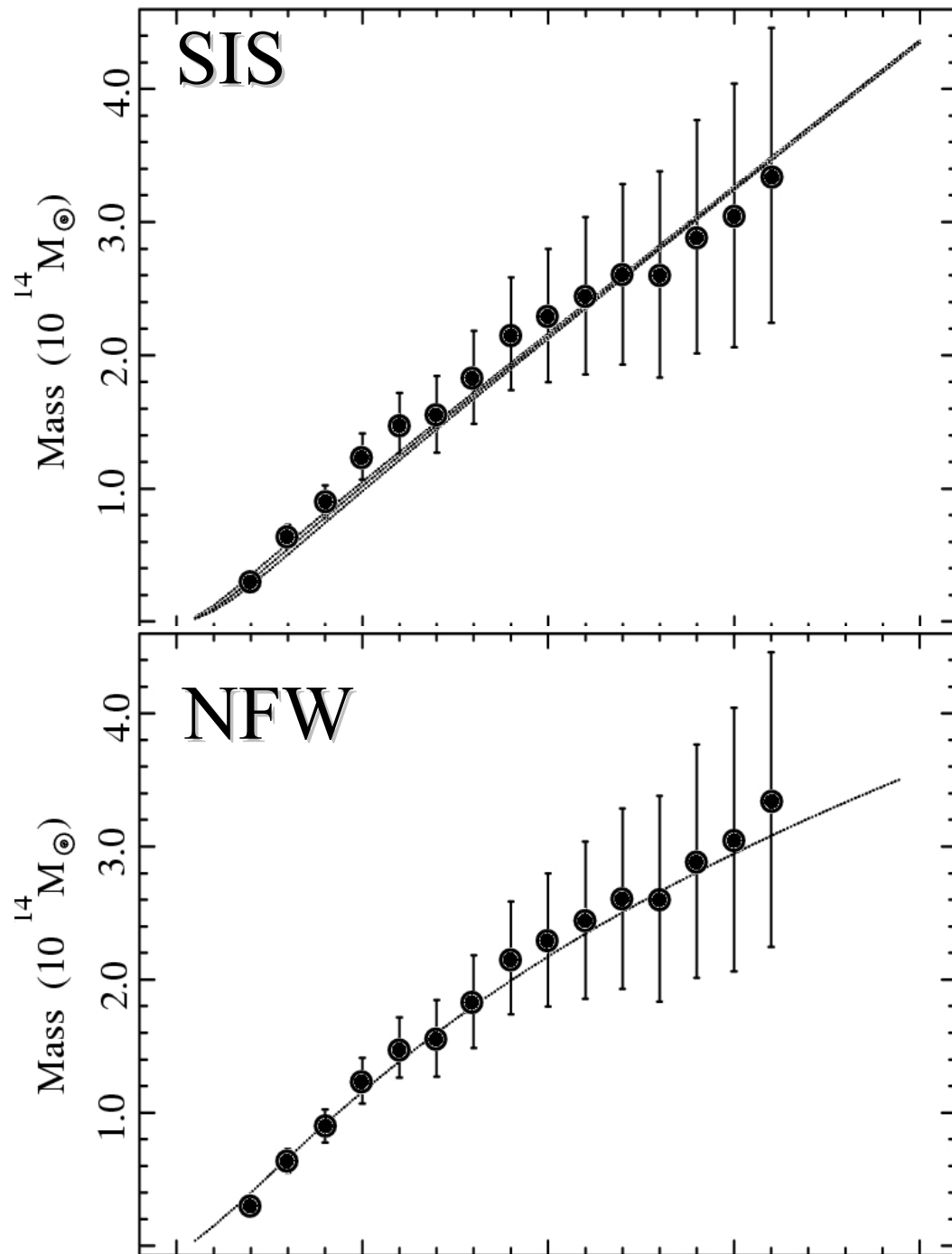
MS0016+16

MS0451-03

MS2053-04



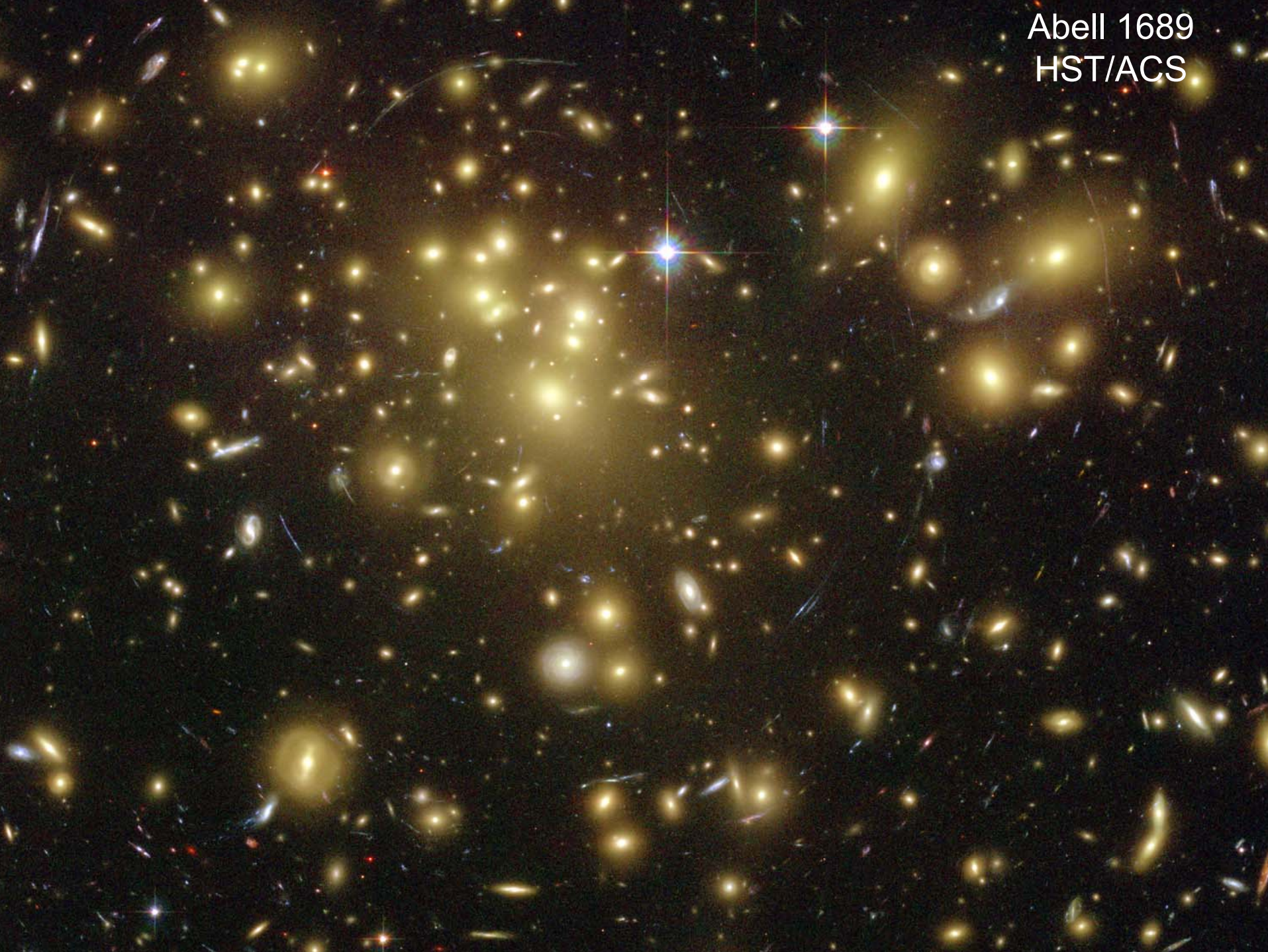
Clowe et al 2004



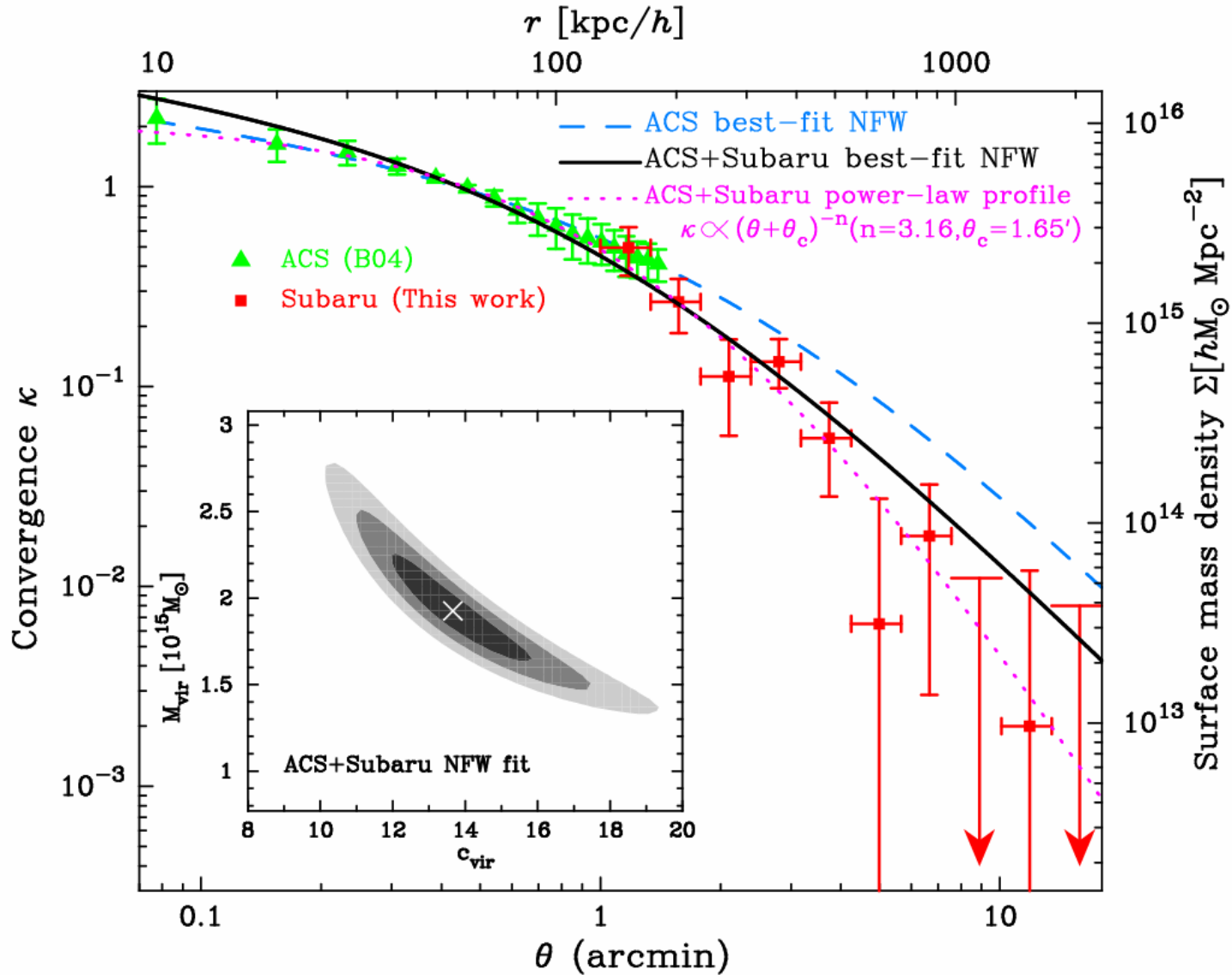
MS1008-1224:

Athreya et al 2002 ,
Lombardi et al 2001

Abell 1689
HST/ACS

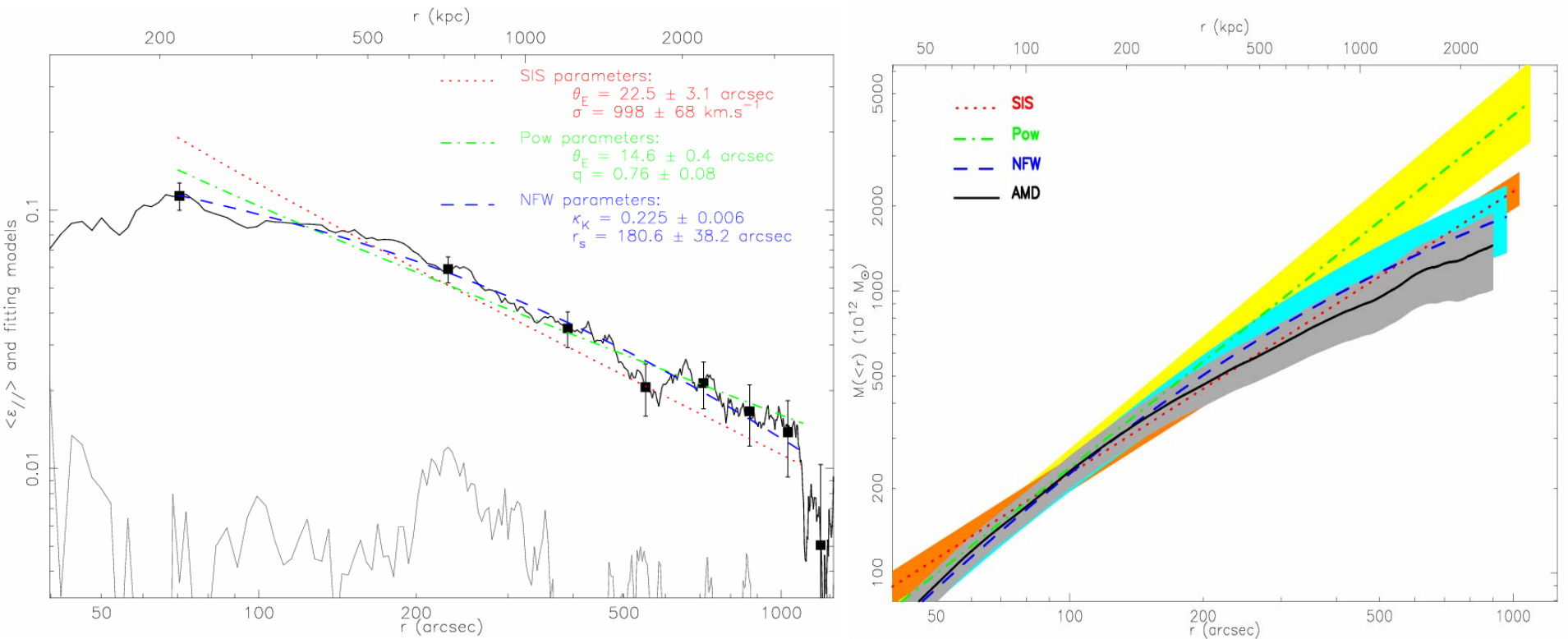


Abell 1689 HST/ACS

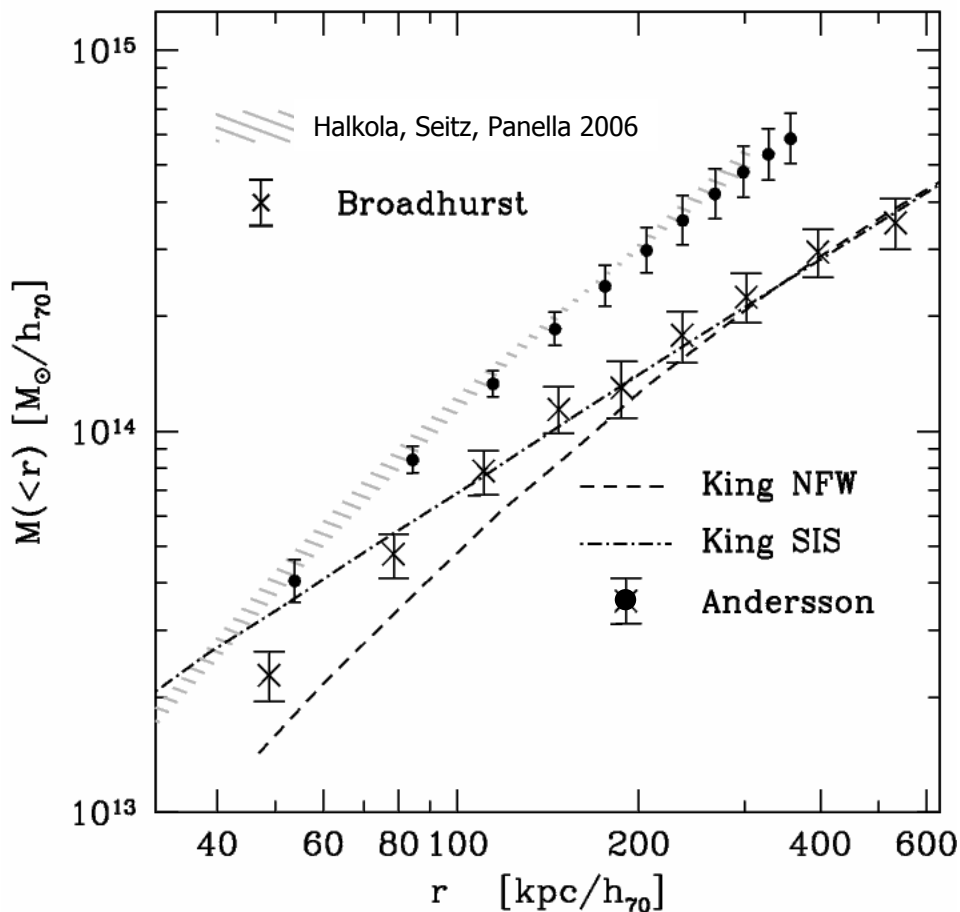


Abell 1689 ; CFH12k

Bardeau et al 2004



Abell 1689 HST/ACS revisited



Halkola, Seitz, Panella 2006

NFW Parameters

| Method | C | r_{200} (Mpc) | Reference |
|--------|---------------------|-----------------|---------------------------|
| SL | 6.0 ± 0.5 | 2.82 ± 0.11 | this work |
| SL | $6.5^{+1.9}_{-1.6}$ | 2.02 | Broadhurst et al. 2005a |
| X-ray | $7.7^{+1.7}_{-2.6}$ | 1.87 ± 0.36 | Andersson & Madejski 2004 |
| WL | 4.8 | 1.84 | King et al. 2002 |

NSIE Parameters

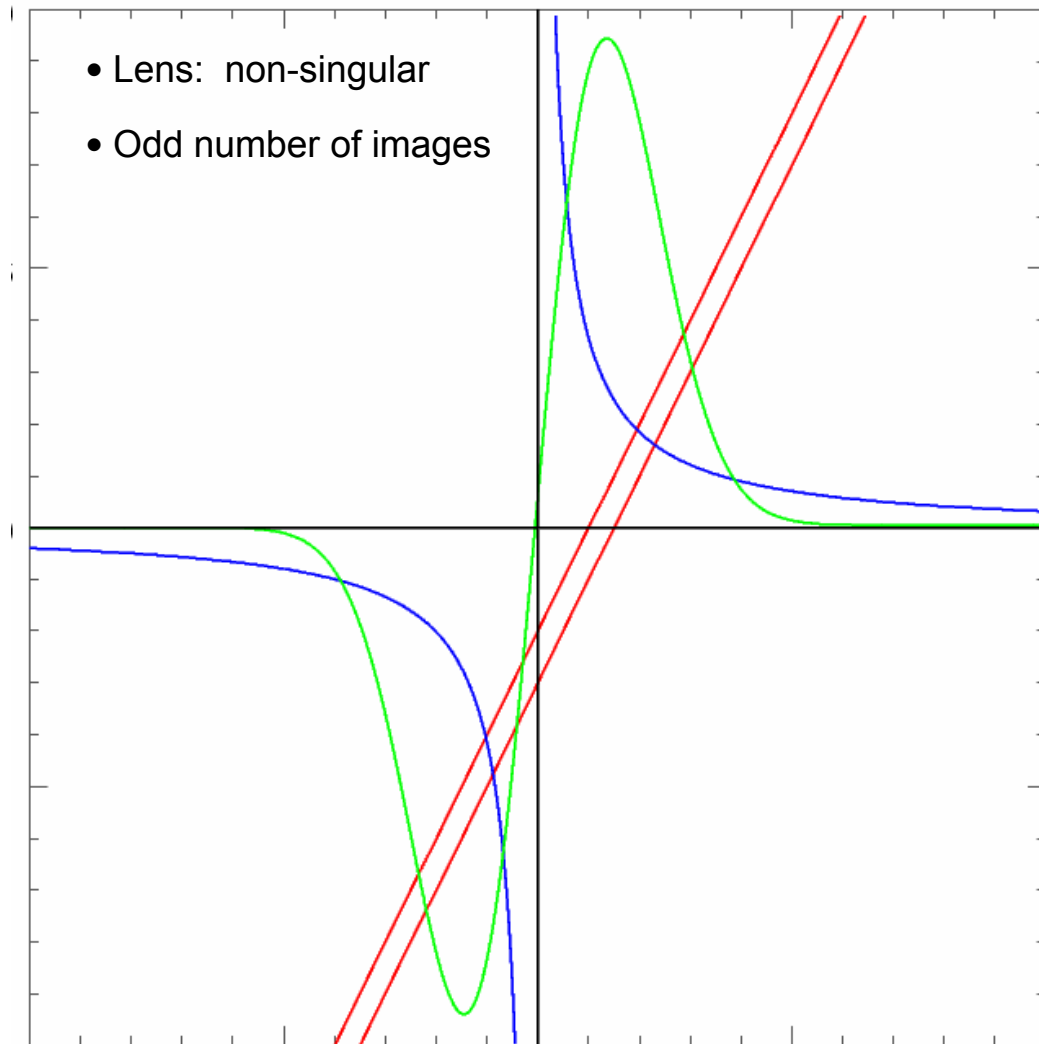
| Method | σ (km/s) | r_c (kpc) | Reference |
|--------|---------------------|-------------|----------------------------|
| SL | 1514 ± 18 | 71 ± 5 | this work |
| SL | 1390 | 60 | Broadhurst et al. 2005a |
| X-ray | 918 ± 27 | SIS | Andersson & Madejski 2004 |
| X-ray | 1190 | 27 | Andersson & Madejski 2004* |
| WL | 998^{+33}_{-42} | SIS | King et al. 2002 |
| LOSVD | 1429^{+145}_{-96} | - | Girardi et al. 1997 |

* data from Andersson & Madejski 2004, fitting done in this work.

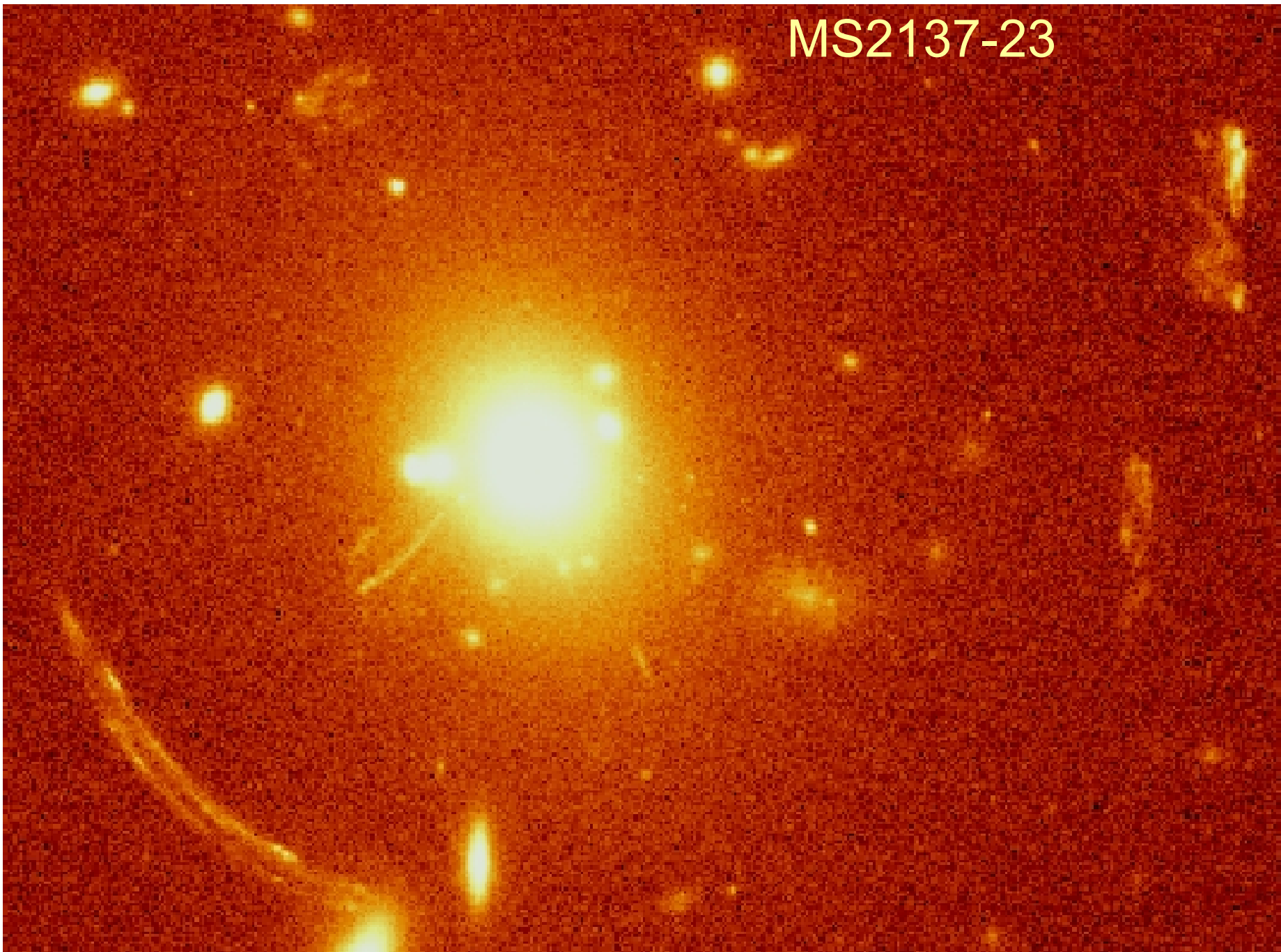
Table 6. Comparison between mass estimates for Abell 1689 from different methods. The mass measured by Andersson & Madejski (2004) are underestimates of the total mass if the cluster is undergoing a merger. For our work the mass at $r=0.25$ Mpc/ h_{70} is an extrapolation since the multiple images do not extend to such large clustercentric radii.

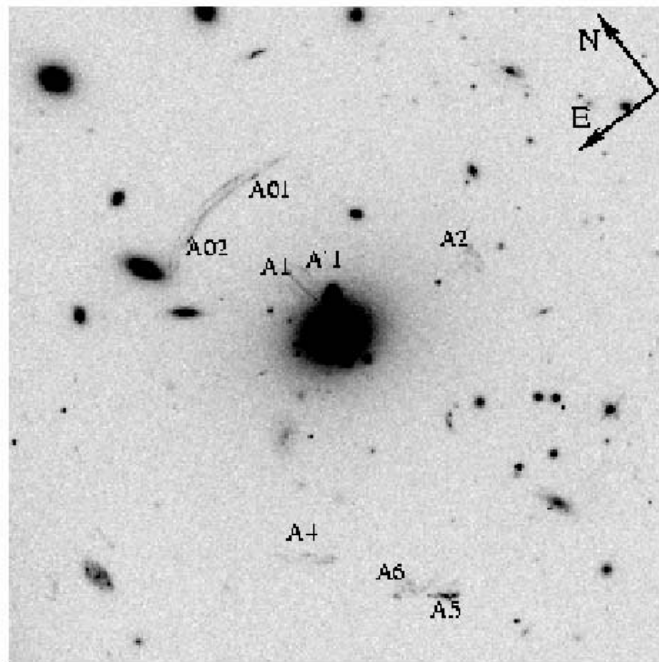
| $M(<r)$ ($10^{15} M_{\odot} h_{100}^{-1}$) | r (Mpc h_{100}^{-1}) | Reference |
|---|------------------------------|-----------------------------|
| 0.14 ± 0.01 | 0.10 | this work, Model III |
| 0.082 ± 0.013 | 0.10 | Andersson & Madejski (2004) |
| 0.43 ± 0.02 | 0.24 | Tyson & Fischer (1995) |
| 0.20 ± 0.03 | 0.25 | Andersson & Madejski (2004) |
| 0.37 ± 0.06 | 0.25 | this work, Model III |
| 0.48 ± 0.16 | 0.25 | Dye et al. (2001) |

Using radial arcs to constrain mass profile

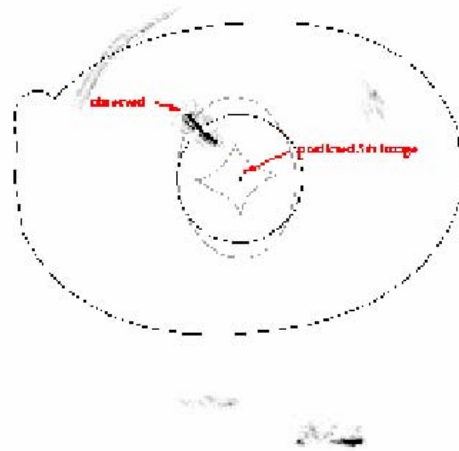


MS2137-23



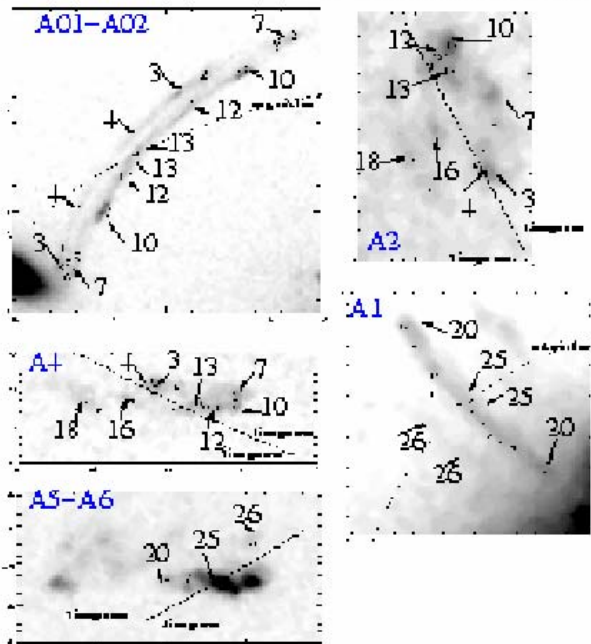


Softened isothermal

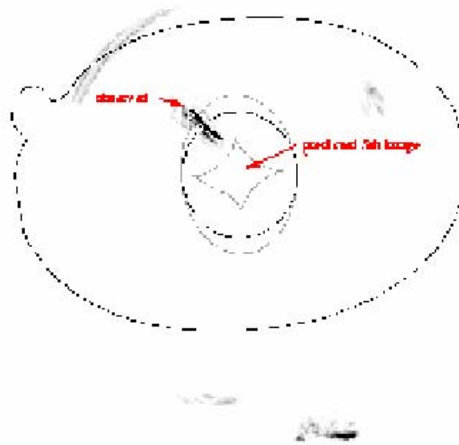


MS2137-23

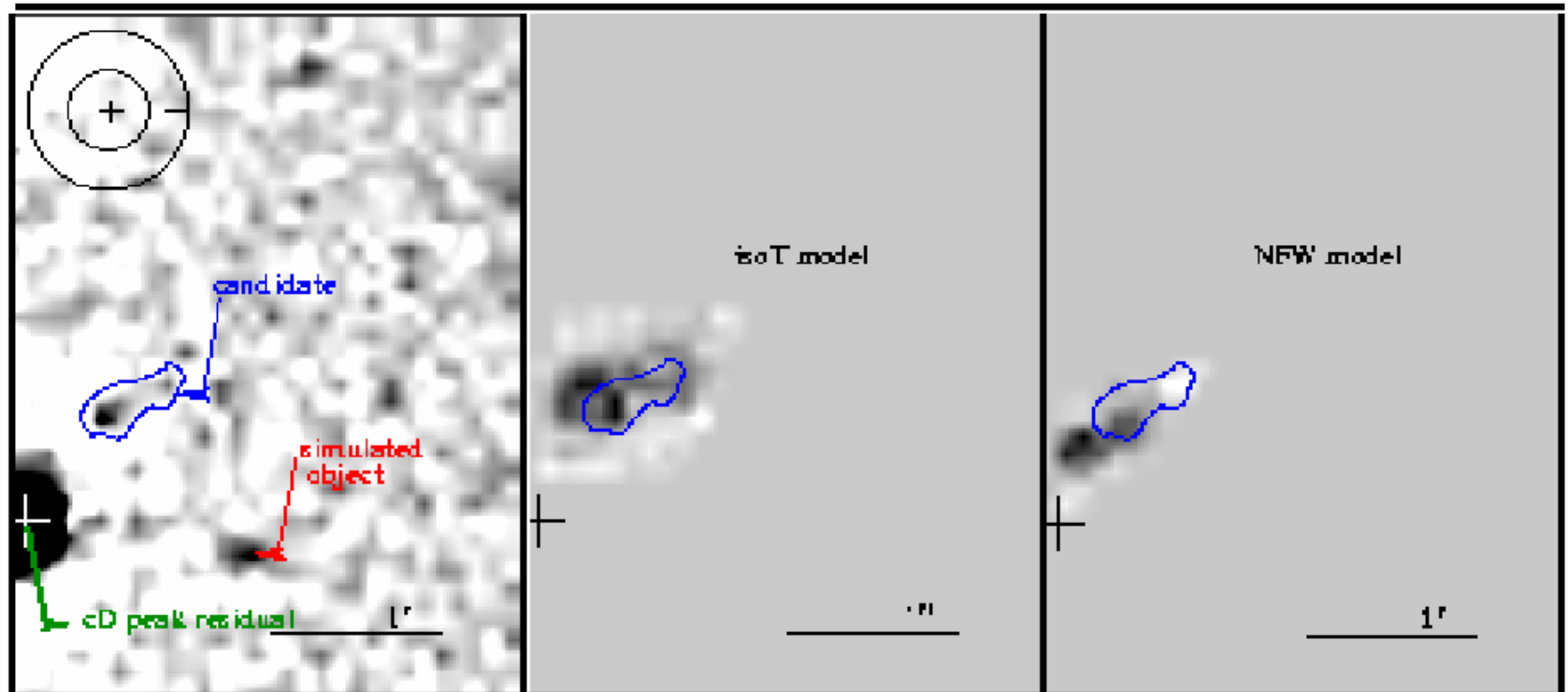
Gavazzi et al 2004



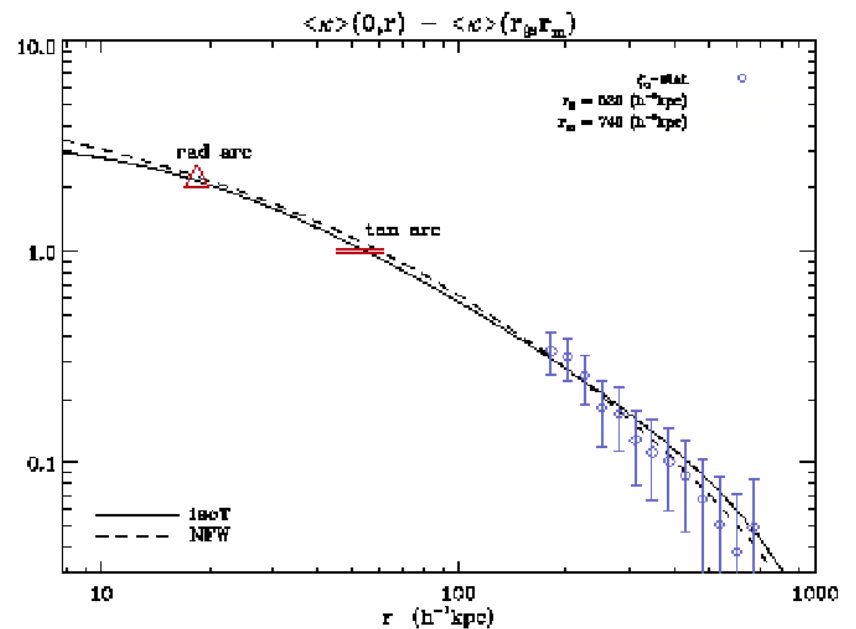
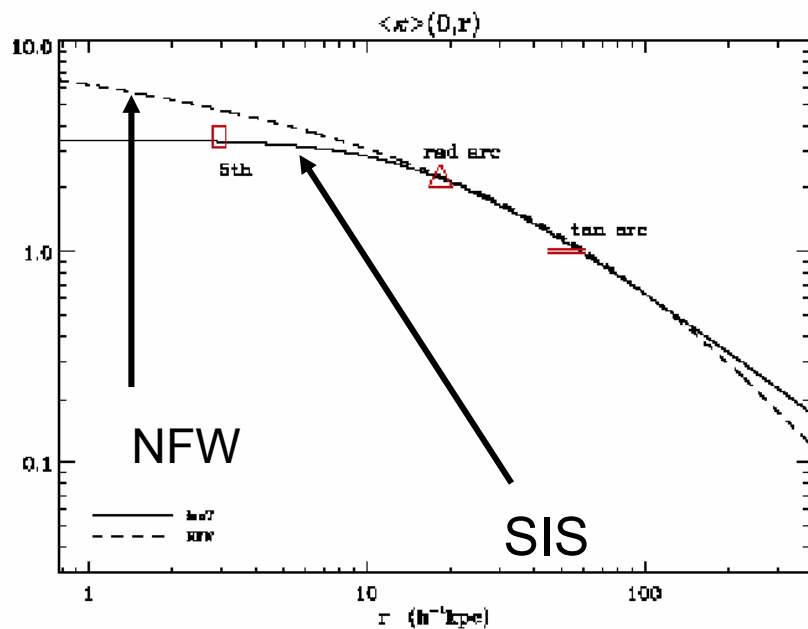
NFW



MS2137-23 Gavazzi et al 2004



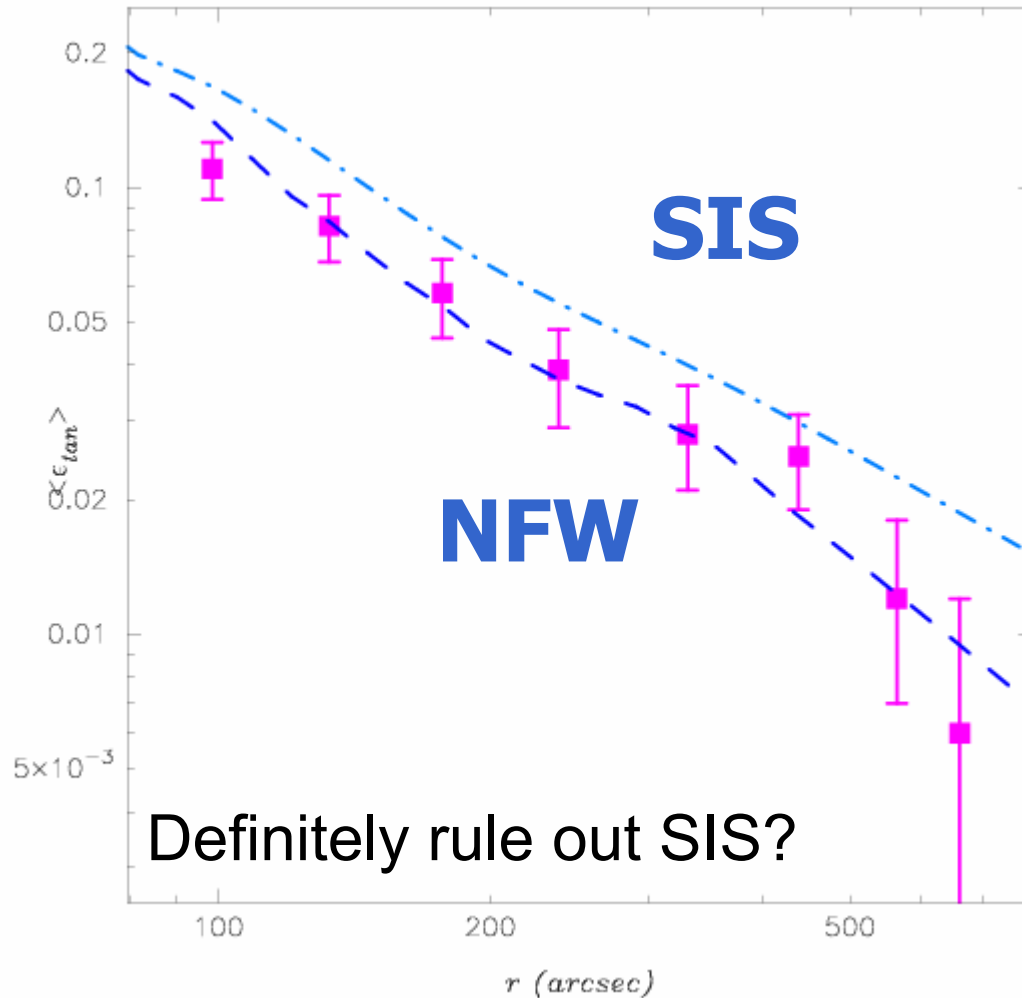
MS2137-23: strong + weak with the 5th image



Gavazzi et al 2004

CI0024 HST wide field data

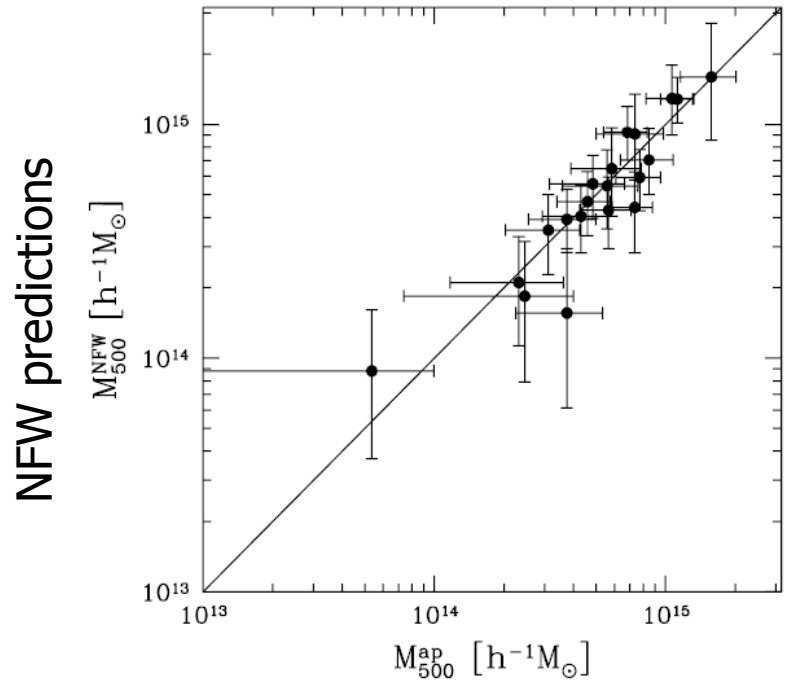
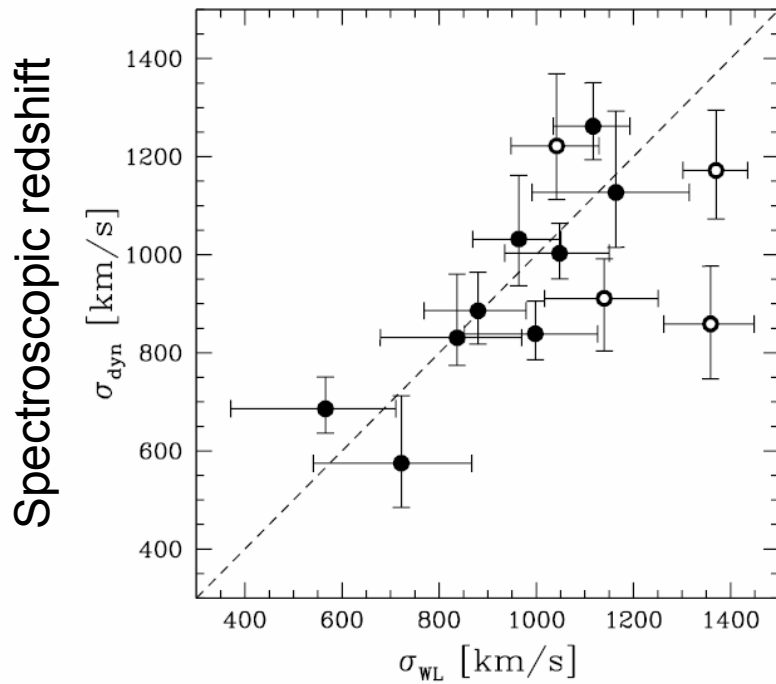
Kneib et al 2003



Summary

- Most Weak and/or Strong lensing data agree with NFW and SIS
- NFW not rejected (all data compatible with CDM predictions)
- Still hard to get a final answer, if any...

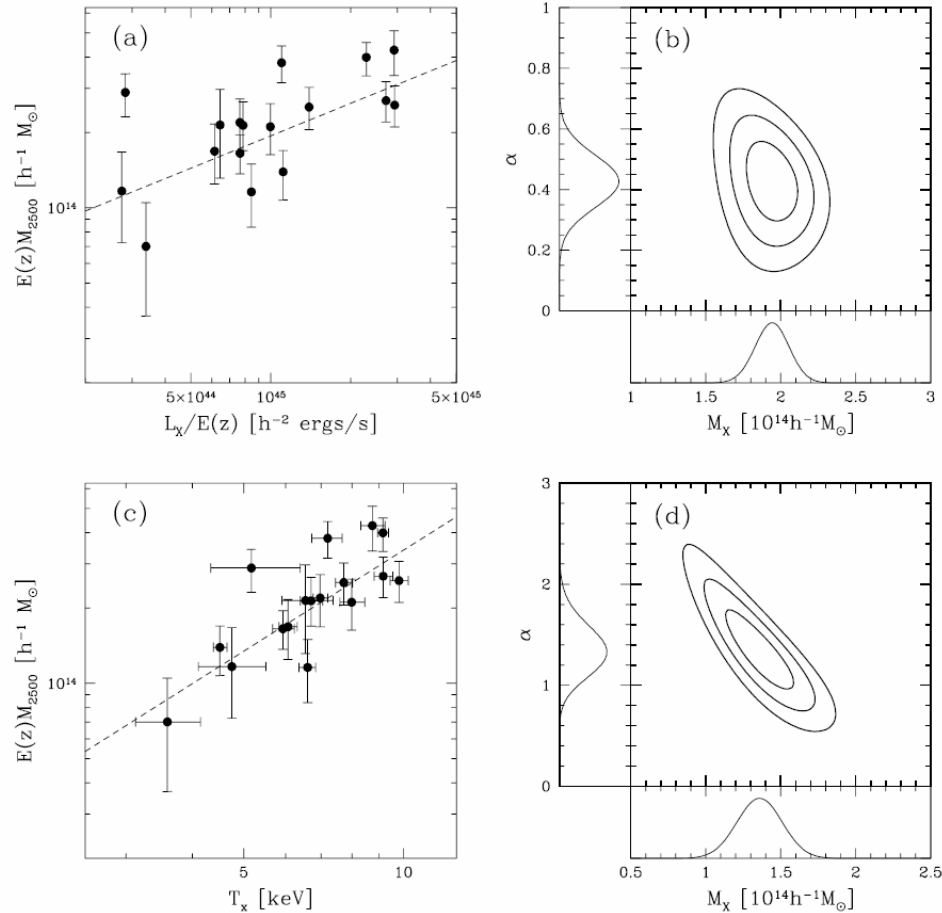
Most recent cluster survey



Map

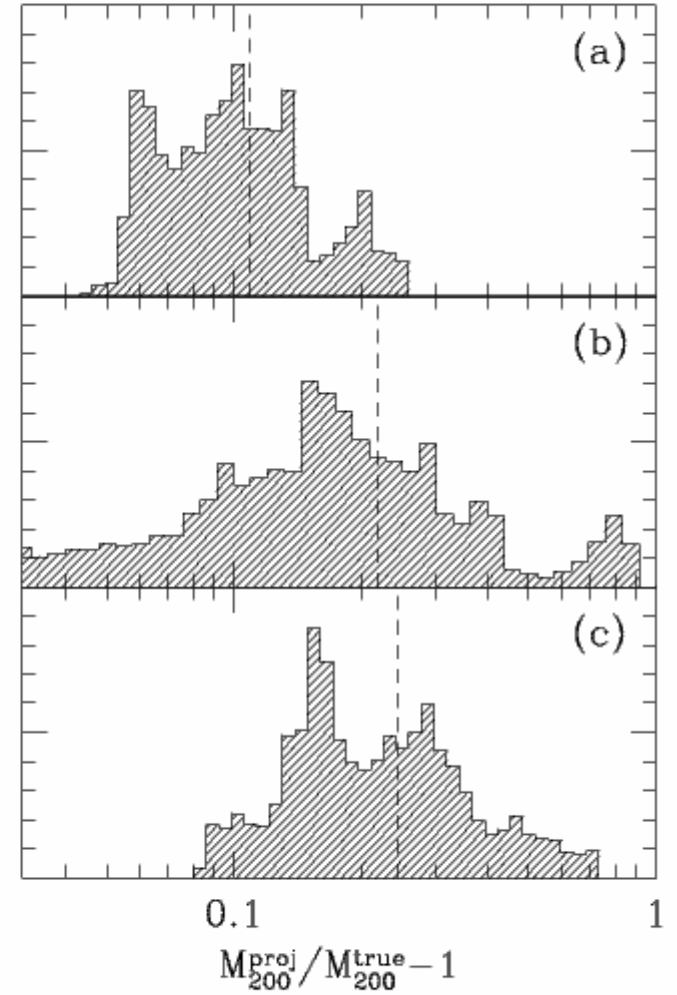
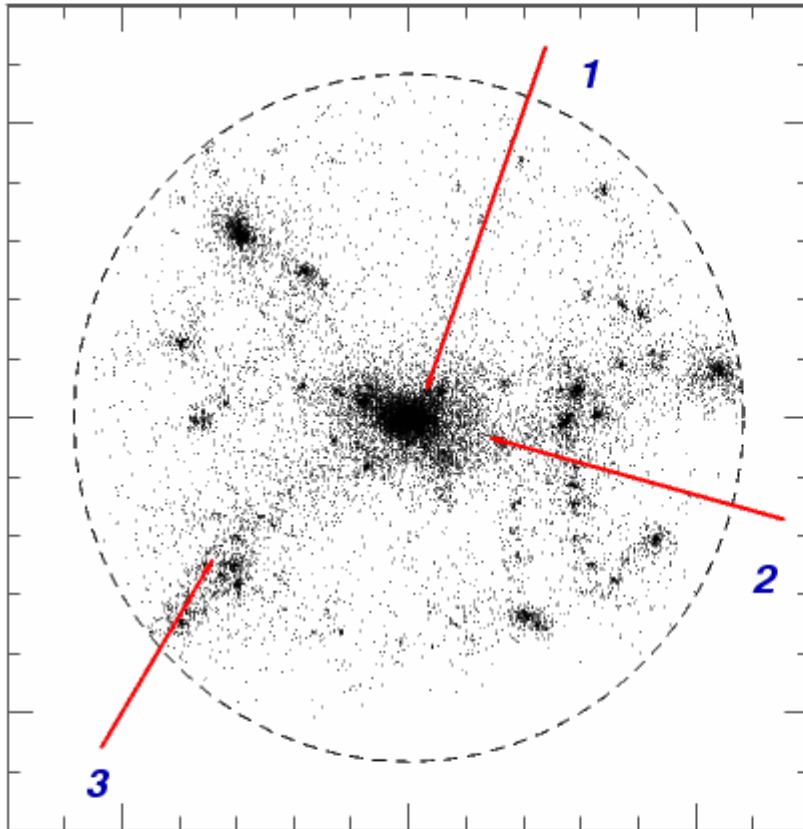
Hoekstra 2007

Most recent cluster survey: mass vs. L_x and T_x relations



Projection effects:
non negligible contamination

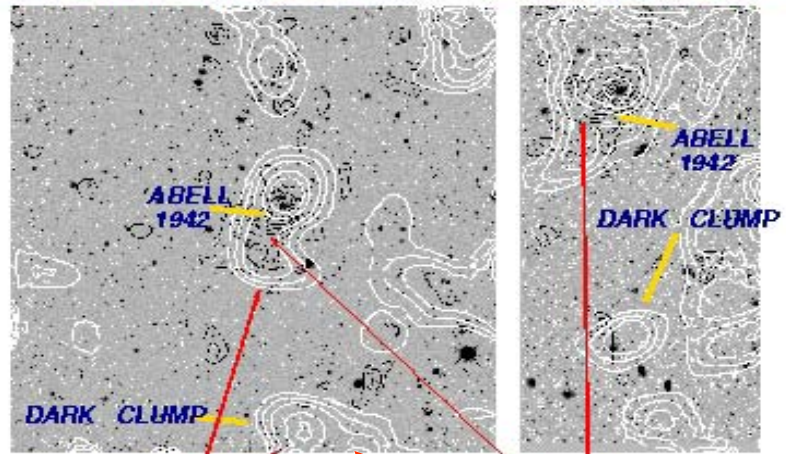
Metzler et al 2000



Dark Cluster ?

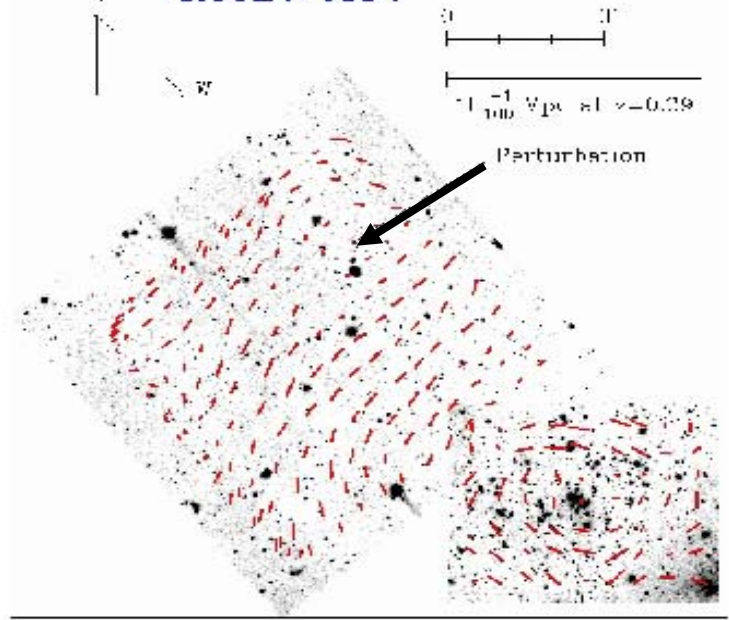
A DARK CLUMP IN Abell 1942
 ERBEN, van WAERBEKE, MELLIER et al 2000

MOCAM 4Kx4K CFHT V BAND 1995 UHSK 1CCD CFHT I BAND 1995

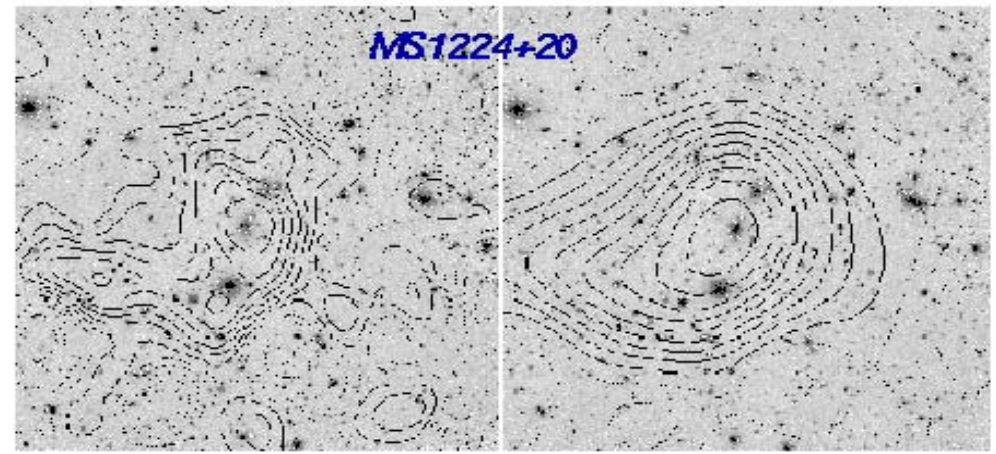


MASS DISTRIBUTION FROM WEAK LENSING (WHITE) LIGHT DISTRIBUTION (BLACK)
 No high-z cluster detected (Gray et al 2000) Bonnet, Mellier, Fort 1994

Cl0024+1654

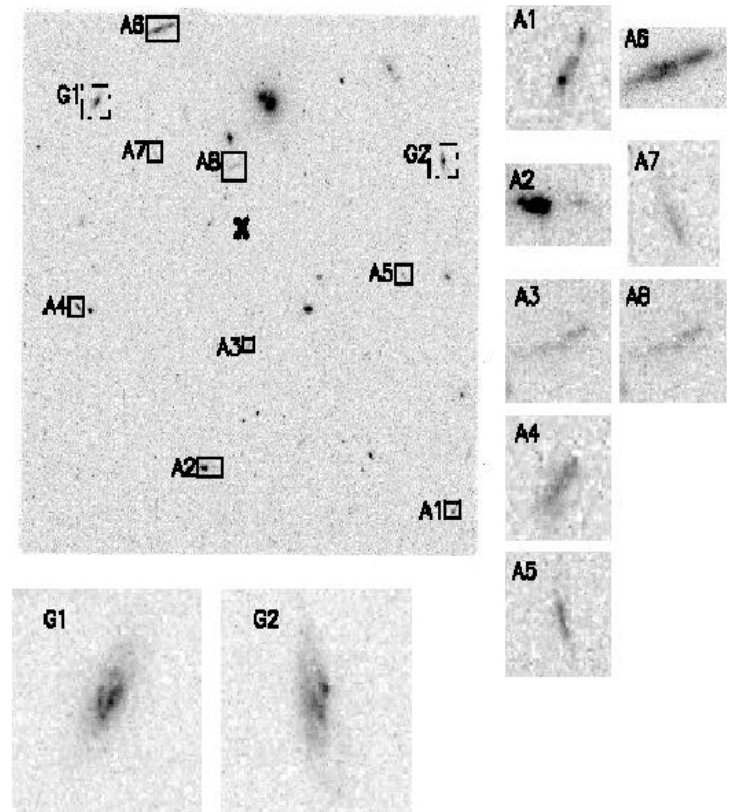


Dark Clusters ?

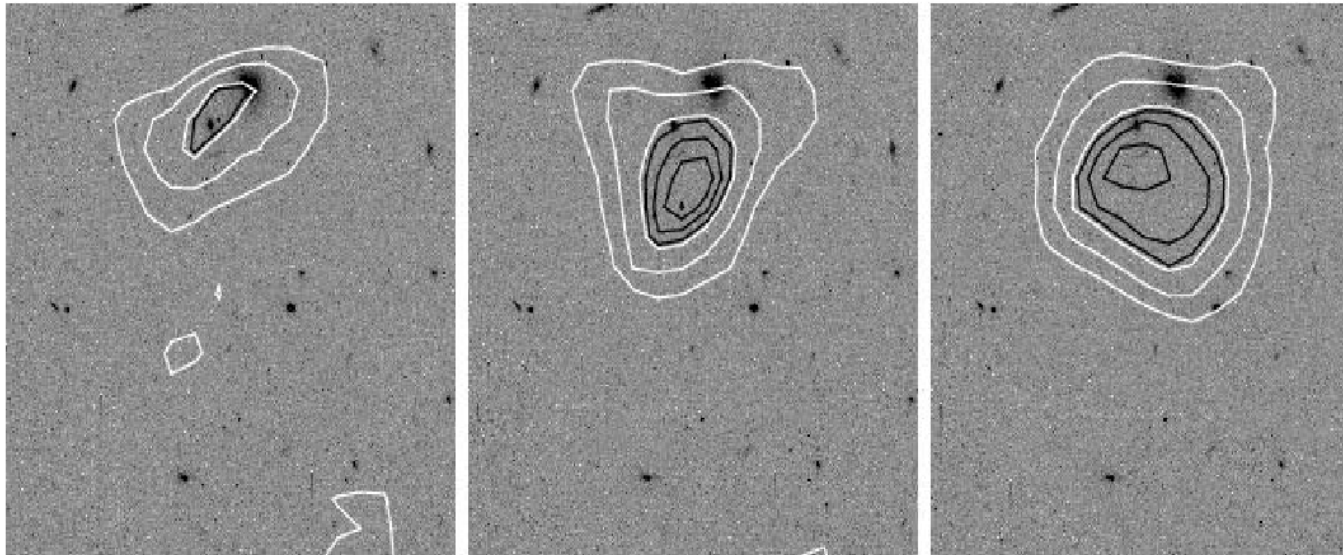


Fischer 2000 (see also Fahlman et al 1994)

An impressive candidate
with a remarkable
alignment of galaxies and
coherent mass map.....



Miralles, Erben, Haemmerle et al 2002



HST/STIS
data



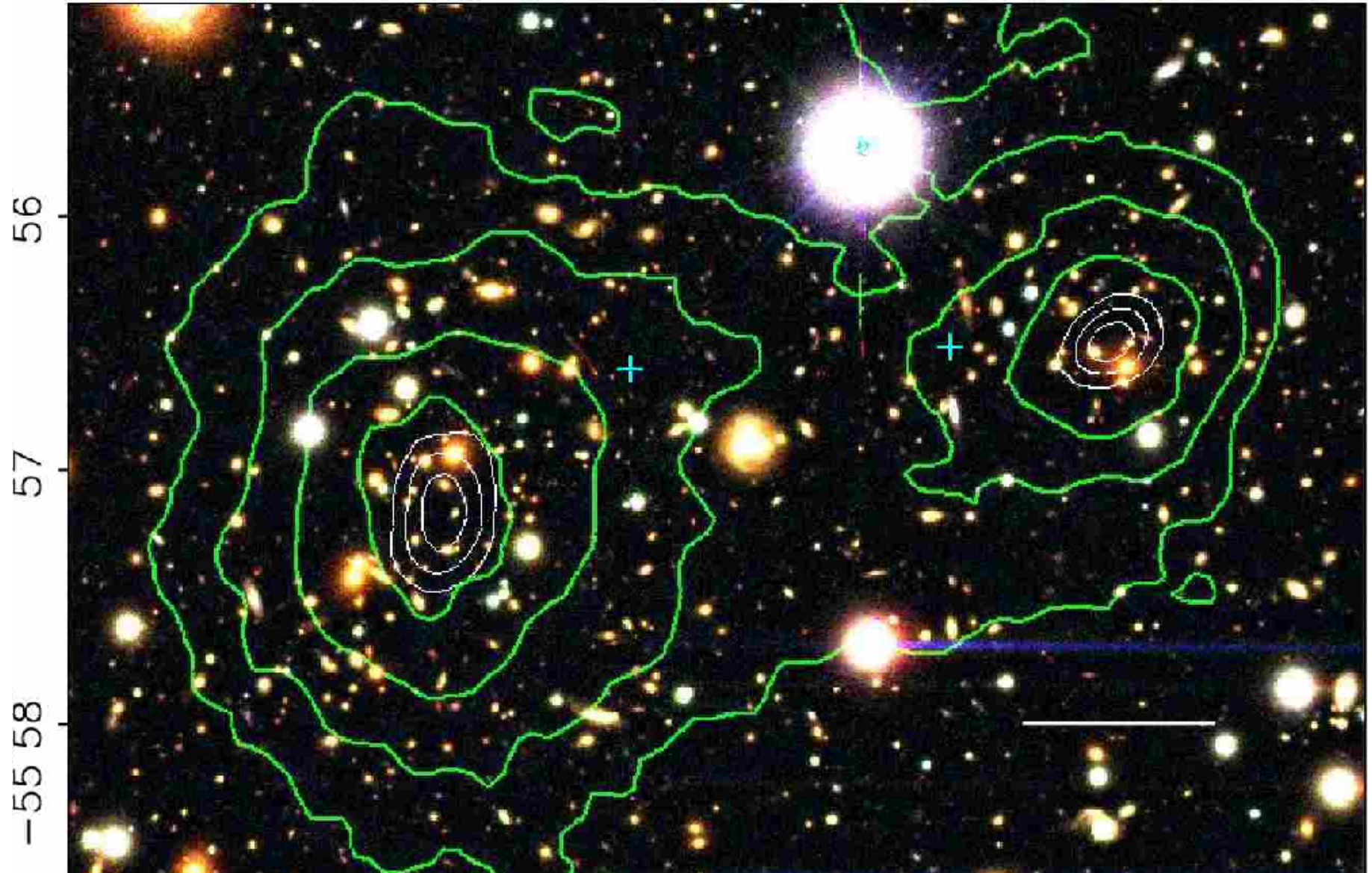
Dark clusters...

not yet convincing
evidence they exist...

The « Bullet » cluster

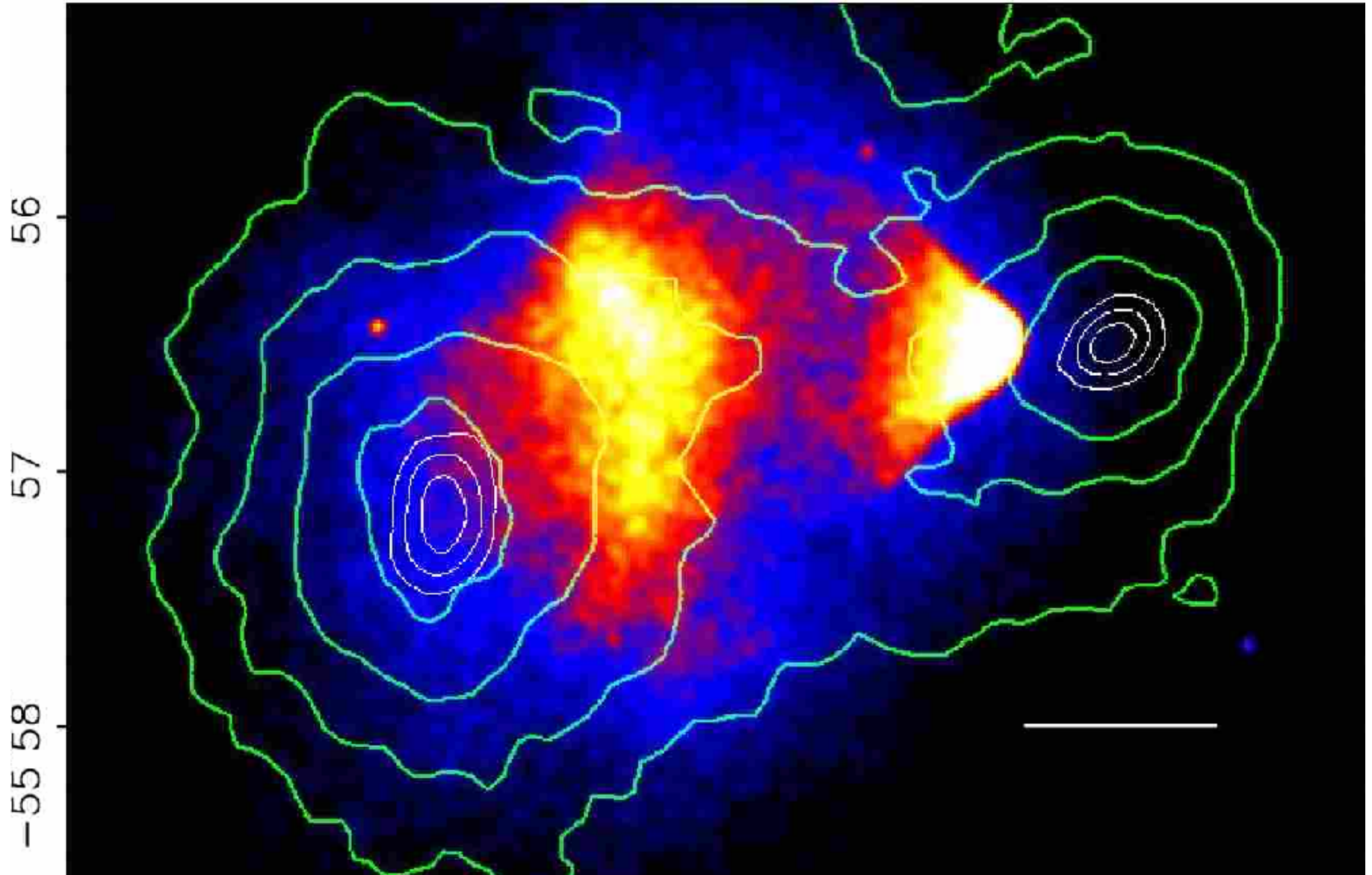
Bullet cluster

Clowe et al 2006



Bullet cluster

Clowe et al 2006



Bullet cluster : example of the interest of lensing

Clowe et al 2006

Mass map from Ellipticity->convergence: total matter

X-ray: baryonic matter

Bullet: baryonic matter decoupled from total mass

-> Clowe et al (2006): Dark matter exists!

Q1: X-ray emissivity is thermal bremsstrahlung? ... or shock?

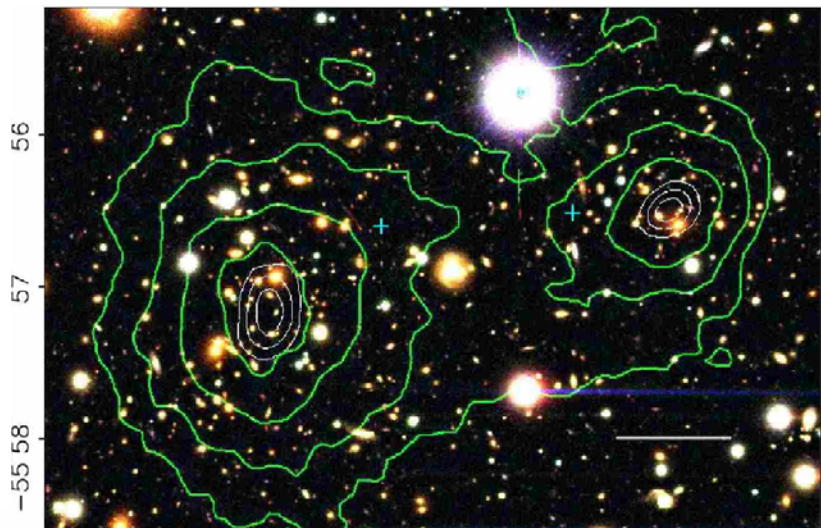
Q2: If shock, X-ray from baryons should be visible anyway and center mass positions, but not visible at the kappa center positions

Q3: Is ellipticity->gamma-> kappa calibration correct?

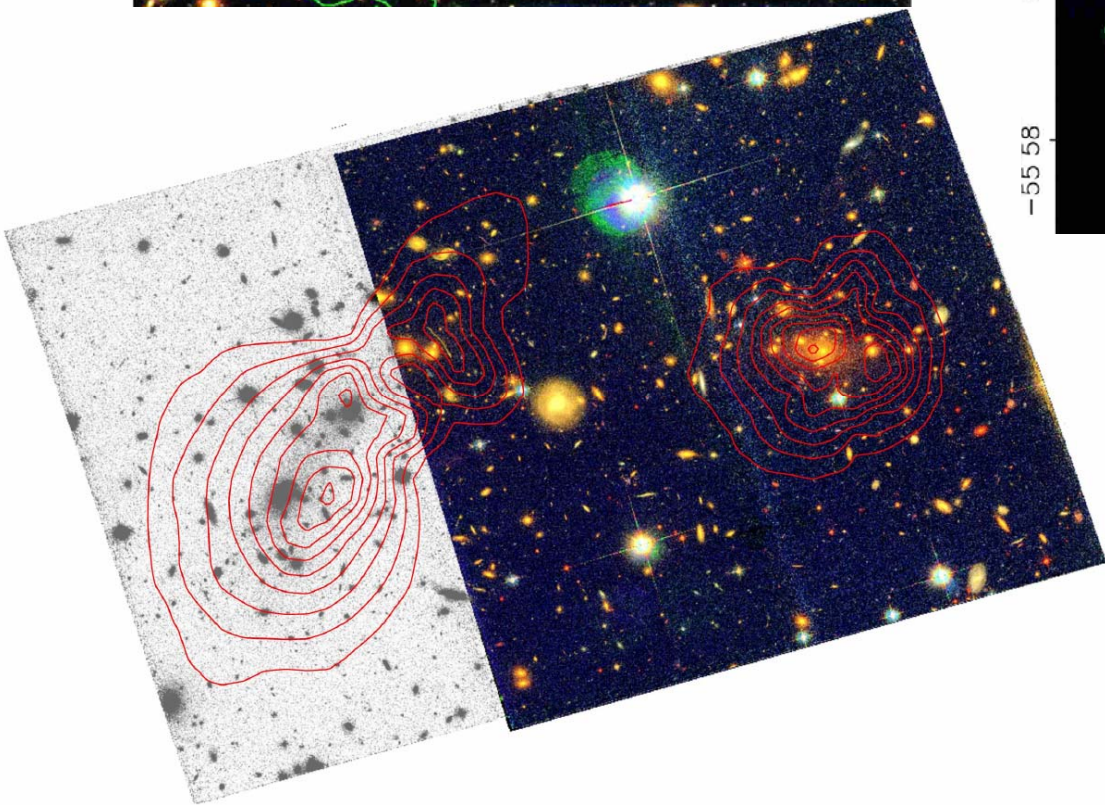
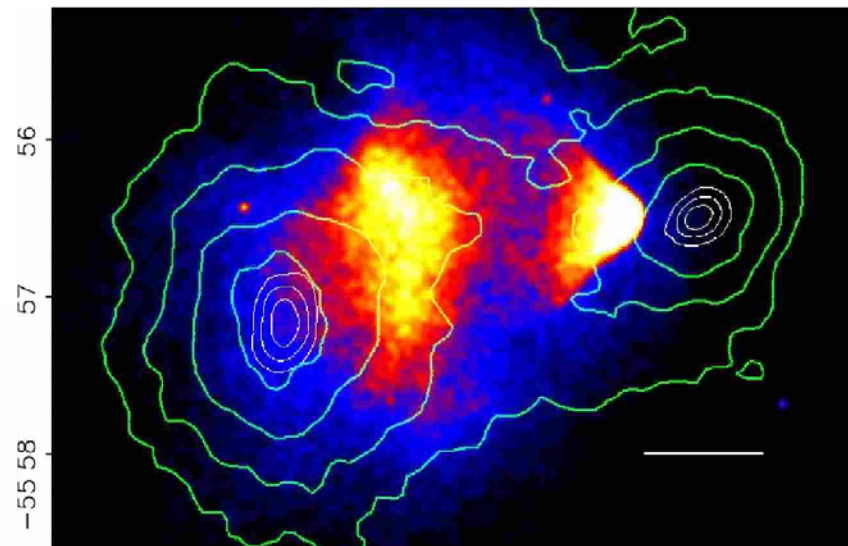
Q4: Is kappa=mass density (MOND: Berkenstein; Angus et al 2006)

Robust statement: the cluster is dominated by collisionless matter, but could be CDM or neutrino with mass~2eV?

Ground: weak



Chandra+weak



HST: strong+weak
(importance of depth: sampling
the mass density)

DM or collisionless matter (neutrino)?

Clowe et al: ground +weak +Chandra: DM exists!
MOND rejected!

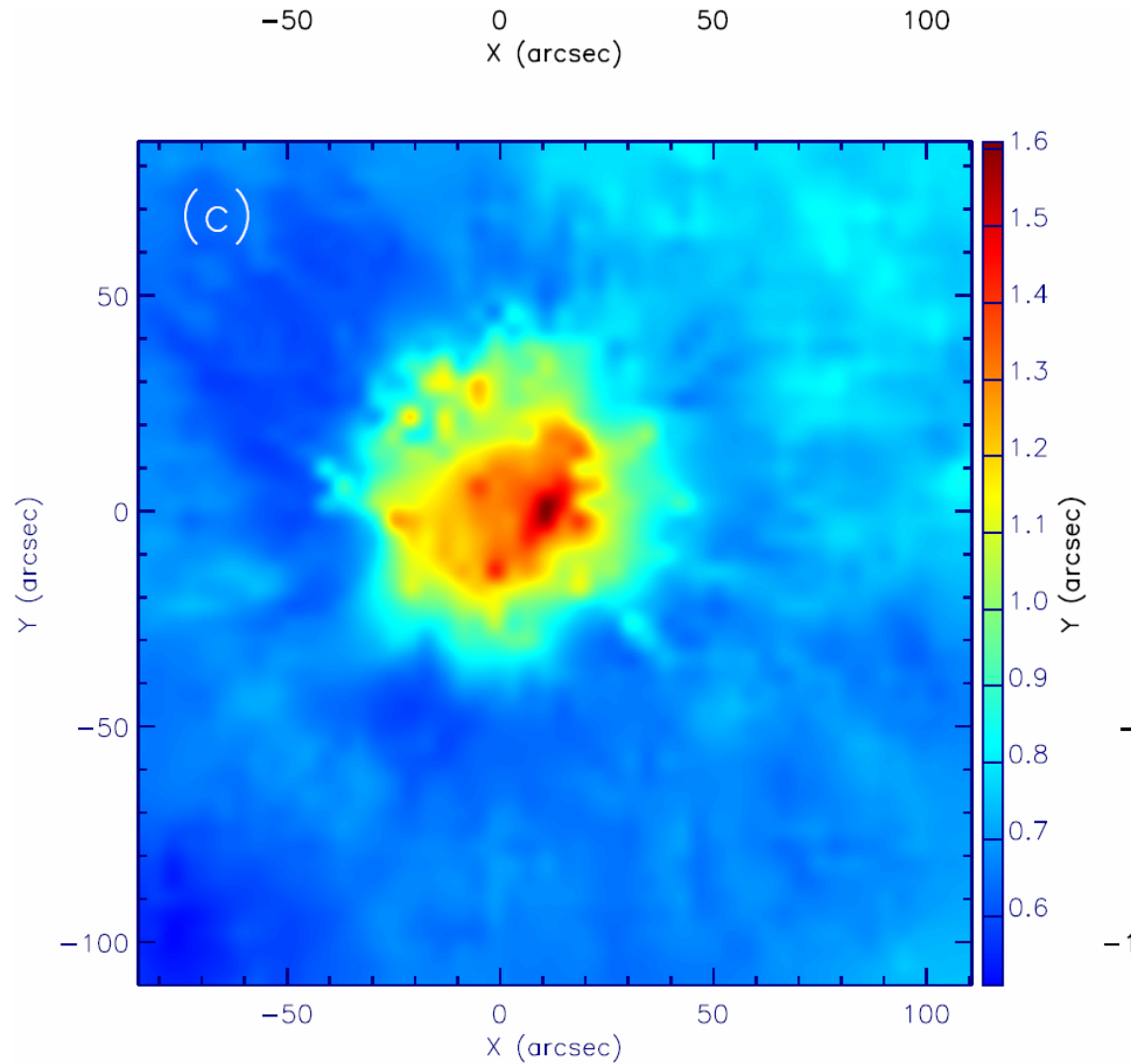
Angus et al: ground data + weak + chandra
compatible with modifies gravity AND neutrino with
mass ~ 2 eV

Clowe et al : HST strong+Weak + chandra : new
mass distribution would imply neutrino with mass of
3.6 eV. Already rulled out !

Bartelmann et al 2007: confirm Clowe et al

The « Ring » in C10024+1654

The « Ring » in Cl0024+1654



Jee et al 2007

III. Gravitational Lensing:

galaxy-size halos

Galaxy-Galaxy lensing

Distortion of foreground halos on the background galaxies

In the weak lensing regime:

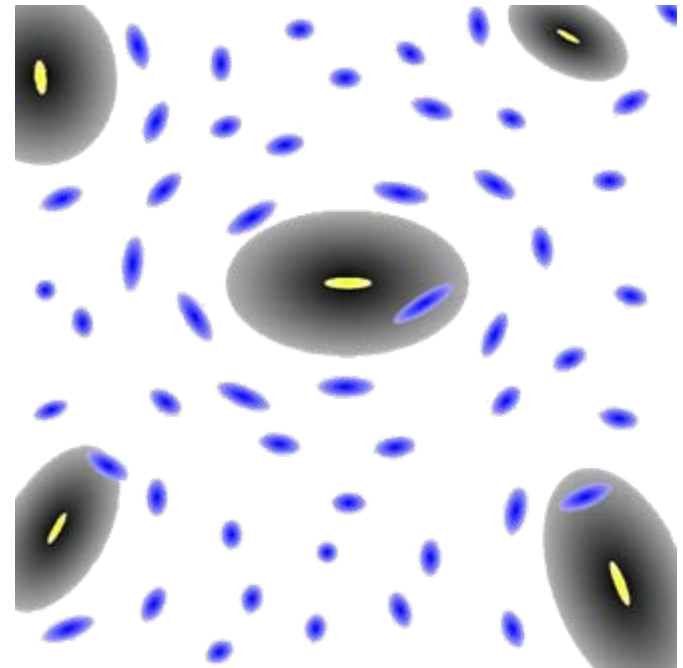
$$\epsilon^s = \epsilon - \gamma$$

Therefore:

$$p(\epsilon) = p^{(s)}(\epsilon - \gamma) = p^{(s)}(\epsilon) - \gamma_\alpha \frac{\partial}{\partial \epsilon_\alpha} p^{(s)}(\epsilon)$$

$$\int d^2\epsilon p(\epsilon) = 2\pi \int d\epsilon \epsilon p(\epsilon) = 1$$

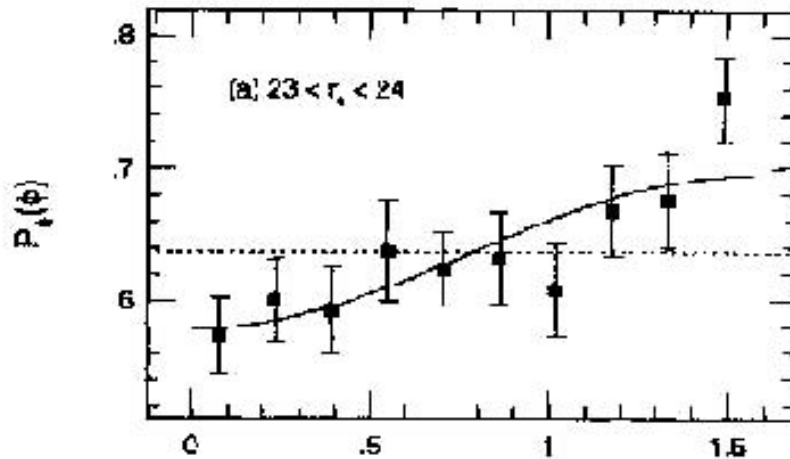
$$\left\langle \frac{1}{\epsilon} \right\rangle = \int d^2\epsilon \frac{p(\epsilon)}{\epsilon} = 2\pi \int d\epsilon \epsilon \frac{p(\epsilon)}{\epsilon}$$



Galaxy-Galaxy lensing

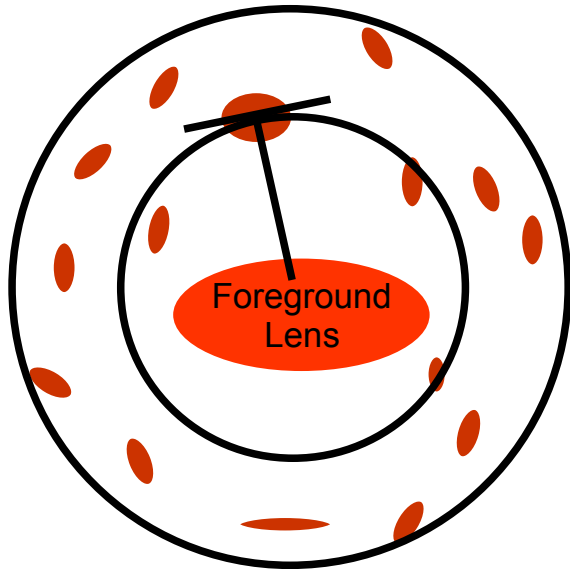
One can then express the modification of the orientation distribution produced by the foreground

$$p(\phi) = \frac{2}{\pi} \left[1 - \langle p \rangle \cos(2\phi) \left\langle \frac{1}{\epsilon} \right\rangle \right]$$

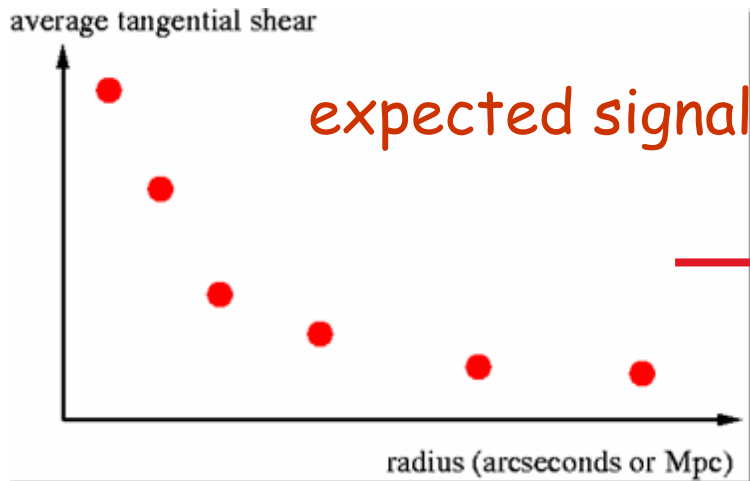


Brainerd et al 1996

Galaxy-Galaxy lensing



- Measure tangential component of shape in bins
- Need to stack signal around MANY foreground lenses

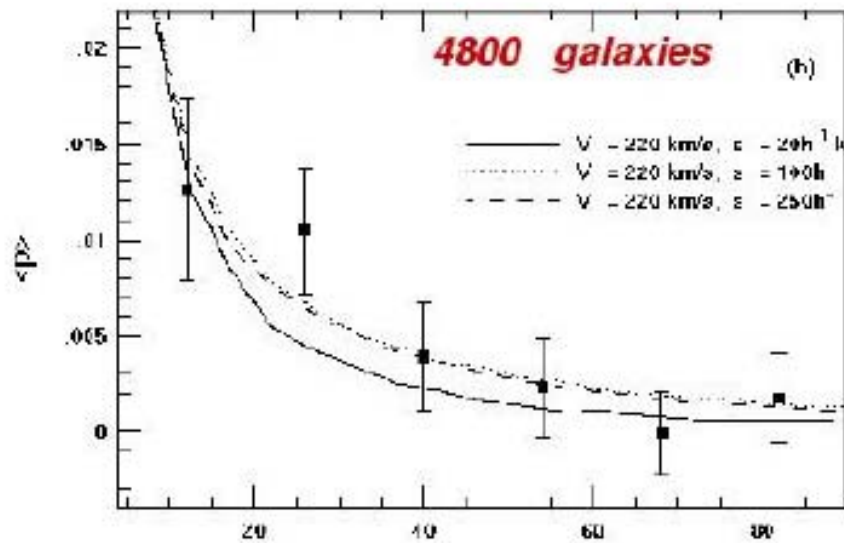


fit signal with your favourite mass profile

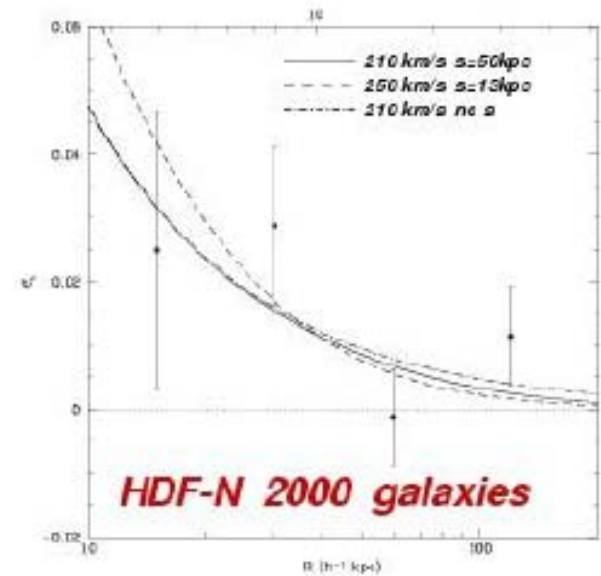
(From Parker 2007)

Galaxy-Galaxy lensing

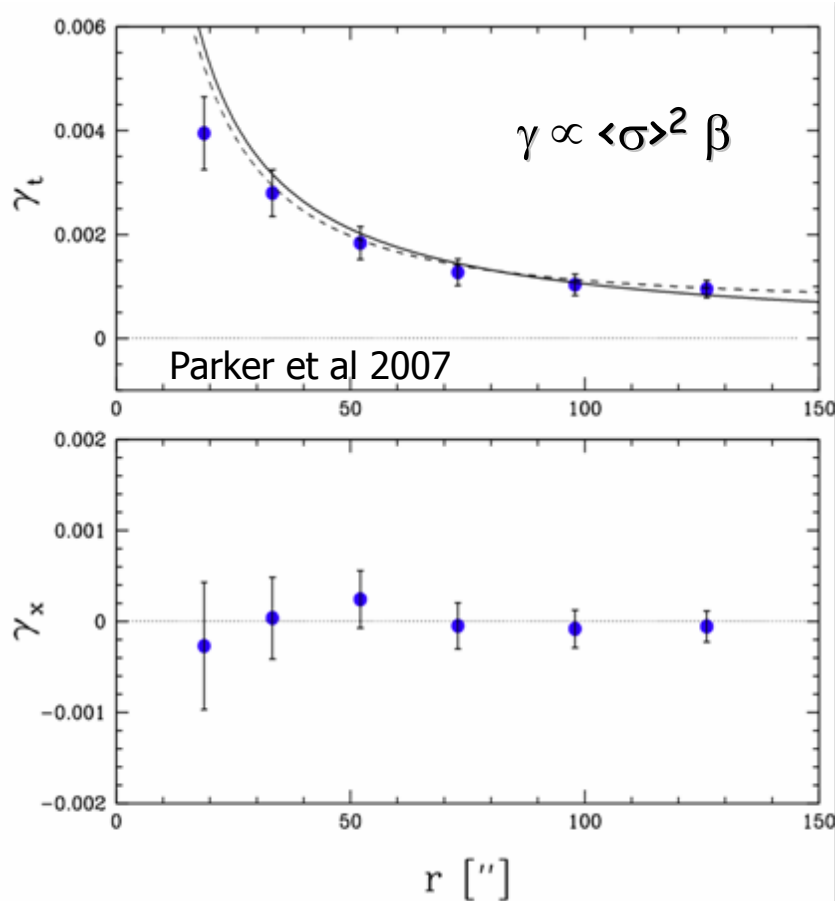
Brainerd et al 1996



Hudson et al 1999.



Galaxy-Galaxy lensing in CFHTLS



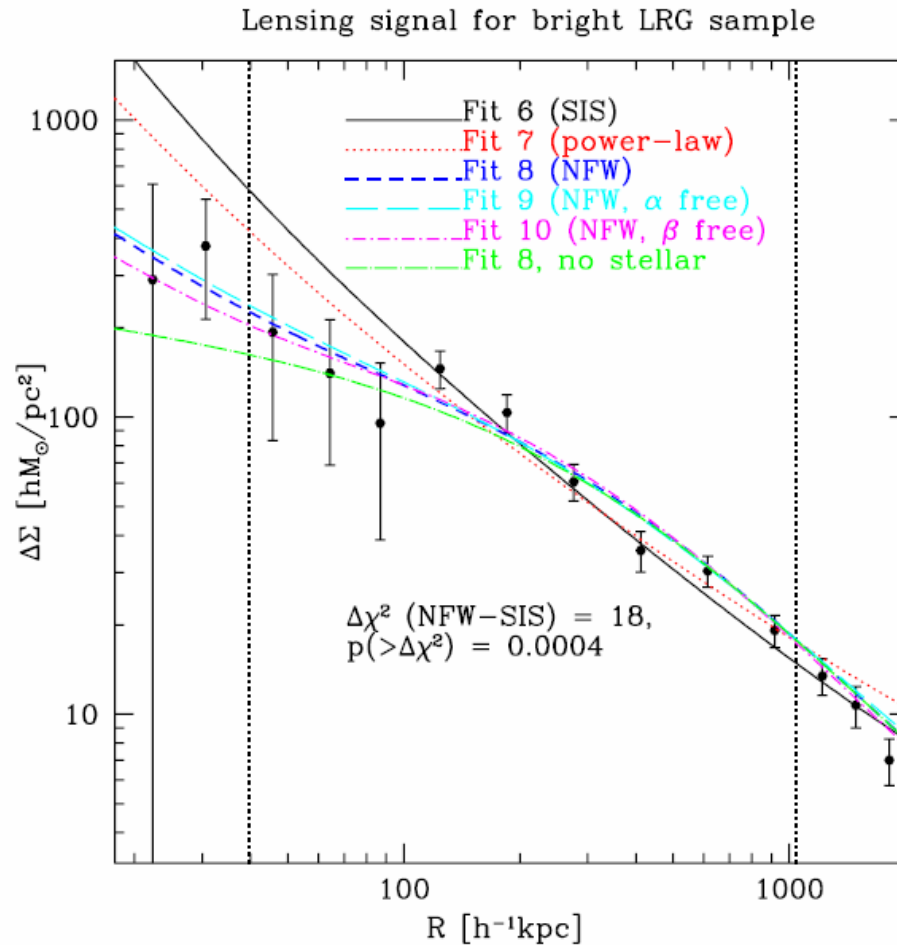
- Velocity dispersion depends on the lens sample.
- Must scale to some typical L^* galaxy, based on an assumed relation between L and velocity (σ prop.to $L^{0.25}$, for example)
- Use σ^* to estimate the total mass of the halo assuming a cut-off radius

| $\langle \sigma \rangle$ km/s | $\langle \sigma \rangle^*$ km/s | Mass total | Mass at r_{200} | $\langle M/L \rangle$ R- |
|----------------------------------|------------------------------------|---------------|----------------------|-----------------------------|
| 132+/-10 | 137+/-11 | 2.2e12 | 1.1e12 | 170+/-30 |

- well-fit with a SIS with a velocity dispersion of 132 +/- 10 km/s
- best fit NFW (dashed) has $r_{200} = 150 h^{-1} \text{kpc}$

(From Parker 2007)

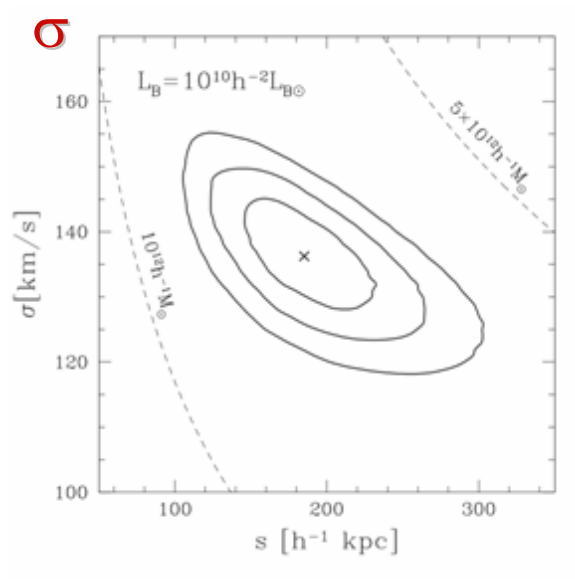
Mass density profile of Luminous Red Galaxies in SDSS using galaxy-galaxy lensing



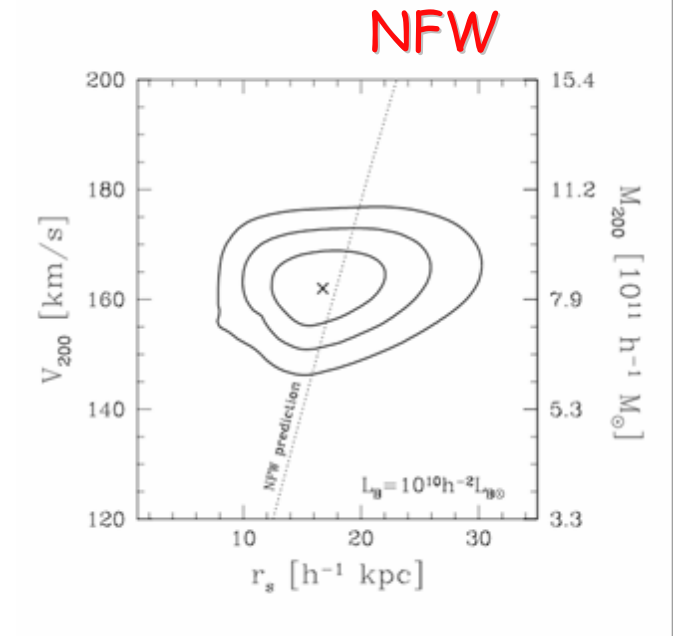
Maudelbaum et al 2006: reject SIS and favor NFW

Extents of halos: CFHTLS

- Maximum likelihood technique to fit for halo model
- For each source you determine the influence from all nearby foreground lenses with a parameterised lens model

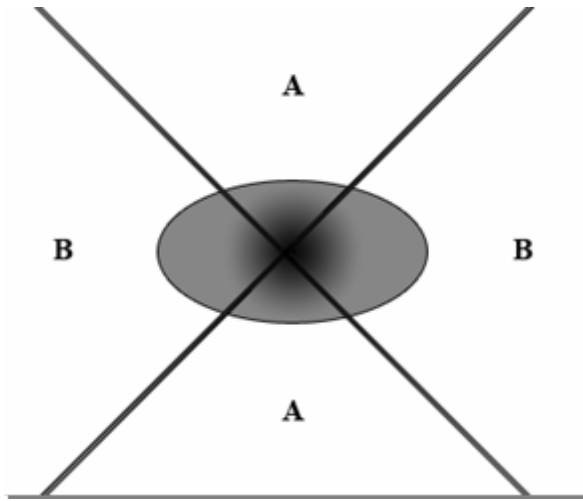


$$\rho(r) = \frac{\sigma^2 s^2}{2\pi G r^2 (r^2 + s^2)}$$



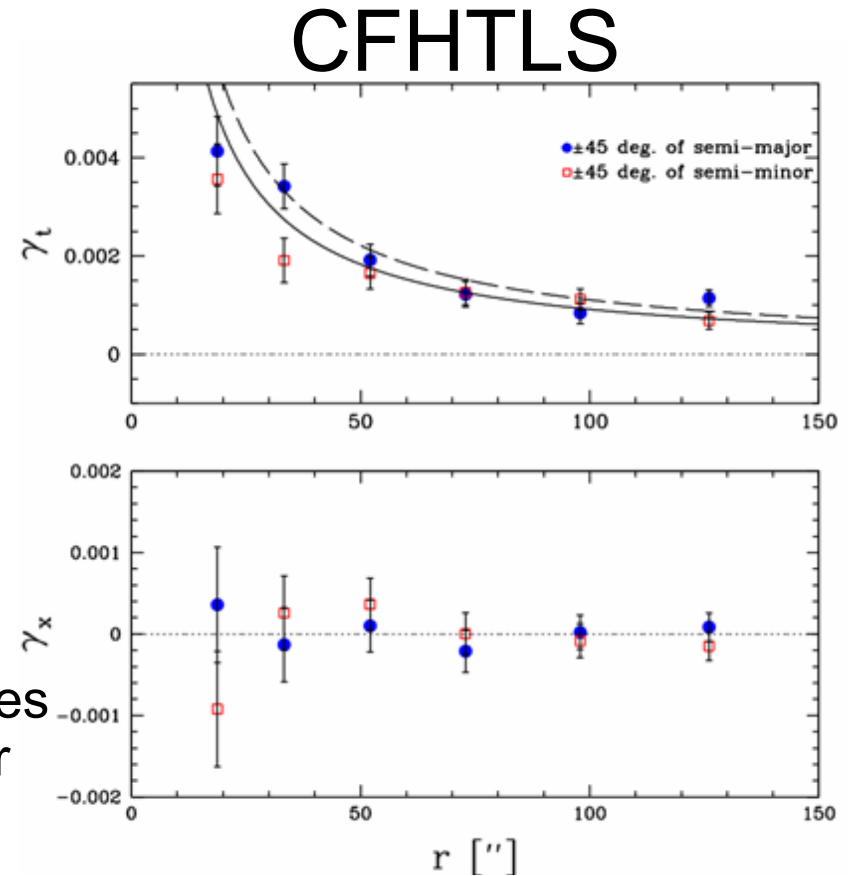
$$\rho(r) = \frac{\delta_c \rho_c}{(r/r_s)(1+r/r_s)^2}$$

Halo shapes from galaxy-galaxy lensing



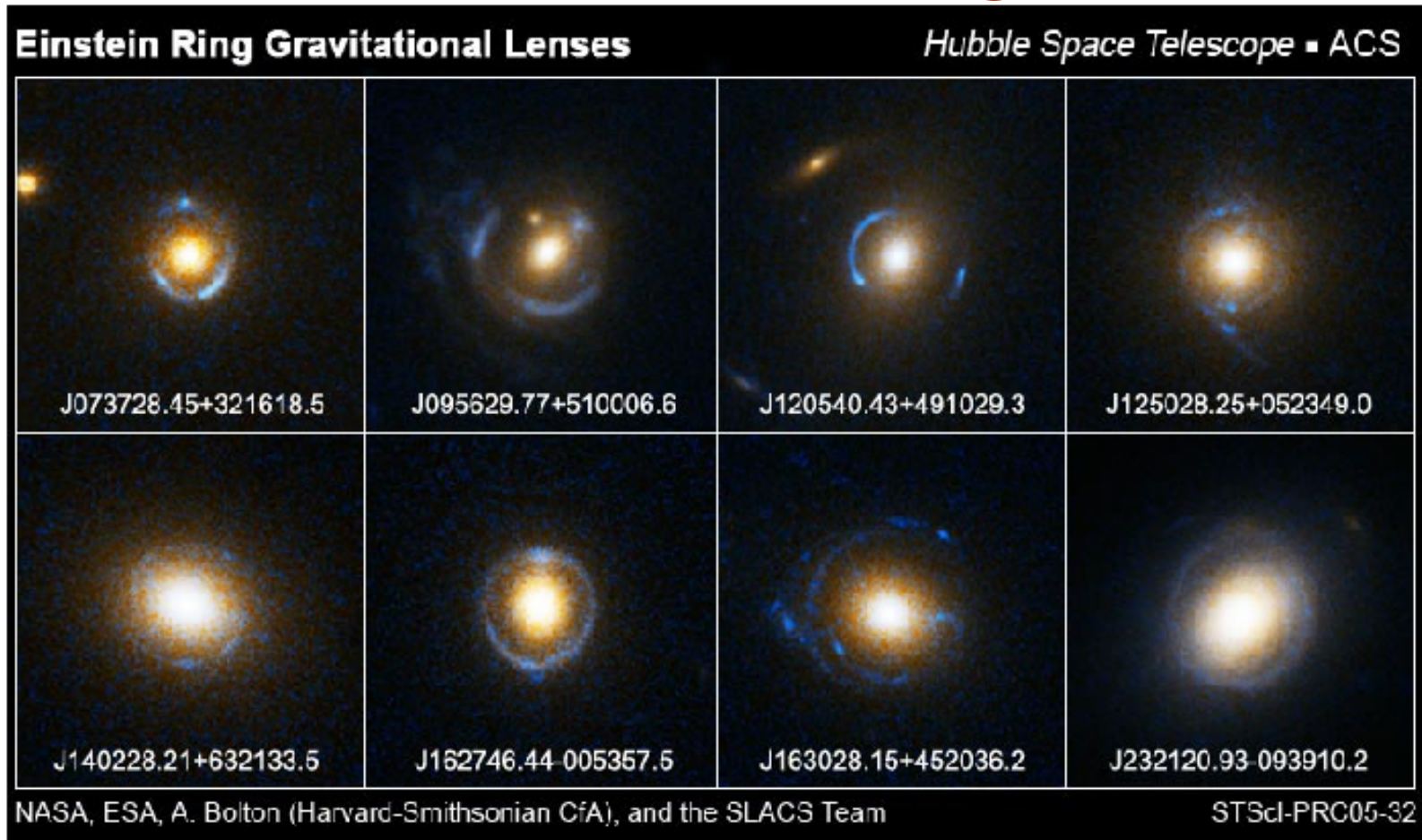
- Look for non-spherical halo shapes by comparing the tangential shear from sources near the major axis to those near the minor

- Halo flattening was observed in a weak lensing analysis of RCS data (Hoekstra et al., 2004), but not in SDSS by Mandelbaum et al. (2005)



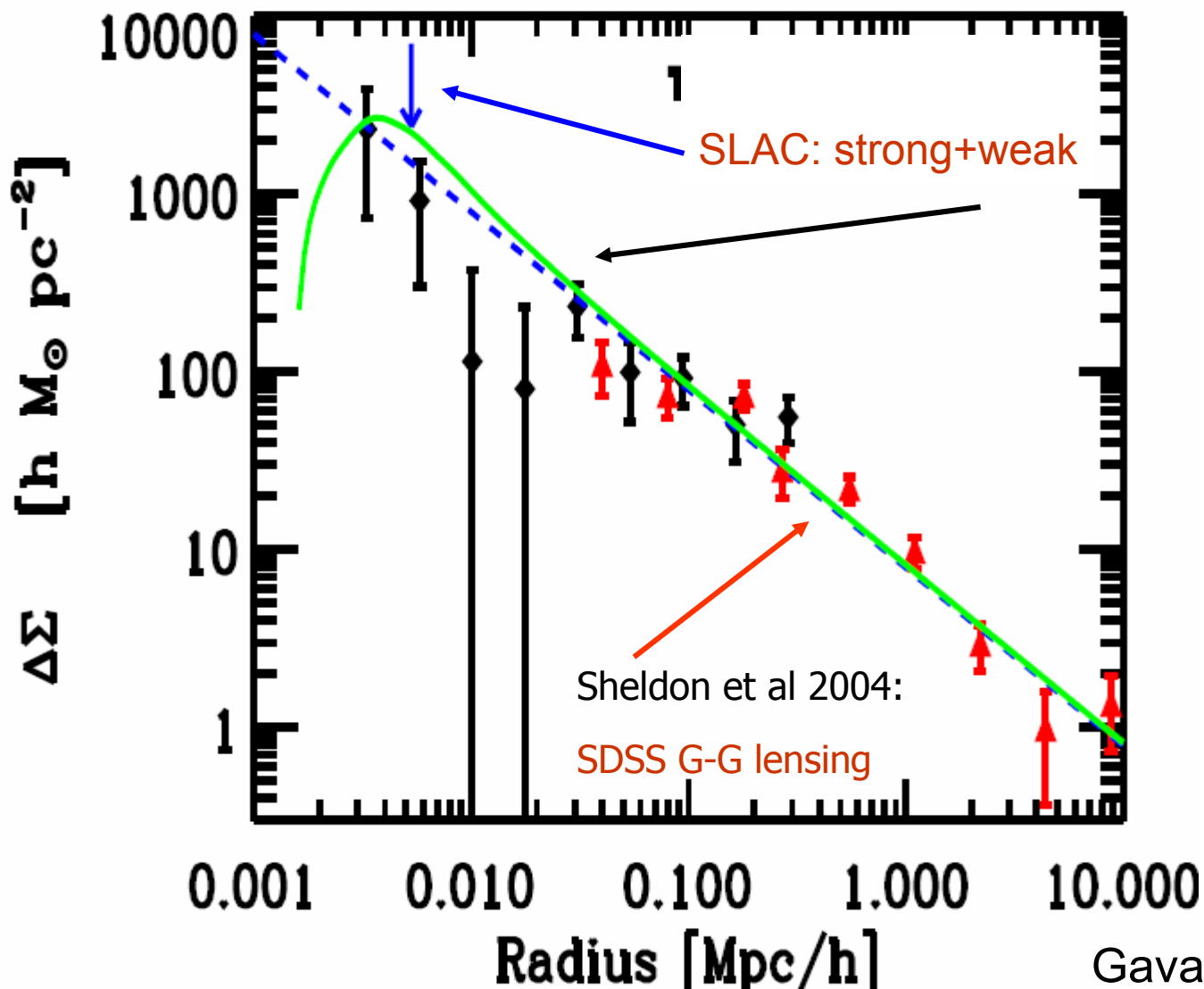
(Parker 2007)

Properties of galaxy halos using Einstein Rings

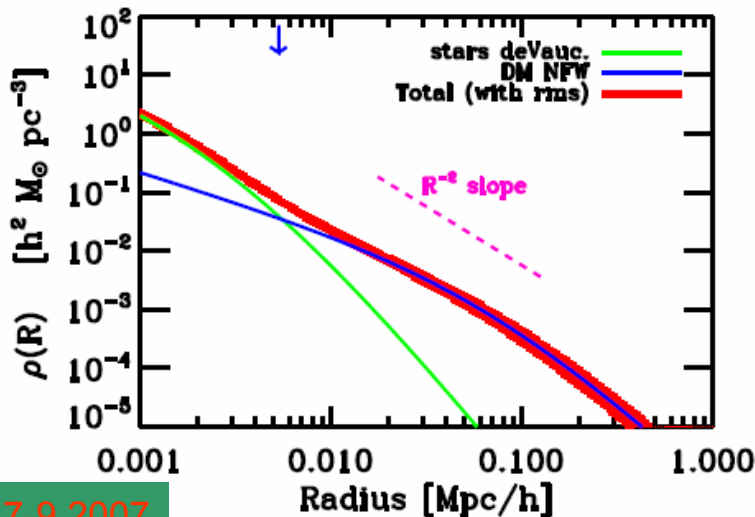
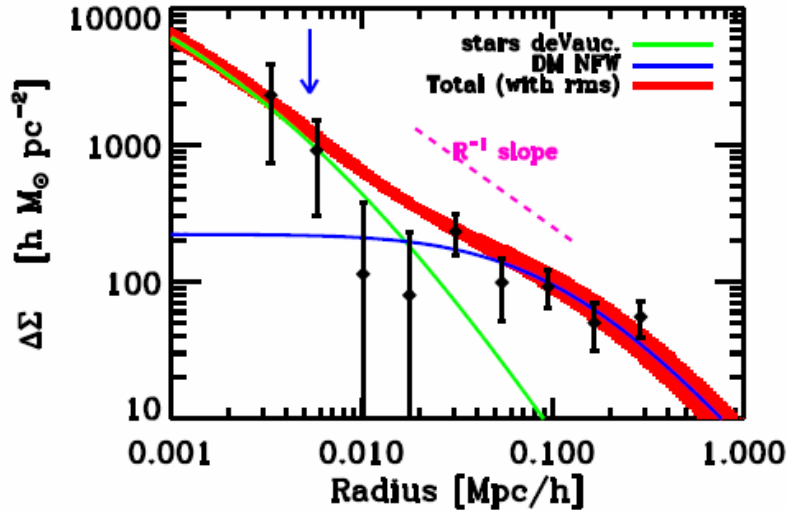


SLOAN Lens ACS Survey: Bolton et al 2006, Treu et al 2006, Koopmans et al 2006

Strong+Weak lensing of galaxies with rings in SLAC



Strong+Weak lensing of galaxies with rings in SLAC



Gavazzi et al 2007:

- Fit SIS
- Does not fit NFW

• Contradict Mandelbaum et al 2006?

• Why? :